

**IMMUNOPHENOTYPIC ANALYSIS OF PERIPHERAL BLOOD AND SYNOVIAL
FLUID LYMPHOCYTES FROM PATIENTS WITH FAILED HIP IMPLANTS**

Thesis as submitted to the Faculty of Graduate and Postdoctoral Studies in
partial fulfillment of the requirements for the degree of Master of Science, in
Biochemistry

The Faculty of Medicine

Department of Biochemistry, Immunology and Microbiology

University of Ottawa

© Ian Hurda, Ottawa, Canada, 2013

Abstract

Metal-on-metal (MM) bearings have been considered as an alternative to conventional metal-on-polyethylene (MPE) bearings because of their lower volumetric wear, but concern exists due to potential metal hypersensitivity. Metal hypersensitivity reactions have been thought to be T-cell-mediated delayed type hypersensitivity (DTH) reaction. However some of the MM periprosthetic tissues show the presence of B- and plasma cells, as well as massive fibrin exudation, which are not characteristic of a DTH reaction. Therefore, the exact nature of the hypersensitivity reaction(s) MM implants remains unclear. The present study aimed to compare the phenotypes of lymphocytes from the peripheral blood and synovial fluid of patients with failed MM and MPE implants, and from volunteers with no implant (peripheral blood only). Results in peripheral blood showed differences in the T-cell populations depending on the implant type. This included differences in the proportions of T-helper and T-cytotoxic cells, and T-cells expressing IFN- γ . Results in synovial fluid showed a significant difference between MM and MPE groups for the B-cells. Both groups depicted a predominance of T-cell lymphocytes in synovial fluid and overall larger proportions of memory cells than in peripheral blood, but group sizes were rather small. Overall, T-cell cytokine expression (analyzed in peripheral blood only because of the limited number of synovial fluid samples) did not exhibit characteristics of a DTH reaction and the proportions of memory lymphocytes did not indicate activation of a specific subset in the MM group. Nevertheless, group sizes still remain to be increased.

List of Abbreviations

μL	microlitre
μm	micrometer
μM	micromolar
ALVAL	aseptic lymphocyte-dominated vasculitis-associated lesion
ANOVA	analysis of variance
APC	antigen presenting cells
BC	Beckman Coulter
BD	Beckton Dickson
CC	ceramic-on-ceramic
Co	cobalt
CPE	ceramic-on-polyethylene
Cr	chromium
DTH	delayed type hypersensitivity
EB	eBioscience
ECD	energy coupled dye (PE-Texas Red)
FBS	fetal bovine serum
FITC	fluorescein isothiocyanate
FL1 to 5	flow cytometer channels for fluorochrome specific wavelengths
FS	forward scatter channel
<i>g</i>	standard gravity units
HLA-DR	human leukocyte antigen encoded MHC II receptor
IL	Interleukin

LTT	lymphocyte transformation test
M-CSF	macrophage colony stimulating factor
MHC	major histocompatibility
mL	millilitre
MM	metal-on-metal
MNGC	multinucleated giant cells
MPE	metal-on-polyethylene
n	sample size
NFκB	nuclear factor kappa-B
NK	natural killer cells
NKT	natural killer T-cells
nm	nanometer
OC	osteoclast
PB	peripheral blood
PBS	Phosphate buffered saline
PE	phycoerythrin
PE-Cy5	phycoerythrin cyanine-5 conjugate
PE-Cy7	phycoerythrin cyanine-7 conjugate
PGE2	Prostaglandin E2
PMA	phorbol-12-myristate
RANK	receptor activator of NFκB
RANKL	RANK-ligand
RPMI-1640	cell medium formulation
SF	synovial fluid

SS	side scatter channel
STD	standard deviation
T _c	T-cytotoxic cells (CD8+)
TCR	T-cell receptor
T _h	T-helper cells (CD4+)
THA	total hip arthroplasty
THR	total hip replacement
TNF- α	tumor necrosis factor- α
TRAF6	tumor necrosis factor associated receptor 6
UHMWPE	Ultra high molecular weight polyethylene

Acknowledgements

It is with great pleasure for me to extend my deepest thanks to those who have made this possible. First, and foremost, I extend the greatest thanks to my supervisor Dr. Isabelle Catelas for her dedication, expertise, and guidance, in the completion of my research and thesis. In combination with my supervisor, I am lucky to have had an active and intelligent co-supervisor, Dr. Daniel Figeys, and advisory committee, Dr. Lionel Filion and Dr. Natalie Goto.

I would also like to thank my colleagues in the lab, in particular Dr. Eric Lehoux, Stephen Baskey and Robilyn VanOs for their support, experience, and providing a fun and stimulating environment in which to learn and grow.

Much gratitude is also extended to Dr. Paul Beaulé, for his clinical perspective, and the entire Division of Orthopaedic Surgery at the Ottawa hospital, for without their support this work would not have been possible. I would also like to extend my acknowledgements to the Hans K Uthoff Fellowship award for personal funding in my research in orthopaedics.

Finally, many thanks go to my family and friends for their support and encouragement which has kept me inspired and made this process fulfilling.

Table of Contents

Abstract	i
List of Abbreviations	ii
Acknowledgements	v
Table of Contents	vi
List of Figures	viii
List of Tables	x
1 Introduction	1
1.1 Total Hip Arthroplasty	1
1.2 Hip Implant Failure	3
1.3 Wear Particle-Induced Inflammation and Osteolysis	4
1.4 Implant Wear Particle Characteristics	6
1.5 Metal-on-Metal Bearings – Clinical Perspective	7
1.6 Metal Sensitivity and Orthopaedic Implants	11
1.7 Metal-on-Metal Bearings and Hypersensitivity	14
1.8 T-cell Cytokine Expression in DTH and Osteoclastogenesis	19
1.9 Study Hypothesis and Objectives	22
2 Methods	23
2.1 Subjects	23
2.2 Samples	24
2.3 Mononuclear Cell Isolation	25
2.3.1 Heparinized Whole Blood	25
2.3.2 Synovial Fluid	25
2.4 Flow Cytometry Analysis	26
2.4.1 Optimization of the Acquisition Protocol Set-up: Identification of Lymphocyte Subsets	26
2.4.2 Extracellular Staining: Lymphocyte Phenotype	29
2.4.3 Intracellular Staining: T-cell Cytokine Expression	31
2.5 Statistical Analysis	33
3 Results	35
3.1 Peripheral Blood Lymphocytes	35
3.1.1 Lymphocyte Subsets	35
3.1.2 T- and B-cell Phenotypes	37
3.1.3 T-cell Intracellular Cytokine Expression	41

Table of Contents (continued)

3.2 Synovial Fluid Lymphocytes	43
3.2.1 Synovial Fluid vs. Peripheral Blood Lymphocyte Subsets	44
3.2.2 Synovial Fluid vs. Peripheral Blood Lymphocytes: T- and B-cell Phenotypes	46
4 Discussion	47
4.1 Peripheral Blood Lymphocyte Subsets	48
4.2 Naive and Memory Lymphocytes	51
4.3 T-Cell Intracellular Cytokine Profile	53
4.4 Lymphocyte Phenotype and Circulation	55
5 Conclusions and Future Considerations	58
References	62
Appendix A: Patient Group Demographics	70
Appendix B: Flow Cytometry Acquisition Protocols	73
Appendix C: Comparison of New Antibody Clones	81
Appendix D: T-Cell Cytokine Stimulation Protocol Development	86
Appendix E: Raw Data Collected from Flow Cytometry Analysis	90
Appendix F: Peripheral Blood Lymphocyte Population Distributions	97

List of Figures

Figure 1: Radiograph of (A) a MM total hip replacement using a femoral stem; and (B) a hip resurfacing, where the femoral head is resurfaced with an artificial head.	1
Figure 2: Bearing surfaces for hip replacements expressed as the percentage of bearing types implanted in patients in Canada between 2006 and 2007.	3
Figure 3: Periprosthetic tissue from a MM case with a suspected metal sensitivity.	9
Figure 4: (A) Representative Forward-Side Scatter dot plot from the ficoll density isolated mononuclear cells; (B) Identification of CD3+ (red) T-cells and CD19+ (blue) B-cells from the distribution of FL1-FL3 dot plot.	27
Figure 5: Workflow of the gating criteria used to identify specific lymphocyte subpopulations using extracellular markers.	31
Figure 6: Workflow of the gating criteria used to identify T-cells as either CD4+ (T helper) or CD8+ (T cytotoxic) cells and intracellular cytokine expression from each subset.	
Figure 7: Model-gating strategy for characterizing lymphocyte subpopulations, T-, B- and NK-cells.	36
Figure 8: Flow cytometry analysis of peripheral blood lymphocyte immunophenotypes, expressed as the percentages of lymphosum.	37
Figure 9: Model-gating strategy for characterizing CD4 ⁺ and CD8 ⁺ T-cells.	38
Figure 10: (A) Peripheral Blood T-cells phenotypes expressed as the ratio of the percentages of CD4 ⁺ over CD8 ⁺ T-cells. (B) Percentages of total T-cells expressing memory marker CD45RO.	39
Figure 11: Model-gating strategy for the identification of naïve and memory B-cells.	40
Figure 12: Percentages of memory B-cells.	40
Figure 13: Model-gating strategy for the characterization of T-cell intracellular cytokine expression.	41
Figure 14: Percentages of T-cells expressing IFN- γ .	42
Figure 15: Acquisition data from the titration of anti-CD3-PE-Texas Red.	75
Figure 16: Compensation matrices for five-colour flow cytometry of peripheral blood and synovial lymphocytes.	76
Figure 17: Single-colour antibody control dot-plots, for antibodies used in the extracellular panels for peripheral blood lymphocytes.	77

List of Figures (continued)

Figure 18: Single-colour antibody control dot-plots, used in the intracellular cytokine analysis panel for peripheral blood lymphocytes.	78
Figure 19: Single-colour antibody control dot-plots, for antibodies used in the extracellular panels for synovial fluid lymphocytes.	79
Figure 20: Single-colour antibody control dot-plots, used in the intracellular cytokine analysis panel for synovial fluid lymphocytes.	80
Figure 21: Evaluation of CD19 antibodies by single-colour extracellular staining.	82
Figure 22: Evaluation of CD3 antibodies by single-colour extracellular staining.	83
Figure 23: Evaluation of CD3 antibodies by single-colour extracellular staining of stimulated lymphocytes, followed by fixation and permeabilization.	84
Figure 24: Recoverable cells following 5.5 hour incubation, in the presence of 1 μ M ionomycin, GolgiPlug and varying concentrations of PMA.	87
Figure 25: T-cell cytokine expression with varying concentrations of PMA.	87
Figure 26: Cytokine expression of CD4 ⁺ and CD4 ⁻ (CD8) T-cells, respectively over a time course of 24 hours.	89
Figure 27: Normal distribution plots for the T- and B- cell lymphocyte populations.	98
Figure 28: Normal distribution plots for the NK- and NKT- cell lymphocyte populations.	99
Figure 29: Normal distribution plots for the CD4/CD8 ratio and percentage of memory (CD45RO+) T-cell lymphocyte populations.	100
Figure 30: Normal distribution plot for the percentage of memory B-cells.	101
Figure 31: Normal distribution plots for the percentage of IFN- γ cytokine expression in CD4 ⁺ and CD4 ⁻ (CD8 ⁺) T-cells.	102
Figure 32: Normal distribution plots for the percentage of IL-4 cytokine expression in CD4 ⁺ and CD4 ⁻ (CD8 ⁺) T-cells.	103
Figure 33: Normal distribution plots for the percentage of IL-17 cytokine expression in CD4 ⁺ and CD4 ⁻ (CD8 ⁺) T-cells.	104

List of Tables

Table 1: Representative T-cell cytokine profiles and their effects on osteoclastogenesis.	20
Table 2: Subject group demographics.	24
Table 3: Antibodies used in the immunophenotyping panels of lymphocytes, including concentration used for analysis.	28
Table 4: Test panels performed for the characterization of lymphocyte subpopulations.	29
Table 5: Subject group sample sizes by analysis.	35
Table 6: Cytokine expression of peripheral blood CD3 ⁺ CD4 ⁺ and CD3 ⁺ CD4 ⁻ T-cells.	43
Table 7: Synovial fluid lymphocyte phenotyping results.	44
Table 8: T-, B-, and NK- cell percentages in the synovial fluid and peripheral blood of patients with failed MM and MPE implants.	45
Table 9: Percentages of memory lymphocyte subsets in the synovial fluid and peripheral blood of patients with failed MM and MPE implants.	47
Table 10: Demographics of patient samples analysed.	70
Table 11: Detector settings for Flow cytometry analysis of peripheral blood and synovial fluid lymphocyte subpopulations.	73
Table 12: T-cell phenotype analysis using the two alternative CD3 antibodies.	85
Table 13: B-cell phenotype analysis using the two alternative CD3 and CD19 antibodies.	85
Table 14: Lymphosum analysis using the two alternative CD3 and CD19 antibodies.	85
Table 15: Intracellular cytokine expression analysis using the two alternative CD3 antibodies.	85
Table 16: Example calculations for Extracellular lymphocyte phenotyping.	90
Table 17: Extracellular phenotyping results.	91
Table 18: Example calculations for Extracellular lymphocyte phenotyping.	94
Table 19: T-cell cytokine expression results.	94

1. Introduction

1.1. Total Hip Arthroplasty

Total hip arthroplasty (THA) is the surgical replacement of the hip joint with an artificial prosthesis, which is a reconstructive procedure for those suffering from degenerative joint diseases. It is the most successful treatment for degenerative hip joints, resulting in dramatic relief of pain, improvement of the joint function and patient quality of life. It is also considered a routine surgery, with over 24,000 hip replacements reported to the Canadian Joint Replacement Registry in the year 2006-2007 [1]. A THA can be performed with a total hip replacement (THR) device using a femoral stem (where the femoral head and acetabulum are replaced) (Figure 1A) or with a resurfacing implant (a bone-conserving method where the femoral head is resurfaced and the acetabulum is replaced) (Figure 1B). Stem-type devices are by far the more practiced option, accounting for 94.2% of replacements between 2006-2007 [1].

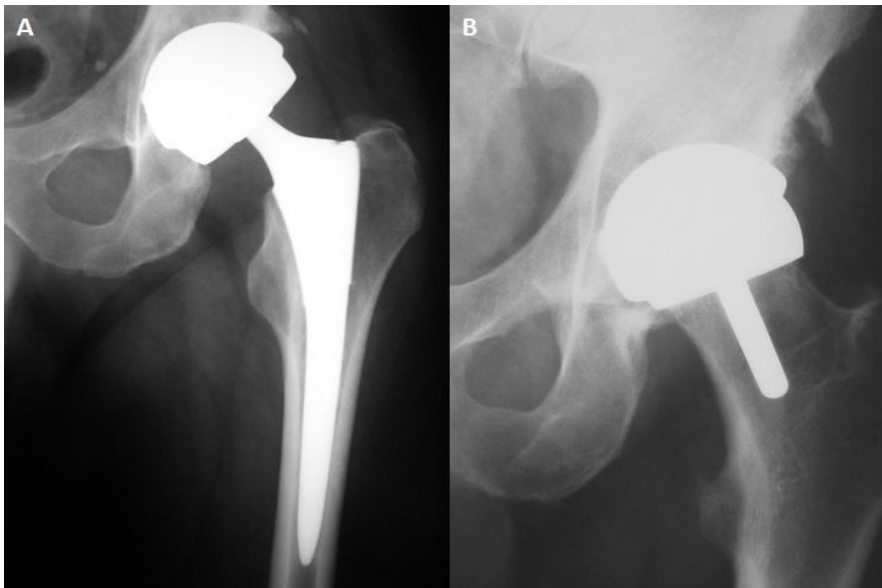


Figure 1: Radiograph of (A) a metal-on-metal (MM) total hip replacement using a femoral stem; and (B) a hip resurfacing, where the femoral head is resurfaced with an artificial head. Taken from Shimmin *et al.*, 2008 [2].

The most commonly used hip implants are metal-on-polyethylene (MPE) bearings, made of an ultra-high molecular weight polyethylene (UHMWPE) acetabular cup (and more recently, highly cross-linked polyethylene) coupled to a cobalt-chromium-molybdenum alloy femoral head. Other bearing couples include ceramic-on-ceramic (CC), metal-on-metal (MM) and ceramic-on-polyethylene (CPE) (Figure 2). Articulation of the bearing surface causes the production of wear particles and hard-on-hard surfaces, such as MM bearings have been introduced due to lower volumetric wear compared to conventional MPE bearings (using UHMWPE). MM implants were first introduced in the 1960's, however they were phased out in favour of MPE bearings [3]. In retrospect, the long-term follow-up of the first generation MM bearings indicated promising survivorship, and the increasing evidence of wear-related osteolysis surrounding conventional MPE bearings led to a resurgence of interest in MM implants due to their lower volumetric wear rates, and the possibility of using larger femoral heads, thereby reducing the risk of dislocation [3–7]. A second generation of MM implants was therefore introduced in the 1980's.

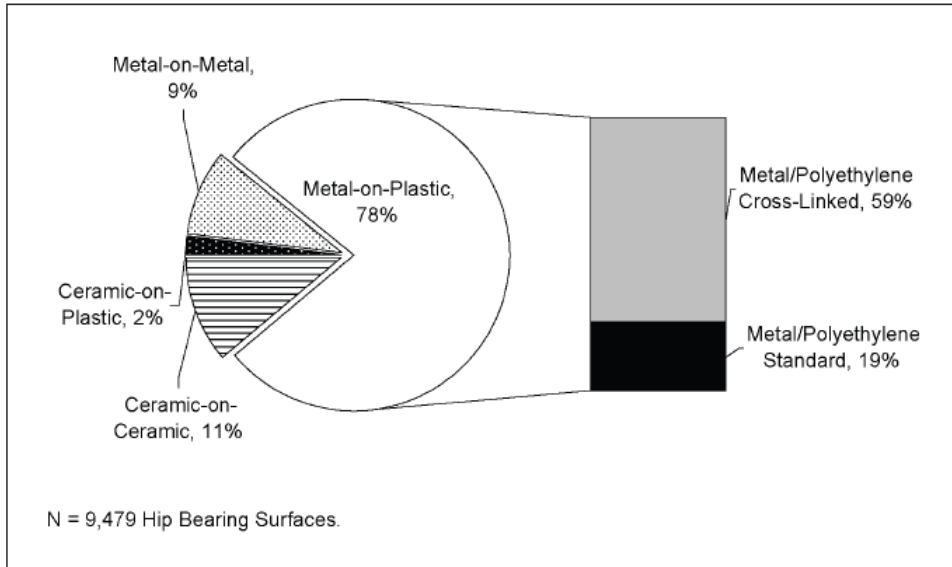


Figure 2: Bearing surfaces for hip replacements expressed as the percentage of bearing types implanted in patients in Canada between 2006 and 2007. Taken from the Canadian Joint Registry's report [1].

1.2. Hip Implant Failure

Over 13% of THA surgeries performed between 2006 and 2007 in Canada were revision surgeries of a failed implant [1]. THR failure rates are reported to be approximately less than 1% per year for the first 10 years. The implications of implant failure are of increasing concern as the incidence of younger patients having hip replacements has been increasing. For example, between 1997 and 2007, the number of hip replacements in male and female patients under the age of 55 has increased 104% and 51%, respectively [1]. These younger patients are much more likely to outlive their implant and therefore, it is important to develop materials and designs that increase survivorship. MM bearings have become an attractive bearing option for these younger patients, due to their lower wear volume compared to conventional MPE bearings. MM resurfacings, in particular, have been considered because they allow preserving the femoral bone stock and using

large diameter heads, thereby reducing the chance of dislocation. Nevertheless, different implant designs from different manufacturers have been shown to have varying degrees of success.

Aseptic loosening accounts for over 75% of THA failures [1,8]. The primary cause of aseptic loosening is wear particle-induced periprosthetic osteolysis (i.e., bone loss around the implant), although it may also be partially caused by physical responses, such as fluid pressure, stress shielding at the bone-implant interface, and/or age-related changes inducing bone loss and instability of the implant [9]. Nevertheless, it has been shown that the presence of wear products inducing an inflammatory reaction largely contribute to osteolysis, with clinical evidence supporting the association of implant wear rates and the extent of osteolysis [5,9–11].

1.3. Wear Particle-Induced Inflammation and Osteolysis

Skeletal bone homeostasis is a continuous process of bone resorption carried out by osteoclasts (OC), and bone formation carried out by osteoblasts. The OC arise from cytokine-driven proliferation and differentiation of monocyte precursors which fuse to form OC polykaryocytes. Cytokines required for OC formation are macrophage colony stimulating factor (M-CSF) and receptor activator of nuclear factor kappa-B-ligand (RANKL), produced primarily by bone marrow stromal cells (which also provide the physical support for OC precursors) as well as osteoblasts, macrophages and activated T- and B-cells [12,13]. RANKL is the key osteoclastogenic cytokine which binds to receptor activator of nuclear factor-kappa B (RANK), expressed on OC and OC precursor cells

[12,13]. RANK signalling stimulates the activation of tumor necrosis factor receptor activating factors (TRAFs), and in particular TRAF6 [14]. TRAF6 plays a critical role in activating signalling transduction pathways from interleukin-1 (IL-1) and tumor necrosis factor (TNF) receptors, as well as RANK, which in turn activates transcriptional activity via nuclear factor kappa-B (NFκB), thereby activating transcription of genes responsible for osteoclastogenesis [12–14].

Wear particles induce a foreign body reaction which can lead to bone loss around the implant (periprosthetic osteolysis). Many cell types have been described to play a role in the response to implant wear products resulting in periprosthetic osteolysis, including fibroblasts, macrophages, multi-nucleated giant cells, osteoblasts, etc. However, macrophages have been recognized as the primary cell type involved in this response [9,15]. Histological analyses of tissues surrounding aseptically loosened hip implants indicate consistent features where macrophages dominate a foreign body reaction, composed of osteolytic granulomas [9,12,16,17]. Macrophages attempt to eliminate the foreign-body wear products by means of endocytosis, depending on the size of the wear particles, which leads to their activation and initiation of an inflammatory response. However, macrophages are unable to digest these wear particles thereby inducing a circulating loop of cell recruitment and secretion of pro-inflammatory mediators, such as IL-1, prostaglandin E2 (PGE2), and TNF-α, the extent of which depends on the nature of the particles [18,19]. Retrieval studies of revised hip replacements have also shown elevated levels of pro-inflammatory cytokines as well as proteases, which suggest their role in the tissue destruction in patients with osteolysis [19–21]. For example, IL-1

promotes the expression of RANKL by bone marrow stromal cells and osteoblasts, and increases production of PGE2 by synoviocytes (resident synovial cells), thereby promoting OC precursor multinucleation and enhancing OC bone resorbing potential [22–24]. TNF- α signals the activation of NF κ B via TNF-receptors on OC precursors, thereby working synergistically with RANK/RANKL in the induction of osteoclastogenesis, as well as acting as a promoter of other pro-inflammatory mediators such as IL-1, IL-6 and M-CSF, which also increase the expression of RANKL and OC formation [22,23,25]. Indeed, it has been shown, in models of osteolysis, that by neutralizing these inflammatory mediators (such as IL-1 or TNF- α) [26] or by inducing anti-inflammatory signals (IL-10) [27], the inflammatory response and bone resorption can be decreased, implying that the inflammatory response to wear particles is in large part the cause of osteolysis.

1.4. Implant Wear Particle Characteristics

In perspective, wear rates for MPE have been reported clinically to be between 100-300 μ m per year [5,28], whereas MM bearings have shown to wear less than 10 μ m per year [29]. However, the average wear particle size has been reported to be much smaller with MM bearings, ranging from around 30 to 100 nm [6,30] versus polyethylene wear particles that have been shown to be mostly between 0.5 to 1 μ m in size, with some larger than 100 μ m [31,32]. However, although MM bearings produce lower volumetric wear than conventional MPE bearings, the nano-scale size of MM wear particles produces a significantly higher number of particles with greater bioactive surface area in comparison to MPE particles. Indeed, Doorn *et al.* found that there were between 13 to 500 times

more MM particles, resulting from mechanical wear and corrosion, compared to wear particles from MPE bearings [30]. Due to their size, the exact amounts of metal particles both locally and systemically are currently unknown. These particles presumably disseminate from the local environment (periprosthetic tissues) via the cardiovascular and lymphatic systems to regional lymph nodes, liver and spleen. Nevertheless, concentrations of these MM particles are significantly higher within the periprosthetic environment with mean concentrations of 33 μM and 120 μM within the synovial fluids of MM patients compared to less than 0.5 μM (both Co and Cr) within the peripheral blood of MM patients [30,33–37].

1.5. Metal-on-Metal Bearings – Clinical Perspective

Clinical results of second generation MM bearings are now available, many of which showing promising results [38–42]. Nevertheless, concerns with MM bearings and related wear include potential risks associated to both the short- and long-term effects of elevated metal concentrations, both locally and systemically. These include toxicity, specific immune reactions, and potential carcinogenicity. Indeed, it has been shown that metal ions and particles can induce cytotoxicity and chromosomal damage *in vitro* [43–46]. Nevertheless, to date, there is no clinical evidence to support the carcinogenic effects related to the elevated metal ion concentrations in patients with MM implants.

Histologically, the rationale behind reintroduction of MM implants has been confirmed with reduced histiocytic inflammation in comparison to conventional MPE implants. However, periprosthetic tissues from failed MM implants have shown the presence of

more lymphocytes than in tissues from conventional MPE implants [36,47–50]. This has suggested a role for an adaptive immune response and in particular, a specific T-cell mediated immune response in the periprosthetic environment [36,47,48,50]. For example, in 2000, Willert *et al.* reported perivascular lymphocyte infiltrates from retrieved tissues surrounding MM bearings [49]. These results prompted follow-up studies comparing tissues from failed 2nd generation MM bearings with tissues from CPE, MPE, and 1st generation MM bearings. Such studies reported distinct patterns of inflammation depending on the type of bearing [49,50]. Tissues from patients with either a CPE or MPE implant showed large amounts of PE wear, histiocytic inflammation, including granulomatous tissues, multi-nucleated giant cells (MNGC), and necrosis, with no or limited lymphocyte infiltrates [50]. MM tissues, from both 1st and 2nd generation implants, generally showed lower levels of macrophages and MNGC but depicted much larger perivascular lymphocyte aggregates and/or diffuse lymphocyte distributions (mostly T and some B lymphocytes) [50] (Figure 3). Such reactions have been described histologically by Willert *et al.* as aseptic lymphocyte-dominated vasculitis-associated lesion (ALVAL) [50].

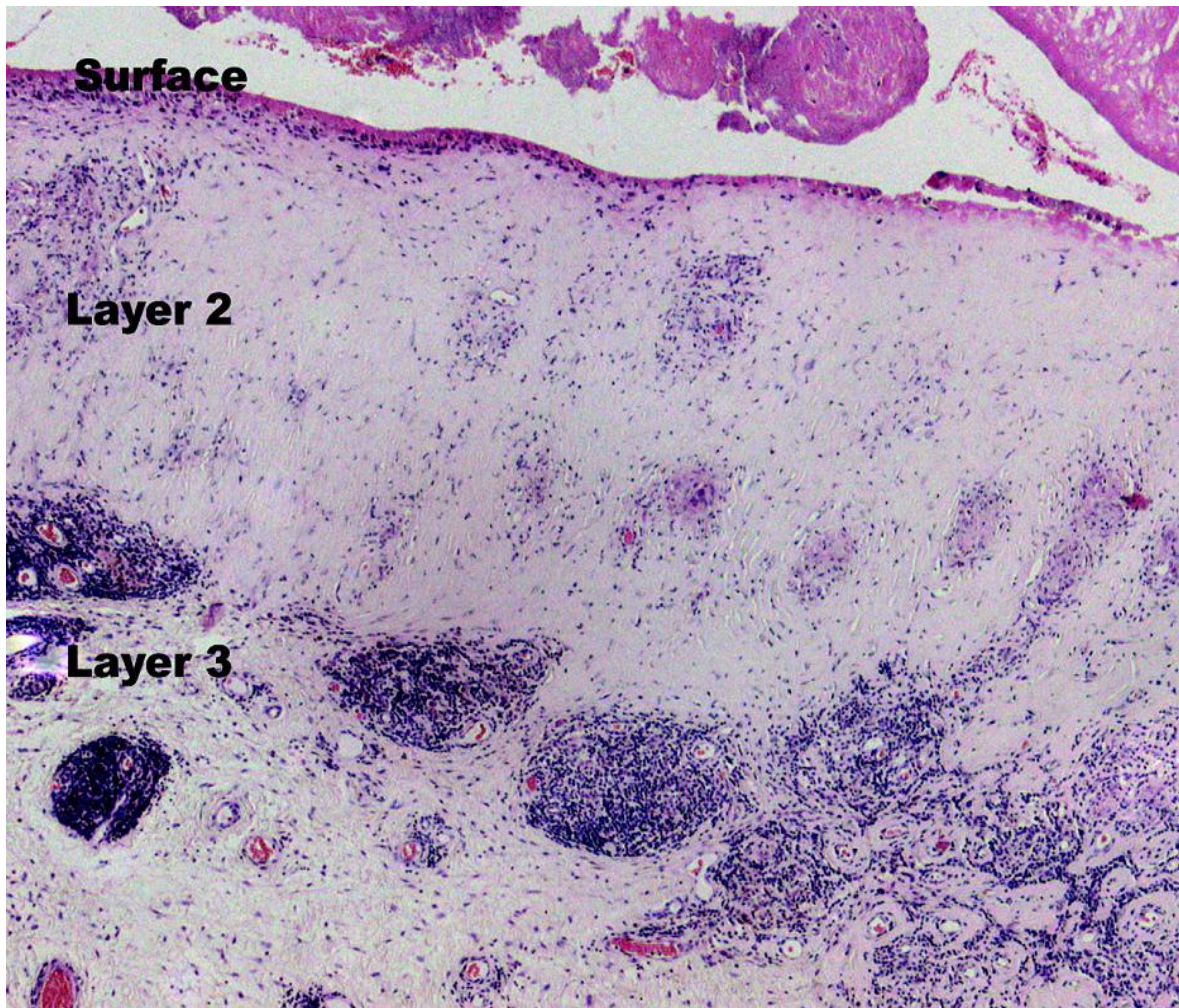


Figure 3: Periprosthetic tissue from a MM case with a suspected metal sensitivity. Section depicts an ulcerated tissue surface, followed by a subsurface layer with little cell infiltration (Layer 2), and a vascular layer (3) with dense perivascular lymphocytic aggregates; haematoxylin and eosin stain, polarized light, 40X magnification, taken from Davies *et al.*, 2005 [47].

Recently, increasing concerns for the use of MM implants has also arisen from reports of soft-tissue masses, termed pseudotumors [36,51]. Histological observations of these masses indicate extensive necrosis of connective tissues, large numbers of macrophages in small granulomatous-like aggregates, heavy lymphocytic infiltrates and lymphoid aggregates (primarily CD4⁺), and occasionally B-cell follicles and/or plasma cells [36,51]. However, the exact causes of these reactions remain unclear, and may include hypersensitivity, excessive wear, or both [52].

Some studies suggest a high wear origin of pseudotumors, and have reported a strong correlation between ion levels from periprosthetic hip aspirates and the presence of pseudotumors [53-54]. For example, Kwon *et al.* found 8 and 10 times higher chromium and cobalt ion levels (respectively) from hip aspirates of patients presenting with pseudotumors versus those without [53]. The authors also reported that both groups had significant lymphocyte reactivity to nickel but not to cobalt and chromium. On the other hand, the analysis of synovial fluid cobalt and chromium concentrations did not show any statistical difference between patients with unexplained pain, which is commonly reported in patients with suspected adverse tissue reactions, and those with a defined cause of failure [34]. Further analysis of failed MM implants by Campbell *et al.* showed that, of thirty-two hip replacements revised because of a pseudotumor, some patients had a high ALVAL score in the absence of high wear, suggesting a hypersensitivity origin in these cases [52]. Therefore, the evidence of high wear as a cause of adverse tissue reactions is still under debate.

Regardless, these failures present severe problems for both the surgeons and patients, as they are difficult for the surgeons to diagnose pre-operatively, and locally destructive and often painful for the patients. This is further compounded because revision surgery, in these cases, has shown to be less successful in comparison to revision surgeries due to other causes, and therefore, reducing the patient's risk of developing these adverse reactions is of great importance [53].

1.6. Metal Sensitivity and Orthopaedic Implants

Metal ions have been shown to have immunogenic potential, where nickel is presently the most common contact allergen, with an estimated prevalence of nickel allergy in the general population of approximately 8.6% [55,56]. Other metal ions, such as cobalt and chromium, may also produce allergic reactions through metal contact with tissues, and therefore implant components containing cobalt and chromium can also potentially cause metal sensitivity problems [56].

In the case of MM hip implants, a hypersensitivity reaction has been implicated as a likely cause of the pathophysiology observed with ALVAL [10,57,58]. However, while histological observations of ALVAL reactions indicate lymphocyte response, preliminary developments for diagnostics, including skin patch testing and lymphocyte transformation testing (LTT) to implant metals have not provided reliable markers for testing metal sensitivity reactions in these patients.

For example, Hallab *et al.* reviewed multiple cohort studies using skin patch testing and reported that about 60% of the patients with a failed (or poorly performing) implant tested positive for metal sensitivity, compared to 25% of the patients with a stable implant and 10-15% of the general population [59]. Although this review did not differentiate the types of implant, it only included implants with a metal component. Interestingly, a more recent study by Granchi *et al.* using skin patch testing reported that 60% of patients with a stable implant tested positive for at least one implant-related hapten, compared to 40% of the patients with either no implant or with a failed implant

[60]. When they looked further into the failed implant group, they found that patients with CoCrMo alloy components were less likely to test positive for metal allergy than those with another bearing type. They also reported that patients with a stable CoCrMo implant had a similar reactivity response as those with a failed CoCrMo implant (41.7 and 32.3%, respectively). All together, these studies show that skin patch testing may not be the most reliable test for hypersensitivity to orthopaedic implant components. Namely, the mechanism by which an allergic reaction occurs on the skin may be considerably different than what may be occurring around the implant.

With regards to LTT, when comparing patients with well-functioning MM and MPE implants, healthy controls and osteoarthritis patients, Hallab et al. found a positive linear correlation between lymphocyte reactivity and the concentration of chromium and cobalt ions in the MM group [57], demonstrating that there was an increased prevalence of cobalt and chromium reactivity with increased blood concentration (which is usually used as an indicator of total wear of the implant). However, their study was performed with patients with well-functioning implants and therefore, it does not indicate whether there was an increase in metal sensitivity in patients with poorly functioning implants. Kwon *et al.* performed a similar study to evaluate the incidence of metal sensitivity in failed MM patients with or without a pseudotumor [61]. LTT assays with chromium, cobalt, and nickel showed a higher incidence of lymphocyte reactivity to nickel but not to chromium and cobalt in both patient groups when compared to control [61]. These results may indicate that there is a higher prevalence of metal sensitivity in failed MM implants compared to control. However, they showed no correlation with the incidence of

pseudotumor. A more recent report by Hallab *et al.* investigated metal sensitivity by both LTT and indications of lymphocyte activation by T- and B-cell activation markers by flow cytometry [62]. In this study, they reported no significant differences in metal reactivity between MM and MPE patient groups (admittedly their MM group sample size was small) [62]. Interestingly, 82% of the patients depicting increased reactivity, irrespective of implant type, exhibited an exclusively T- or B-cell activation response to chromium, cobalt and nickel. They also found that 27% of the patients exhibited activation of only B-cells, whereas 55% showed exclusive activation of T-cells and the remaining patients (18%) showed mixed (T- and B-cell) activation [62]. While analyzing T- and/or B-cell-activation upon metal exposure, they did not find a correlation between the LTT stimulation index and the expression of activation markers. Thus, when using LTT, the study did not indicate increased reactivity in MM patients, but that immune reactivity to metal exposure was patient-dependent, irrespective of their implant type.

Overall, the histological analysis of MM tissues and *in vitro* testing of lymphocyte reactivity in patients with MM implants have indicated the potential for a hypersensitivity response in some patients. However, to date, there are no reliable tests to diagnose hypersensitivity responses pre-operatively. Imaging may help in the identification of solid masses (i.e., pseudotumors) but not hypersensitivity reactions. Skin-patch testing and LTT have shown that MM patients have increased reactivity to metals but results could not be correlated to the function of the implant. Finally, while blood ion concentrations may be helpful in cases of high wear, they do not always correlate with the presence of hypersensitivity and/or pseudotumors.

1.7. Metal-on-Metal Bearings and Hypersensitivity

Hypersensitivity reactions are classified into 4 types, of which I, II and III are mediated, for the most part, by B-cell production of antibodies and clearance by complement. Delayed type hypersensitivity (DTH) reactions (type IV) are driven predominantly by T-cells. Metal implant-related hypersensitivity reactions have been thought to be T-lymphocyte cell-mediated, delayed-type IV hypersensitivity immune reactions [17]. However, B-cells and plasma B-cells have been observed in the periprosthetic tissues of MM patients [50]. Hence, the mechanisms involved in adverse tissue reactions around MM implants are not fully understood. B-cells may also play a role, which may also have an influence on osteolysis since activated B-cells are capable of producing many pro-osteoclastogenic cytokines, including RANKL, TNF- α , and IL-6 [63].

In all hypersensitivity reactions, lymphocytes are the key component in antigen recognition and activation of specific immunity. The elicitation of this reaction in DTH occurs via the T-cell recognition of non-self via T-cell receptor (TCR) signalling. Each T-cell expresses many identical TCRs. However, this receptor is highly variable between T-cells and the wide range of variability (TCR repertoire) exists so that the T-cell compartment of the immune system may recognize a wide variety of antigens. Metal ions are not thought to be antigens by themselves, but they are highly chemically reactive and therefore, can form complexes with proteins via aspartate, cysteine, glutamate and histidine amino acid residues [64]. In the process of haptenization, the small molecule (i.e., in the present context a complex of metal ions with proteins) undergoes chemical modification,

potentially altering the endogenous protein native structure and/or function, thereby producing a protein with antigenic potential [64]. Alternatively, metal ions can potentially bind to major histocompatibility (MHC) proteins already expressed on antigen presenting cells (APCs), such as macrophages and dendritic cells, to produce a processing-independent antigen and promote T-cell mediated immunity [64]. APCs process these metal:protein complexes (antigens), circulate through the lymphatic system to regional lymph nodes where they encounter naïve T-cells specific to the MHC:antigen presented on their surface, leading to T-cell activation and proliferation of hapten specific memory/effector T-cells.

T-helper (T_h) cells express the CD4 TCR co-receptor which facilitates binding of T_h cells to the MHC class II:peptide complex on APCs. Thus, when 'self' proteins are derivatized by metal ions, the peptide may be recognized as non-self and elicit T-cell activation. Cytotoxic T-cells (T_c) do not express CD4 but instead express the CD8 co-receptor, which restricts their immune response to MHC class I receptors (present on all nucleated cells). As the name suggests, T_c cells are responsible for eliciting cytotoxicity in infected cells, whereas T_h cells elicit immune responses by 'helping' other immune cells in neutralization of antigen through activation of other immune cells, including macrophages, B-cells and T_c cells. Activation and proliferation of T-cells require TCR triggering, as well as co-stimulation via co-receptors on the surface of T-cells and APCs. The co-stimulation of T-cell-associated CD28 and APC associated-CD86 is one signal which promotes TCR-activated signal transduction pathways for mutual stimulation [65].

In the context of MM implants, it has been shown that CD86, required for T-cell response, is significantly upregulated on APCs in patients with a MM bearing compared to those with a MPE bearing [65], suggesting an increased antigen presentation to T-cells. Interestingly, after the revision of a failed MM to a non-MM bearing, the levels of CD86 expression appear to be no longer elevated [65]. Also, studies have shown that in MM patients, CD28 expression on T-cells is significantly lower, which is transiently down-regulated following T-cell activation, thus suggesting T-cell activation in these patients [65,66]. Therefore, there are indications of the adaptive immune system activation in MM patients, depicted by the increase in antigen presentation and increased T-cell activity.

The activation of a naïve T-cell includes mutual recognition and stimulation by hapten-presenting APCs and hapten-specific T-cells producing anti-apoptotic signals to ensure both prolonged presentation to T-cells and active proliferation of resulting memory/effector T-cells specific to the hapten. The result is the expansion of hapten-specific T-cells (oligoclonality) which has been reported within the synovial T-cell isolate of a MM patient presenting with chromium-related sensitivity [67]. However, to date, there is no comparison to other implant types or larger patient groups.

Lymphocytes circulate throughout the body and have a differential distribution of phenotypes across body compartments. For example, activated memory T-cells have a higher capacity to enter peripheral tissues and sites of inflammation than naive T-cells, and are present in larger numbers at these sites relative to the blood and non-inflamed tissues [68]. It is therefore potentially difficult to identify T-cells specific for a known

antigen when analyzing a peripheral blood sample because in a typical *in vitro* test from peripheral blood, there may be only a small percentage of T-cells specific for the antigen in comparison to the site of inflammation. Nevertheless, peripheral blood still represents an extremely useful and accessible source of T-cells for study, as many more T-cells can be isolated from blood relative to tissues [69]. For example, Granchi *et al.* investigated the systemic changes in white blood cell populations (WBCs) in patients with well-functioning THRs and found a significantly lower concentration of WBCs in the peripheral blood of patients with a hip replacement (MM, MPE, and CC) compared to healthy controls [70]. The lower concentration of WBCs was even more prominent in the patients with a metal component (MM and MPE). It is also likely that the reduced lymphocyte counts were due to a specific decrease in the CD8⁺ T-cell subset which the authors attributed to the presence of the metal component, as the significance was much higher in the MM group, followed by MPE and CC groups [70]. Hart *et al.* then studied the lymphocyte concentrations of T-, B- and NK cells in patients with a MM resurfacing in comparison to MPE implant and reached the same conclusions by showing reduced lymphocyte concentrations in patient peripheral blood as a consequence of reduced CD8⁺ T-cells in MM patients [71]. Further work has indicated that this reduction in CD8⁺ T-cells was correlated to the level of wear, as indicated by the concentration of blood cobalt and chromium ion levels [72]. However, interestingly, a more recent investigation on the lymphocyte populations in MM patients did not find reduced cell proportion in the total CD8⁺ population, but did find that there was an elevated percentage of HLA-DR⁺ (an MHC class II receptor) CD8⁺ T-cells, which is an indication of CD8⁺ T-cell activation and suggests

a role in response to MM implants [37]. Therefore, there appears to be contradictory observations on CD8⁺ T-cell phenotype in MM patients, as demonstrated by the conflicting results of these recent studies [37,70-72].

CD8⁺ T-cells have not been reported to be the predominant T-cell subset in MM periprosthetic tissues. Instead, CD4⁺ T-cells have been shown to be the primary lymphocytic infiltrate [36]. However, CD8⁺ T-cells are MHC-I restricted, which is expressed by all nucleated cells, such as osteoclasts and all other resident synoviocytes (synovial cells). Interestingly, there is *in vitro* evidence of anti-osteoclastogenic effects of CD8⁺ T-cells [73]. However, the mechanism by which they would exert this effect has yet to be determined. Therefore, the current knowledge may suggest that CD8⁺ T-cells may either be disrupted from 1) an as of yet unknown bone-saving mechanism (i.e. immunosuppressive or cytotoxicity); or 2) activated by the presence of metallic wear to another function, such as cytotoxic effects on synoviocytes or expression of pro-inflammatory cytokines.

Following activation, T-cells generally exhibit a 'Type 0' T-cell profile, for which they secrete a broad array of cytokines, including IL-2, IL-4, IL-10, IFN- γ and TNF- α [74]. Within days, these T-cells can be polarized towards a more specific cytokine profile, depending on multiple factors, such as the cytokine environment at the site of inflammation and the molecular nature of the antigens. After being activated, T-cells take on memory and/or effector phenotypes, which can be characterized by the expression of a cell surface receptor CD45RO. For example, CD4⁺CD45RO⁺ T-cells have been shown to be over-

represented as the primary responding T-cell population to nickel challenge [75]. The T-cell cytokine profile of metal-mediated DTH reactions is of current debate: infiltrates in skin allergy to metals have been shown to be predominantly CD4⁺ T-cells of a type-1 cytokine profile (i.e., primarily IFN- γ and IL-2 secretion), and as such, have been reported as the primary responding cells in DTH [76]. However, both CD8⁺ T-cells and CD4⁺ T-cells of other cytokine profiles have also been reported to play a role in DTH to nickel [76].

1.8. T-cell Cytokine Expression in DTH and Osteoclastogenesis

While other cytokine profiles have been reported, DTH has been primarily characterized by the activation of a T-cell subpopulation with a type 1 cytokine profile (Table 1). The release of these cytokines attracts and activates macrophages which produce many pro-inflammatory and pro-osteoclastogenic mediators, including IL-1, IL-6, PGE₂, and TNF- α [77]. Once activated, macrophages can then trigger the activation of more T-cells, and thus create a sustained immune response to antigen.

Table 1: Representative T-cell cytokine profiles and their effects on osteoclastogenesis. [78]

T-cell subset	Cytokines	Effects on osteoclastogenesis
1	IFN- γ	Stimulation/Inhibition*
	IL-2	Stimulation
	IL-18	Stimulation
	GM-CSF	Stimulation
	TNF- α	Stimulation
2	IL-4	Inhibition
	IL-6	Stimulation
	IL-10	Inhibition
	IL-13	Inhibition
17	IL-17	Stimulation
	RANKL	Stimulation
	IL-23	Stimulation

* Under debate (see text)

In an *in vitro* study, Hallab *et al.* have reported a predominance of the type 1 cytokine profile in T-cells isolated from peripheral blood of MPE patients and stimulated with chromium, cobalt and nickel. This suggests that a type 1 T-cell cytokine profile may occur *in vivo* in MM patients [79]. In the context of periprosthetic osteolysis, it has been previously reported that cytokines including IL-2, IL-4, IFN- γ , and IL-10 are present in periprosthetic tissues [80,81]. Nevertheless, these reports are not representative of comparative differences between MM and non-MM bearings, and the T-cell cytokine profile in the periprosthetic environment of MM implants remain largely unknown [80,81]. This is compounded by the fact that the mechanisms of T-cell activity on bone homeostasis are not completely understood. In general, the activation and subsequent polarization of T-cells to specific profile of cytokine secretion may have inhibitory or stimulatory effects, either directly or indirectly, on the bone remodeling process (Table 1). For example, IFN- γ , a type 1 T-cell cytokine, can have both inhibitory and stimulatory

effects on bone resorption, i.e.: 1) IFN- γ inhibits RANK-dependent osteoclastogenesis by downregulating and/or degrading an adaptor protein of RANK, TRAF6 in OC precursors, thereby preventing signal transduction of the RANK/RANKL activation for osteoclastogenesis [14]; and 2) it stimulates T-cell activation as well as secretion of RANKL from T-cells, osteoblasts, and macrophages, further stimulating osteoclastogenesis and bone resorption [82]. In the context of an inflammatory environment, IFN- γ net effect *in vivo* is speculated to be pro-osteoclastogenic, but it is under debate [82].

In contrast to type 1 T-cell profile, type 2 cytokines are most often associated with humoral immunity, and therefore, the types 1-3 hypersensitivity reactions. Among type 2 cytokines is IL-4, which has been shown to inhibit osteoclastogenesis through various mechanisms, including the inhibition of RANK signal transduction and the activation of signal transducer and activator of transcription 6 (STAT6, a transcription factor). STAT6 inhibits activation of NF κ B genes in OC precursors, thereby inhibiting osteoclastogenesis [83].

Finally, a more recent addition to the subsets of T-cell cytokine profiles has included type 17. Type 17 T-cells have now been shown to be involved in a variety of autoimmune disorders and secrete cytokines with potent osteoclastogenic potential including RANKL and IL-17, which promotes osteoclastogenesis by upregulating RANKL in osteoblasts and stromal cells [84].

1.9. Study Hypothesis and Objectives

The presence of lymphocyte infiltrates in failed MM tissues suggests the presence of a metal hypersensitivity reaction in the periprosthetic environment. Implant-related hypersensitivity reactions have been thought to be T-lymphocyte cell-mediated, delayed-type IV hypersensitivity (DTH) immune reactions [17]. However, B-cells and plasma B-cells have been observed in the periprosthetic tissues of MM patients. Therefore, the type(s) of the hypersensitivity reaction, the specific lymphocyte populations involved in the immune response around MM implants and their correlation to implant failure has yet to be determined.

The hypothesis of the study was that a DTH reaction is predominant in the early failure MM patients and as such, a T-cell subpopulation with a memory/effector phenotype and type 1 cytokine profile may be over-represented in these patients.

Therefore, the objective of the current study was to quantify the proportions of lymphocyte subsets in peripheral blood and synovial fluid of MM patients compared to MPE patients and control subjects, in order to determine whether there is an increased activation in a subset of lymphocytes in MM patients. Such activation could indicate mechanisms of the aetiology (type of hypersensitivity) of the T-cell and/or B-cell response to metal wear. T-cell cytokine expression was also evaluated to determine if a T-cell specific response is occurring so that its potential role in MM failure may be further explored.

To fulfill the study objective, lymphocytes were isolated from peripheral blood and synovial fluid and analyzed by flow cytometry to specifically determine:

- 1) The proportions of T-, B-, NK- and NKT-cells,
- 2) The lymphocyte activation by analysis of memory T- and B-cell proportions,
- 3) The cytokine profile of T-cells by studying some cytokines specific to type 1, 2 and 17 T-cell profiles.

2. Methods

2.1. Subjects

The study has been approved by the Ottawa Hospital Research Ethics Boards. Patients with failed hip implants were classified by type of implant bearing: MM and MPE. Healthy volunteers were also recruited as a control group for the peripheral blood analysis. Patients were recruited by the Division of Orthopaedic Surgery of The Ottawa hospital as they were scheduled for a revision of a failed implant. The primary causes for revision were either a loose component and/or excessive wear. Other reasons included fracture or unexplained pain. Appendix A lists all causes for revision.

Table 2: Subject group demographics.

Patient Groups	MM (n=16)	MPE (n=20)	Control (n=15)
Male	11	10	8
Female	5	10	7
Age (years)			
Mean +/- STD	55±12	66±11	35±16
Range	47-79	44-83	20-86
Time to Revision (years)			
Mean +/- STD	2.4±1.2	11.9±6.3	N/A
Range	1-4	2 - 25	

Note: for some tests, not all patients could be analyzed (see details in sections 2.2 and 2.5)

2.2. Samples

Peripheral blood samples were obtained by venipuncture into sodium heparin vacutainer (GE Healthcare, Piscataway, NJ, USA) at the Ottawa hospital. Samples were obtained at the time of the patient pre-operative appointment or on the day of surgery, immediately prior to surgery. Samples from control group subjects were collected at similar hours of the day (between 9am to 2pm). Synovial fluid samples were obtained at the time of revision surgery by aspiration in the hip joint cavity. A total of 16, 20, and 15 blood samples were analyzed for MM, MPE and control, respectively. Synovial Fluid samples were only obtained from patients undergoing surgery. A total of 7 MM and 6 MPE samples were analyzed. Total lymphosum and cytokine expression were not analyzed for all samples because the tests were not finalized at the time of sample collection and/or due to a too small volume of sample. Details on the number of samples analyzed for each test are given in section 2.5).

2.3 Mononuclear Cell Isolation

2.3.1 Heparinized Whole Blood

Heparinized whole blood samples were diluted 1:1 in room temperature phosphate buffered saline (PBS) (Wisent, Montreal, PQ, Canada) and placed on an equal volume of Ficoll Hypaque (GE Healthcare, Piscataway, NJ, USA), under aseptic conditions using a class II biosafety cabinet (Labconco, Kansas City, MO, USA). Density centrifugation was performed at 400 x *g* for 30 minutes at 20°C on a Sorvall Legend RT+ centrifuge (Thermo Scientific, Ottawa, ON, Canada). The plasma layer was removed, followed by aspiration of the lymphocyte buffy coat which was immediately washed in 3 volumes of RPMI-1640 (Wisent) supplemented with 2% of heat-inactivated fetal bovine serum (FBS) (Wisent), and centrifuged for 5 minutes at 300 x *g*. The cells were washed once more with RPMI-1640/2% FBS, and mononuclear cells were enumerated under an inverted light microscope (VWR, Mississauga, ON, Canada) using a haemocytometer (VWR). They were then resuspended at a concentration of 1.5×10^6 cells/mL in RPMI-1640 supplemented with 10% FBS. Two aliquots of 1 mL each were used immediately for extracellular staining (Section 2.4.2) and the remaining suspension was cultured in 1 mL aliquots for culture stimulation and intracellular cytokine staining (Section 2.4.4).

2.3.2 Synovial Fluid

Isolation of synovial lymphocytes was performed as previously described [85]. Freshly obtained synovial fluid was diluted 1:1 in room temperature PBS under aseptic conditions, using a class II biosafety cabinet. When the synovial fluid was too viscous for aspiration,

the fluid suspension was incubated for 30 minutes at 37°C, 5% CO₂ on a rotator, with 25µg/ml hyaluronidase (Fisher, ON, Canada) to digest hyaluronan, thereby reducing viscosity [85]. The digested product was then filtered through a 70 µm cell strainer and mononuclear cells were isolated by standard Ficoll density gradient, as described for whole blood (Section 2.3.1).

2.4 Flow Cytometry Analysis

2.4.1 Optimization of the Acquisition Protocol Set-up: Identification of Lymphocyte Subsets

Flow cytometry was used to identify different lymphocyte subpopulations, with a FC500 flow cytometer including software package, CXP 2.2 (Beckman Coulter, Mississauga, ON, Canada). Lymphocytes possess distinct size and granularity and therefore, are depicted as a consistent population with distinct 'Forward Scatter' (FS) and 'Side Scatter' (SS) characteristics, allowing their identification easily. In order to evaluate cell subsets, cells were labelled with fluorochrome-conjugated antibodies, which bind to specific proteins on or within the cells. Quantity and fluorescence intensity data were then be visualized as frequency distributions of the cell refraction (FS and SS) and fluorescence (channels 1 to 5, FL1 to FL5) (Figure 4).

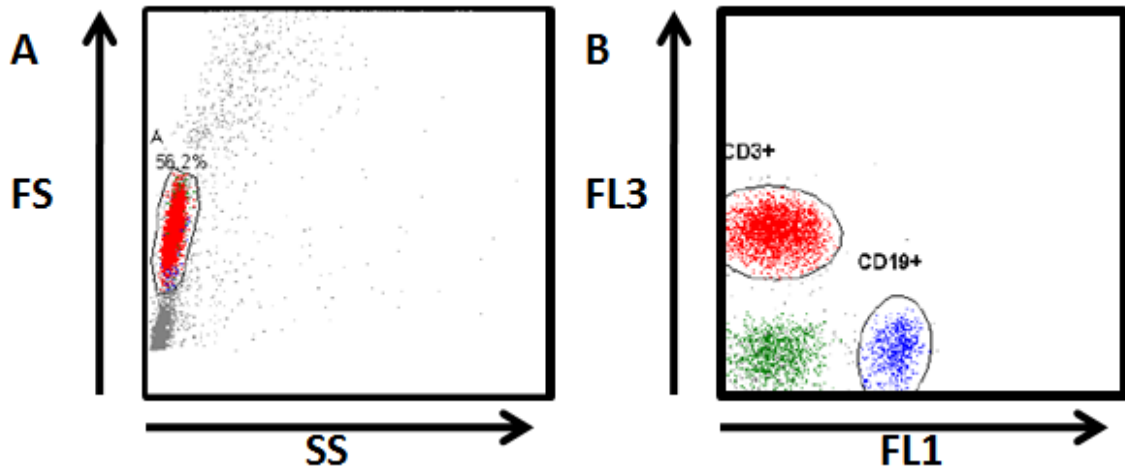


Figure 4: (A) Representative Forward-Side Scatter dot plot from the ficoll density isolated mononuclear cells, with the 'A' population indicating the lymphocyte population; (B) Identification of CD3+ (red) T-cells and CD19+ (blue) B-cells from the distribution of FL1-FL3 dot plot, where anti-CD3 is collected in FL3 and anti-CD19 in FL1.

Optimization of the acquisition parameters (FS, SS and FL1 to FL5) for the analysis of lymphocyte subsets was initially performed. Firstly, an unstained cell suspension was analyzed to optimize the FS and SS detectors to identify the lymphocyte population on the FS-SS dot plot. Each fluorochrome-conjugated antibody marker was then titrated, in dilutions starting at the manufacturer's recommended concentration per test, to determine the optimum concentration (Table 3).

Table 3: Antibodies used in the immunophenotyping panels of lymphocytes, including concentration used for analysis.

Antibody	Optimized Concentration (µg/test)	Fluorochrome	Clone	Supplier
Anti-CD3	0.1/0.2*	ECD	UCHT1	BC
	0.0625/0.125*	PE-Texas Red	UCHT1	BD [†]
Anti-CD4	0.0625/0.125*	PE-Cy5	13B8.2	BC
Anti-CD8	0.25	PE-Cy7	SFC121Thy2D3	BC
Anti-CD45RO	0.25	FITC	UCHL1	EB
Anti-CD56	0.0625	PE	CMSSB	EB
Anti-CD19	0.25	FITC	J3119	BC
	1.0	FITC	H1B19	EB [†]
Anti-CD27	0.0625	PE	1A4CD27	BC
Anti-IL-17	0.125	Alex 488	eBio64DEC17	EB
Anti-IL-4	0.25	PE	8D4-8	EB
Anti-IFN-γ	1.0	PE-Cy7	4S.B3	EB

BC – Beckman Coulter, ON, Canada

EB – eBioscience, CA, USA

*Given as the concentration required for *extracellular/intracellular* staining, respectively.

[†]Anti-CD3 and anti-CD19 antibodies were replaced with clones from Becton Dickinson for patients H80 to H87 and HC13-15

Once the optimum concentration of each antibody had been determined, single-colour control tubes were analyzed to set the negative and positive populations in the 1st and 2nd/3rd decade of the log fluorescence histogram plot, respectively, and the compensation matrix was adjusted to remove spectral overlap of the single fluorochrome from the other four fluorescent detectors. Two-colour control tubes containing optimum antibody concentrations were then analyzed to adjust the compensation matrix for spectral overlap between fluorochromes (i.e.: FITC-PE, FITC-ECD, FITC-PC-Cy5, etc.) until all combinations of fluorochromes had been adjusted. The final detector and compensation settings for

each test panel (Table 4) were saved and used in all subsequent tests. For reference of detector and compensation settings, refer to Appendix B.

Samples were processed and analyzed on the day of reception. For each test, up to 10,000 events were acquired within the lymphocyte A gate. As noted in Table 3 following patient H80, two antibodies were replaced using a new manufacturer and clone. Comparisons of the new antibodies were run in parallel to the previously used ones to ensure reproducibility (see Appendix C).

Table 4: Test panels performed for the characterization of lymphocyte subpopulations. The five channels used for each fluorochrome–conjugated antibody are noted with the specific markers detected in each test.

Test panels	FITC	PE	ECD	PE-Cy5	PE-Cy7
Total lymphocytes	CD19	CD56	CD3		
T-population	CD45RO	CD56	CD3	CD4	CD8
B-population	CD19	CD27	CD3		
Cytokine profile	IL-17	IL-4	CD3	CD4	IFN- γ

2.4.2 Extracellular Staining: Lymphocyte Phenotype

Three test panels were performed to determine T-, B-, NK- and NKT-lymphocyte subpopulations and T- and B-cell memory phenotypes (first three tests of Table 4). Isolated cells from blood or synovial fluid were centrifuged and diluted to a final concentration of 2×10^6 cells/mL in PBS supplemented with 2% FBS and 0.01% NaN_3 (w/v) (staining buffer). For each test, a 50 μ L mix of the appropriate antibodies (Table 3) was added to 100,000 cells, which were then incubated at room temperature for 10 minutes in the dark. The cell suspensions were then filled up to 500 μ L with staining buffer and

analyzed by flow cytometry in duplicates. Lymphocyte subsets were gated by positive or negative staining criteria. T-cells were identified by T-cell surface marker CD3, and were further classified into their respective subsets of CD4⁺ (T-helper (T_h)) or CD8⁺ (T-cytotoxic (T_c)) T-cells [86]. Memory Th and Tc cells were identified by the expression of CD45RO surface marker [87]. B-cells (CD19⁺) were directly stained along with CD27 to differentiate memory/plasma cells (CD27⁺) and naïve cells (CD27⁻) [86,88]. Natural killer (NK) cells were detected as CD3⁻CD56⁺ population, and NKT-cells as the doubly positive CD3⁺CD56⁺ cells. For comparison with previous studies [35,89], the proportion of NK-cells was also calculated as the total CD56⁺ population, without segregation of double positive (CD3⁺CD56⁺) cells (Figure 5).

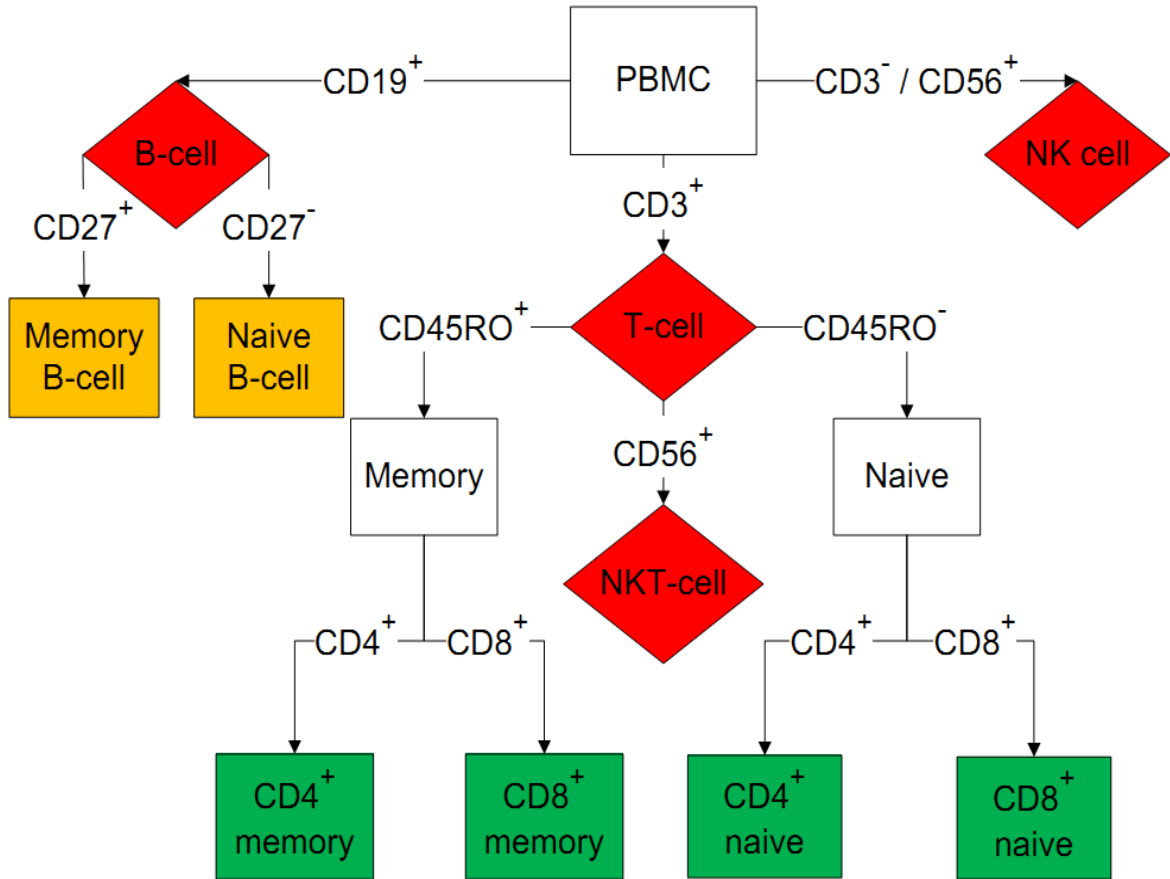


Figure 5: Workflow of the gating criteria used to identify specific lymphocyte subpopulations using extracellular markers. Each red and red box indicates the identification of a lymphocyte subset, from the total lymphocytes panel with further T-cell subsets (green) and B-cell subsets (yellow) from the T- and B-cell panels, respectively.

2.4.3 Intracellular Staining: T-cell Cytokine Expression

Detection of intracellular cytokines was performed as previously described [90,91]. The isolated cells, suspended in 10%FBS/RPMI-1640, were aliquoted in 1 mL (1.5×10^6 cells) in a 24-well plate. Stimulation of cytokine production was performed using a polyclonal activator, phorbol-12-myristate (PMA) (Sigma, Oakville, ON, Canada), and calcium ionophore, ionomycin (Sigma) at concentrations of 15ng/mL and 1 μ M, respectively, as determined by initial protocol development (see Appendix D). Cytokine secretion was inhibited by incorporation of a transport inhibitor, GolgiPlug, containing brefeldin A, as per

the manufacturer instructions (BD Biosciences, Mississauga, ON, Canada). Control cultures included unstimulated cells, with or without GolgiPlug, and stimulated cells in the absence of GolgiPlug. Cells were then incubated at 37°C, 5% CO₂ for 5.5 hours.

Following incubation, cells were harvested and centrifuged for 10 minutes at 300g. The pellet was resuspended in 300 µL of staining buffer and aliquoted to 3 microcentrifuge tubes containing 100 µL each (approximately 500,000 cells each). Cell suspensions requiring anti-CD3 and/or anti-CD4 were stained with the pre-determined concentrations of these antibodies. Following staining, each tube was filled to 500 µL with staining buffer and centrifuged for 5 minutes at 300g. The pellets were then resuspended in 100 µL of fixing reagent (intraprep reagent 1, Beckman Coulter, ON, Canada), briefly vortexed, and left to fix for 15 minutes at room temperature and in the dark. Following fixation, the cell suspension was diluted with 1 mL staining buffer and centrifuged for 5 minutes at 300g. The pellets were then resuspended in 100 µL of permeabilizing reagent (intraprep reagent 2, Beckman Coulter) and incubated for 5 minutes at room temperature in the dark. Cells requiring intracellular staining were then stained with antibodies specific for the intracellular cytokines: IFN-γ, IL-4 and IL-17. Cells were incubated in the dark for 15 minutes, followed by a wash with 1 mL staining buffer (centrifugation at 300g for 5 minutes) and finally resuspended in 500 µL of cold 4% PFA (*w/v*) in 200mM PBS (pH 7.2). Cells were left in the dark and at 4°C until flow cytometry analysis. The initial acquisition protocol as laid out in section 2.4.2 included unstained, single, and double-stained cells to setup the detectors and compensation matrix (Appendix B). Unstained and single-colour

controls were included for each experiment, and each test was run in triplicate to identify T-cell cytokine expression (IFN- γ , IL-4 and IL-17), as laid out in figure 7.

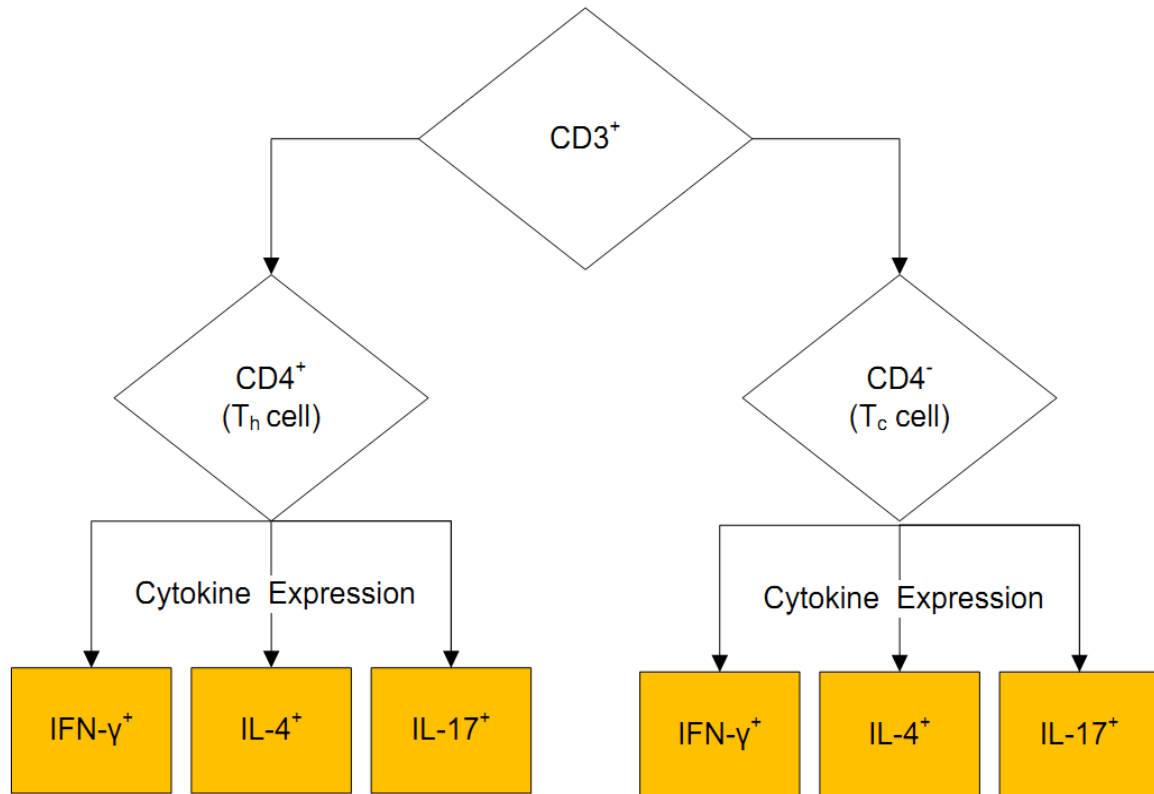


Figure 6: Workflow of the gating criteria used to identify T-cells as either CD4⁺ (T helper) or CD4⁻ (considered to be primary CD8⁺, i.e., T-cytotoxic) cells and intracellular cytokine expression from each subset. Yellow boxes indicate final gating criteria for T-cell cytokine expression.

2.5 Statistical Analysis

Statistical analysis was performed using SPSS 17.0 (IBM, Markham, ON) (for raw data refer to Appendix E). Peripheral blood lymphocyte data distributions for the 3 groups (i.e., MM, MPE, and control), were assumed to be of a near normal distribution, with the exception of NK- and NKT-cells, and T-cell cytokine expression for IL-4 and IL-17, as qualitatively assessed using distribution plots (Appendix F).

Data sets with near normal distributions were analyzed using ANOVA with Welch's correction for cases with unequal variance, as determined by the Levene test, followed by Games-Howell post-hoc test for multiple group comparison. ANOVA without the Welch's correction was used for cases of equal variance followed by Bonferroni's post-hoc test for multiple comparisons. For the analysis of NK- and NKT-cells, which depicted non-normal data distributions and unequal variances, the data was first normalized by transformation followed by one-way ANOVA with Welch's correction for unequal variance (Kruskal Wallis test could not be applied because of the unequal variances) [92]. Kruskal-Wallis was used for the analysis of intracellular cytokines with non-normal data distributions and equal variance (IL-4 and IL-17). Since there was no significant difference between groups for the two cytokines, no post-hoc tests were performed.

For the analysis of synovial fluids (comparing MM versus MPE groups, or blood versus synovial fluid), group sizes were too small to test for data distribution normality, and therefore the non-parametric Mann-Whitney U test was used for group comparisons. For all analyses, $p < 0.05$ was considered significant.

The antibody for NK- and NKT-cells (CD56) was added to the analysis starting at patient H50 and therefore total lymphocyte analysis is not available for patients prior to H50. The cytokine profile was optimized with volunteer samples and was used to analyze patient samples starting with patient H39. Therefore, cytokines were not analyzed for a portion of the patient groups. Finally, synovial fluid samples were not always available, or, in some cases, the volume collected was insufficient to perform intracellular cytokine analysis. The total sample sizes for each test are given in Table 5.

Table 5: Subject group sample sizes by analysis.

Analysis	Fluid Type	MM (n)	MPE (n)	Control (n)
T-cell phenotype	Blood	15	20	15
	Synovial	7	6	N/A
B-cell phenotype	Blood	15	20	15
	Synovial	7	6	N/A
NK cell phenotype	Blood	6	11	13
	Synovial	4	6	N/A
Cytokine expression	Blood	8	19	15
	Synovial	2*	1*	N/A

* Statistical comparison of these samples was not performed due to the low number of samples analyzed thus far.

3 Results

3.1 Peripheral Blood Lymphocytes

3.1.1 Lymphocyte Subsets

The primary lymphocyte subsets, T-, B-, NK- and NKT-cells were analyzed using a gating strategy to identify T- and B- cells ($CD3^+$ and $CD19^+$, respectively) (Figure 7A-B), as well as NK-cells ($CD3^-CD56^+$) (Figure 7C), and NKT-cells ($CD3^+CD56^+$).

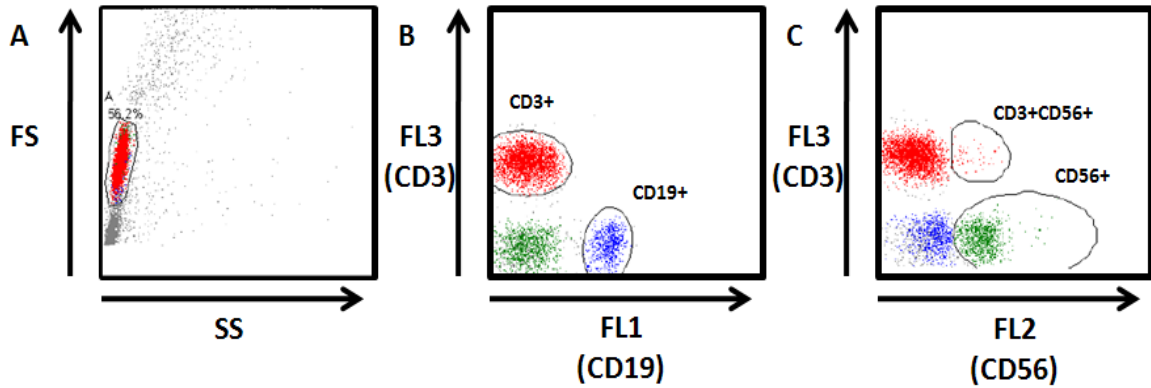


Figure 7: Model-gating strategy for characterizing lymphocyte subpopulations, T-, B- and NK-cells: (A) FS/SS dot plot indicating the lymphocyte population within the 'A' gate. Subsequent dot plots (B and C) were then gated on the lymphocyte 'A' gate; (B) FL1/FL3 detector dot plot of the lymphocyte population indicating T- (CD3⁺) and B (CD19⁺)-cell populations; and (C) FL2/FL3 detector dot plot of the lymphocyte populations indicating NK-cells (CD3⁺CD56⁺) and NKT-cells (CD3⁺CD56⁺) populations.

There were no significant differences in the mean percentages of T-, B-, and NK- cells between the groups (Figure 9A-C). On the other hand, there was a significant difference in the mean percentages of NKT-cells between the groups ($p=0.036$). However, post-hoc tests did not identify any significant difference (Figure 9D). The MM and MPE groups showed the largest difference, with mean values of 2.00% and 5.45%, respectively ($p=0.082$).

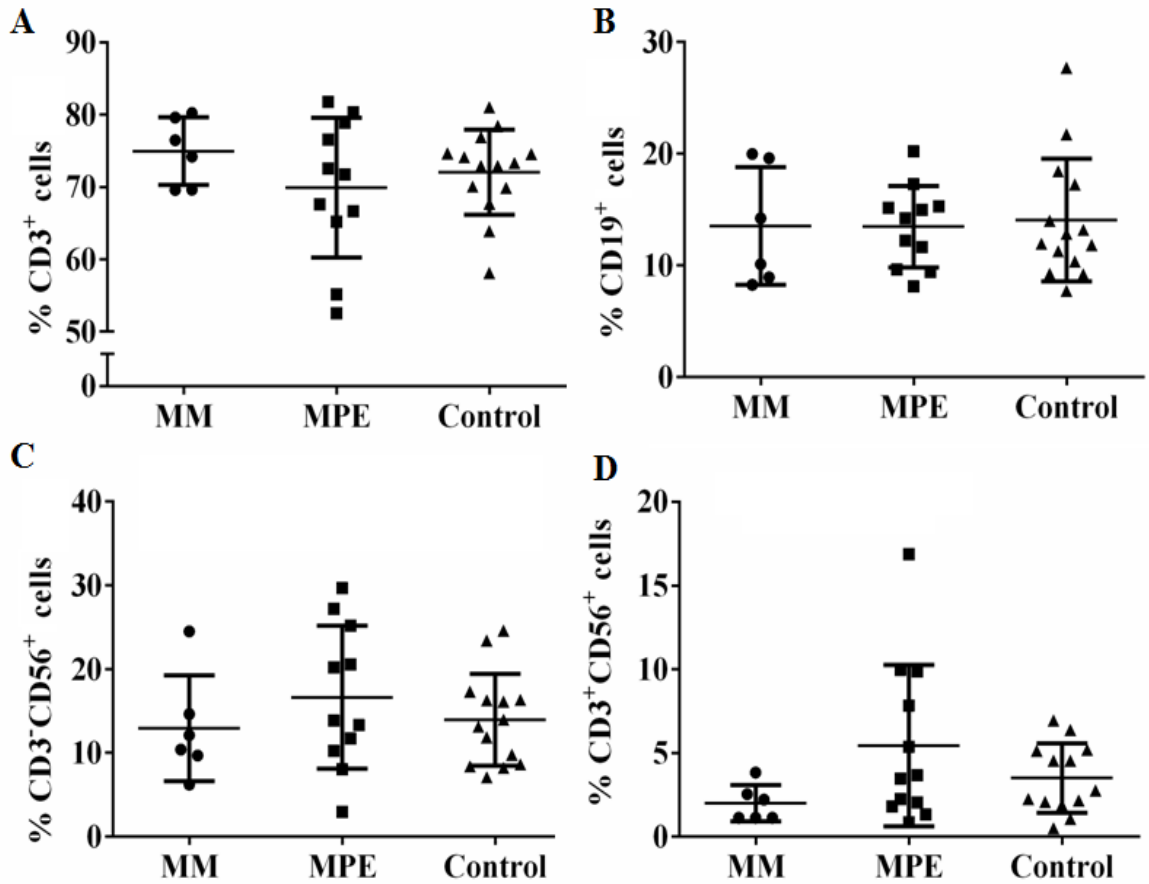


Figure 8: Flow cytometry analysis of peripheral blood lymphocyte immunophenotypes, expressed as the percentages of lymphosum: (A) T-cells (CD3⁺); (B) B-cells (CD19⁺); (C) NK-cells (CD3⁺CD56⁺); and (D) NKT-cells (CD3⁺CD56⁺). Dot plots indicate the mean values and standard deviations.

3.1.2 T- and B-cell Phenotypes

Lymphocyte populations were then analyzed to identify T-cell subsets (T-helper and T-cytotoxic), as well as the expression of CD45RO on T-cells to differentiate naïve (CD45RO⁻) and memory cells (CD45RO⁺) (Figure 9). The CD3⁺ T-cells were categorized by co-expression of CD3 with either CD4 (for T-helper) or CD8 (for T-cytotoxic), which were then classified as either naïve or memory T-cells.

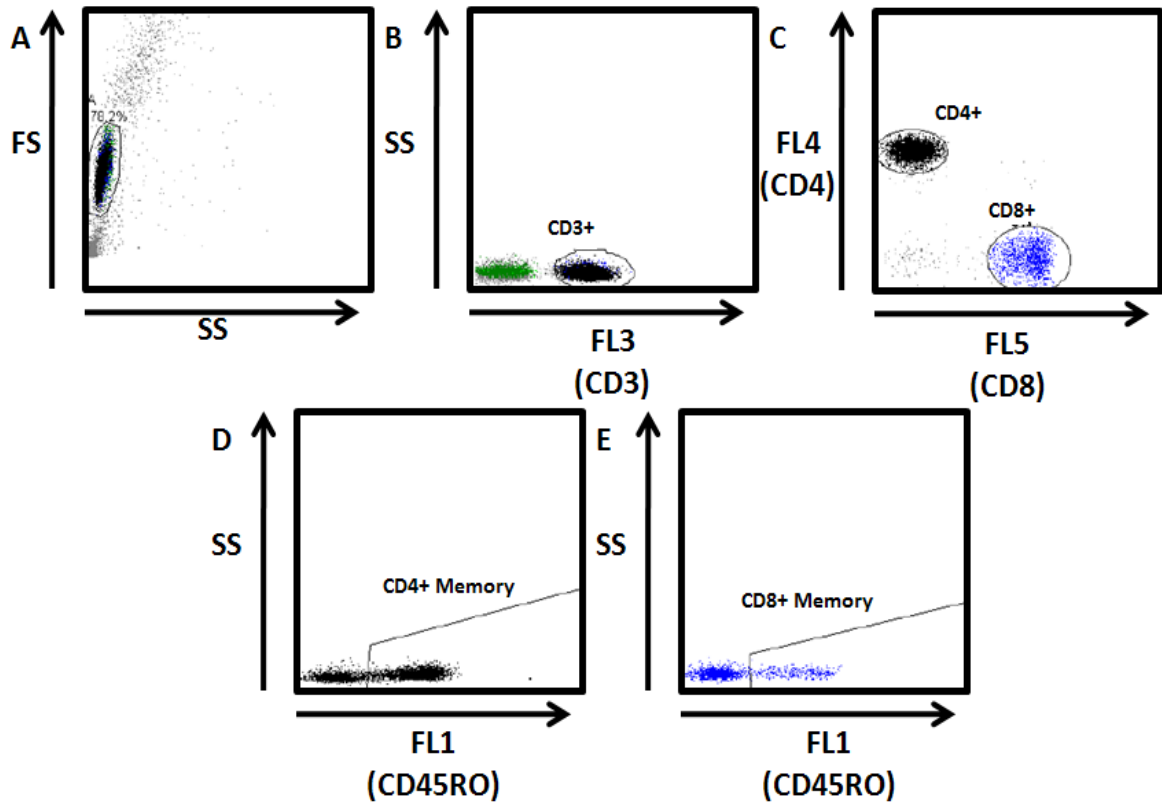


Figure 9: Model-gating strategy for characterizing CD4⁺ and CD8⁺ T-cells: (A) FS/SS dot plot indicating the lymphocyte population, within the 'A' gate.; (B) SS/CD3 dot plot, gated on the lymphocyte 'A' gate, indicating CD3⁺ lymphocytes; (C) CD4/CD8 dot plot, gated on the CD3⁺ lymphocytes identifying the CD3⁺CD4⁺ and CD3⁺CD8⁺ T-cell populations. CD4⁺ and CD8⁺ T-cell populations were then evaluated for the expression of CD45RO ((D) and (E), respectively).

Results indicated a significant difference in the CD4⁺/CD8⁺ T-cell mean ratios between the groups ($p=0.025$), with a significantly larger mean in the MM group compared to control group (mean values of 3.80 vs. 2.18, respectively; $p=0.012$). There was no significant difference between the MM and MPE groups (mean values of 3.80 vs. 2.97, respectively; $p=0.379$), while there was a trend for a higher mean ratio in the MPE group compared to control ($p=0.117$) (Figure 10A).

Within the T-cell subpopulation, the mean percentages of CD4⁺ and CD8⁺ cells expressing CD45RO memory marker were not significantly different between groups ($p=0.168$ for

CD4⁺ cells and p=0.491 for CD8⁺ cells). Nevertheless, the mean percentages of the total memory T-cells was found to be significantly different between the groups (p=0.049). Both implant groups showed a trend for higher percentages than the control group, with mean values of 52.73% and 50.03% for MM and MPE groups, respectively, compared to 41.55% for the control group, but post-hoc tests did not identify any significant difference (p=0.102 for MM vs. control, and p=0.097 for MPE vs. control) (Figure 10 Finally, results showed a significant difference in variances between the three groups (Levene test for all groups: p=0.005), with MM and MPE groups having a larger spread in the result distributions compared to the control group.

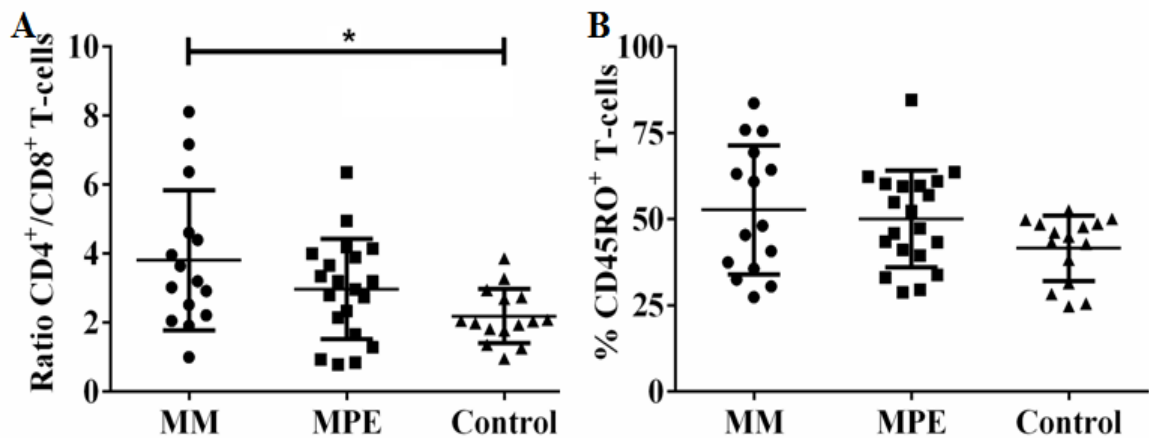


Figure 10: (A) Peripheral Blood T-cells phenotypes expressed as the ratio of the percentages of CD4⁺ over CD8⁺ T-cells. (B) Percentages of total T-cells expressing memory marker CD45RO. *Line connects groups found to be significantly different (p<0.05) by Games-Howell post-hoc test following one-way ANOVA with Welch's correction for unequal variance.

B-lymphocytes (CD19⁺) were then analyzed, where naive (CD27⁻) cells were differentiated from memory (CD27⁺) cells (Figure 12).

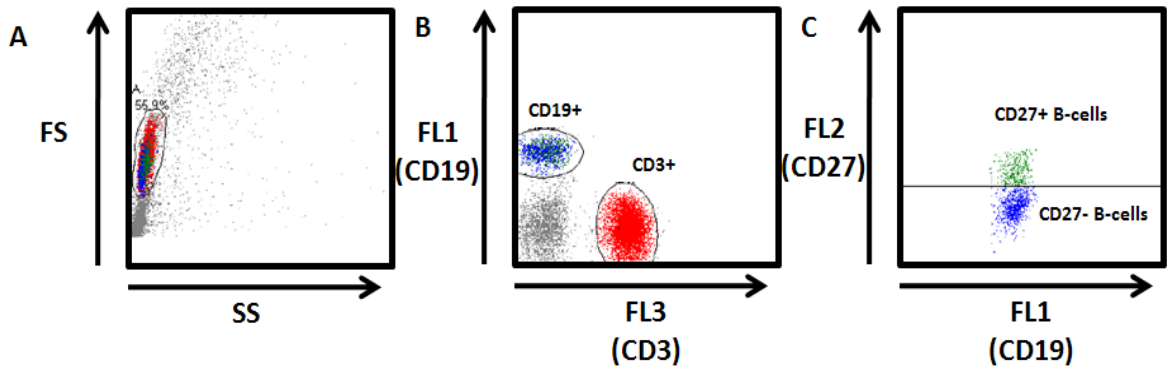


Figure 11: Model-gating strategy for the identification of naïve and memory B-cells. 'A' gated lymphocyte population (A) was analyzed to differentiate T-cells (CD3⁺) and B-cells (CD19⁺) (B), and B-cells were then identified as either CD27⁺ (naïve) or CD27⁺ (memory) (C).

Within the B-cell population, there was no significant difference in the mean percentages of memory cells (CD27⁺) between the groups ($p=0.292$) (Figure 12), with a mean percentage of 27.89% for the MM group compared to 21.77% and 27.47% for the MPE and control groups, respectively.

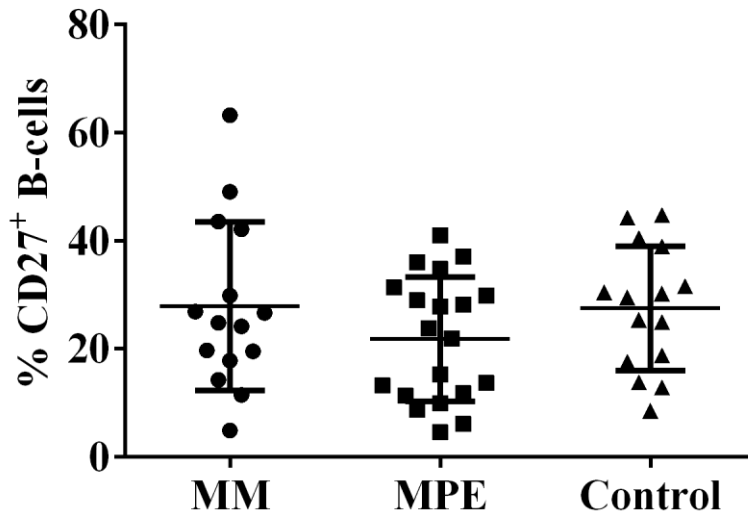


Figure 12: Percentages of memory B-cells.

3.1.3 T-cell Intracellular Cytokine Expression

Within the lymphocyte population, PMA/ionomycin stimulated T-cells ($CD3^+$) were gated as either $CD4^+$ (T-helper cells) or $CD4^-$ (representing primarily cytotoxic T-cells), which were then evaluated for intracellular cytokine expression of IFN- γ , IL-4 and IL-17 (Figure 13).

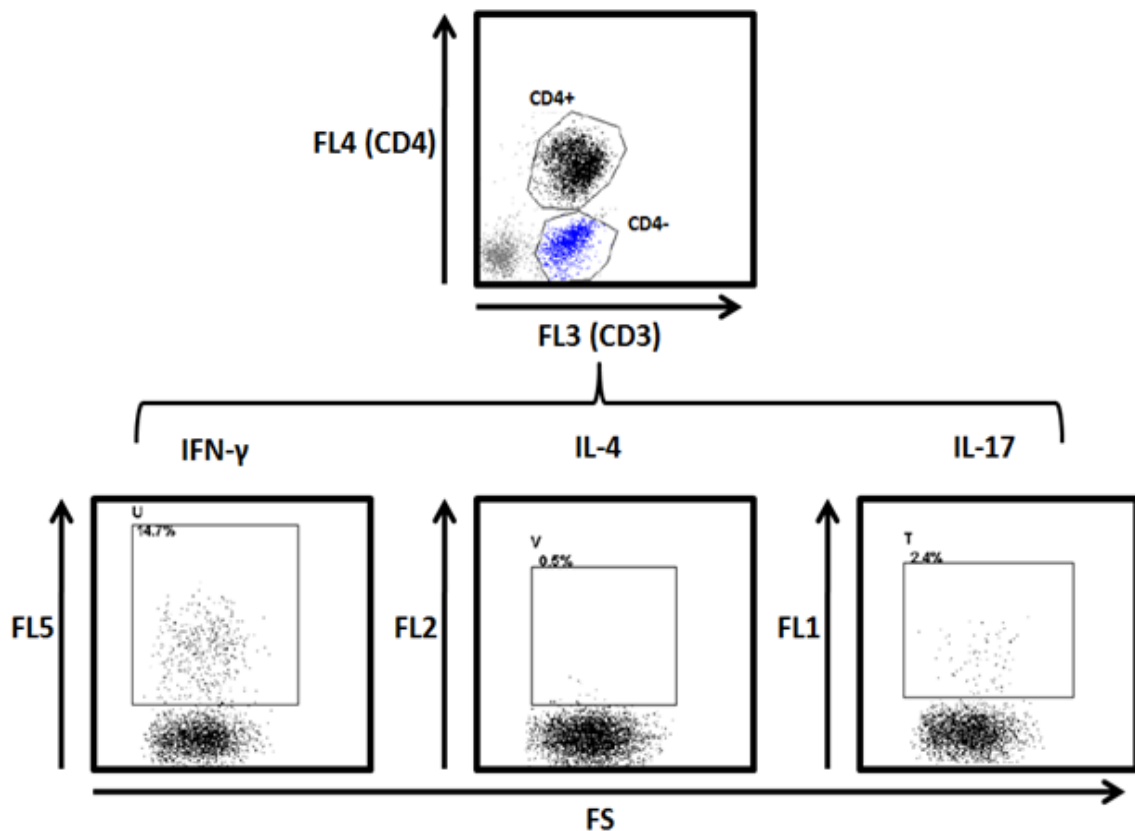


Figure 13: Model-gating strategy for the characterization of T-cell intracellular cytokine expression. The lymphocyte population was gated to identify $CD3^+CD4^+$ and $CD3^+CD4^-$ cells, which were then characterized for expression of IFN- γ , IL-4 and IL-17.

There was no significant difference between the groups for total T-cells ($CD3^+$ lymphocytes) expressing IFN- γ (data not shown). However, within the T-cell subpopulations, the mean percentages of $CD3^+CD4^-$ T-cells (representing primarily $CD8^+$ T-

cells) expressing IFN- γ were significantly different between the groups ($p=0.003$). A significantly higher mean percentage of IFN- γ producing CD8⁺ T-cells was observed in the MPE group when compared to the control group ($p=0.003$), with mean values of 57.03% and 37.91%, respectively. The MPE group also showed a trend for higher percentages than the MM group, but the difference was not statistically significant (mean percentages of 57.03% and 44.10%, respectively; $p=0.187$), and similar means were observed between the MM and control groups (Figure 14B).

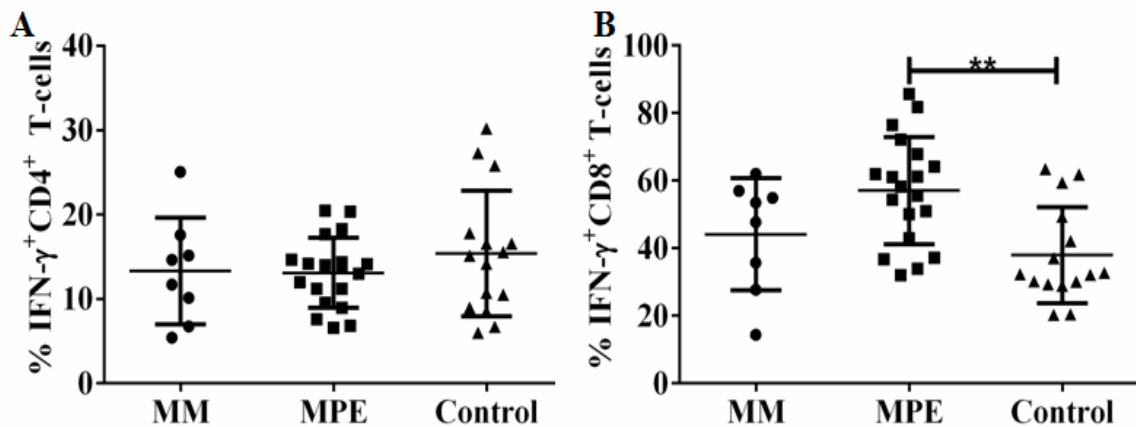


Figure 14: Percentages of T-cells expressing IFN- γ following PMA/ionomycin stimulation. (A) CD3⁺CD4⁺ (T_H) cells; and (B) CD3⁺CD4⁻ (considered to be primarily Tc) cells. Line connects groups found to be significantly different by Bonferroni's post-hoc test following one-way ANOVA (** $p < 0.01$).

Finally, the percentages of T-cells expressing IL-4 and IL-17 remained low in all groups with no significant difference between the groups (Table 6).

Table 6: Cytokine expression of peripheral blood CD3⁺CD4⁺ and CD3⁺CD4⁻ T-cells.

	% of cells expressing IL-4		% of cells expressing IL-17	
	CD3 ⁺ CD4 ⁺	CD3 ⁺ CD4 ⁻	CD3 ⁺ CD4 ⁺	CD3 ⁺ CD4 ⁻
MM				
Median	0.2	0.3	1.5	0.3
25th;75th percentile	0.1;0.2	0.1;0.6	1.3;1.5	0.2;0.3
MPE				
Median	0.1	0.2	0.9	0.3
25th;75th percentile	0.1;0.2	0.1;0.3	0.9;1.4	0.2;0.4
Control				
Median	0.2	0.2	1.1	0.4
25th;75th percentile	0.1;0.2	0.1;0.3	0.9;1.4	0.2;0.6

Results from the flow cytometric analysis of PBMC, following PMA/ionomycin stimulation, from patients with failed MM and MPE implants, or control subjects.

3.2 Synovial Fluid Lymphocytes

Results showed a significant difference between MM and MPE groups for the B-cells in synovial fluid (p=0.027), with higher percentages in the MM group when compared to MPE group (median values of 7.4% and 1.0%, respectively). No statistically significant differences were observed between MM and MPE groups for the other cell types (T-, NK-, and NKT-cells) (

Table 7). The T-cell population was the predominant lymphocyte population in the synovial fluid for both groups, with a majority of CD4⁺ T-cells. A trend for higher NK-cell percentages in the MM group was noticed but the difference between the two groups was not significantly different (p=0.142). Finally, both groups had high percentages of memory T-cells. Results were then compared with those from peripheral blood for each group, as detailed below (sections 3.2.1 and 3.2.2).

Table 7: Lymphocyte populations in synovial fluid of patients with failed MM and MPE implants.

	MM	MPE
% CD3⁺ (T-cells)		
Median	74.2	88.7
25%;75% percentiles	71.0;80.0	85.0;91.7
% CD3⁺ CD4⁺ T-cells		
Median	63.7	57.4
25%;75% percentiles	61.9;72.6	45.5;70.6
% CD3⁺ CD8⁺ T-cells		
Median	36.3	37.6
25%;75% percentiles	27.4;38.1	25.8;50.0
% CD19⁺ (B-cells)		
Median	7.4*	1.0*
25%;75% percentiles	5.4;8.3	0.9;1.2
% CD3⁺ CD56⁺ (NK-cells)		
Median	15.2	6.1
25%;75% percentiles	11.8;17.3	5.2;9.4
% CD3⁺ CD56⁺ (NKT-cells)		
Median	2.7	3.7
25%;75% percentiles	2.0;3.9	1.8;4.9
% CD4⁺ CD45RO⁺ (Memory CD4 T-cells)		
Median	87.4	90.3
25%;75% percentiles	70.0;93.0	84.0;92.1
% CD8⁺ CD45RO⁺ (Memory CD8 T-cells)		
Median	63.3	74.5
25%;75% percentiles	37;80.3	56.5;91.9
% CD19⁺ CD27⁺ (Memory B cells)		
Median	35.5	28.4
25%;75% percentiles	30.9;36.9	20.6;38.7

Mann-Whitney U-test: *p<0.05 when comparing MM versus MPE synovial fluid.

3.2.1 Synovial Fluid vs. Peripheral Blood Lymphocyte Subsets

MM group: There was a significant difference between synovial fluid and peripheral blood for the CD8⁺ T-cells (p=0.037) and B-cells (p=0.019), with more CD8⁺ T-cells and less B-cells in the synovial fluid (median values of 36.3% vs. 23.4% for CD8⁺ T-cells and 7.4% vs. 12.2% for B-cells). However, there was no significant difference for T-, NK- and NKT-cells (Table 8).

MPE group: There was a significant difference between synovial fluid and peripheral blood for the total CD3⁺ T-cells (p=0.002), B-cells (p=0.001) and NK-cells (p=0.047), with more T-cells but less B-cells and less NK-cells in the synovial fluid (median values of 88.7% vs. 71.7% for T-cells; 1.0% vs. 14.2% for B-cells; and 4.8% vs. 13.8% for NK-cells) (Table 7). There was, however, no significant difference between synovial fluid and peripheral blood for T-cell subsets (CD4⁺, CD8⁺ and NKT-cells) (Table 8).

Table 8: T-, B-, and NK-cell percentages in synovial fluid vs. peripheral blood of patients with failed MM and MPE implants.

	MM		MPE	
	Synovial Fluid	Blood	Synovial Fluid	Blood
% CD3⁺ (T-cells)				
Median	74.2	75.3	88.7***	71.7***
25%;75% percentiles	71.0;80.0	71.9;77.2	85.0;91.7	66.3;76.5
% CD3⁺ CD4⁺ T-cells				
Median	63.7	74.9	57.4	72.9
25%;75% percentiles	61.9;72.6	67.6;78.2	45.5;70.6	64.3;76.0
% CD3⁺ CD8⁺ T-cells				
Median	36.3*	23.4*	37.6	24.1
25%;75% percentiles	27.4;38.1	18.1;27.0	25.8;50.0	19.5;29.9
% CD19⁺ (B-cells)				
Median	7.4*	12.2*	1.0***	14.2***
25%;75% percentiles	5.4;8.3	9.5;15.6	0.9;1.2	11.1;15.16
% CD3⁺CD56⁺ (NK-cells)				
Median	15.2	11.3	6.1*	13.8*
25%;75% percentiles	11.8;17.3	10.0;12.7	5.2;9.4	9.2;16.3
% CD3⁺CD56⁺ (NKT-cells)				
Median	2.7	1.7	3.7	3.6
25%;75% percentiles	2.0;3.9	1.1;2.3	1.8;4.9	2.0;7.2

Mann-Whitney U-test: *p<0.05, *** p<0.001 when comparing synovial fluid versus peripheral blood within the same group (MM or MPE).

Overall, both MM and MPE groups exhibited a predominance of T-cells over B- and NK-cells in the synovial fluid and peripheral blood and lower proportions of B-cells in the synovial fluid than in peripheral blood. Finally, the NK-cell population was significantly

different between synovial fluid and peripheral blood of MPE patients, but not MM patients.

3.2.2 Synovial Fluid vs. Peripheral Blood Lymphocytes: T- and B-cell Phenotypes

MM group: There was a significant difference between synovial fluid and peripheral blood for the CD4⁺ memory T-cells (p=0.044), with higher percentages in the synovial fluid (median values of 87.4% vs. 49.7% respectively). There was a trend for higher proportions of CD8⁺ memory T-cells in the synovial fluid compared to the peripheral blood, but the difference was not significant (median values of 63.3% vs. 34.7%) (p=0.117 when comparing the two groups). There was also a significant difference between synovial fluid and blood for memory B-cells (p=0.044), with higher percentages in the synovial fluid (median values of 35.5% vs. 26.6%, respectively) (Table 9).

MPE group: There was a significant difference between synovial fluid and peripheral blood for both memory T-cell subsets (CD4⁺ and CD8⁺) (p=0.005 and p=0.018, respectively), with higher percentages observed in the synovial fluid. On the other hand, there was a trend for higher proportions of memory B-cells in the synovial fluid compared to the peripheral blood, but the difference was not significant (median values of 28.4% vs. 22.8%) (p=0.330 when comparing the two groups) (Table 9).

Overall, both MM and MPE groups presented with larger proportions of memory cells in the synovial fluid. The differences were statistically significant for memory T-helper and memory B- but not memory T-cytotoxic cells (trend only) for the MM group, while they

were significant for memory T-helper and memory T-cytotoxic but not memory B-cells (trend only) for the MPE group.

Table 9: Percentages of memory lymphocyte subsets in the synovial fluid and peripheral blood of patients with failed MM and MPE implants.

	MM		MPE	
	Synovial Fluid	Blood	Synovial Fluid	Blood
% CD4⁺CD45RO⁺ (Memory CD4)				
Median	87.4*	49.7*	90.3**	60.1**
25%;75% percentiles	70.0;93.0	44.1;69.8	84.0;92.1	52.2;65.6
% CD8⁺CD45RO⁺ (Memory CD8)				
Median	63.3	34.7	74.5*	39.1*
25%;75% percentiles	37;80.3	32.5;46.1	56.5;91.9	25.3;57.5
% CD19⁺CD27⁺ (Memory B cells)				
Median	35.5*	26.6*	28.4	22.8
25%;75% percentiles	30.9;36.9	19.5;39.1	20.6;38.7	11.8;29.6

Mann-Whitney U-test: *p<0.05, ** p<0.01 when comparing synovial fluid versus peripheral blood, within the same group (MM or MPE).

4 Discussion

Because of their higher wear resistance compared to conventional MPE implants, MM hip replacements have become more common, especially for younger and more active patients suffering from degenerative joint diseases. However, a recent increase in the number of early adverse tissue reactions in the periprosthetic environment has led to early failure in a subset of patients. Histological studies of early failed MM implants have shown, in some cases, features characteristic of a hypersensitivity reaction, suggesting a role of the adaptive immune system as either a cause or consequence of early failure [50,36]. Therefore, the present study aimed to identify potential differences in the adaptive immune system at the systemic level between patients with failed MM implants,

patients with failed MPE implants, and controls (volunteers with no implant). Specifically, the objectives of this study were to determine whether there are any changes in the proportion of memory lymphocytes and in the cytokine expression of T-cells in the patients with MM hip implants to identify potential lymphocyte subsets which may be involved in a hypersensitivity reaction.

4.1 Peripheral Blood Lymphocyte Subsets

Peripheral blood lymphocytes were analyzed to identify differences in the proportions of lymphocyte subsets, between MM, MPE revision patients and controls. No differences were found in the proportion of T-, B- and total NK-cells between groups. The proportion of NKT-cells was found to be significantly different between the three groups and a trend for higher percentages in the MPE group was noticed compared to MM group, but the post-hoc comparisons did not reveal any significant difference. Larger sample sizes and specific grouping based on causes of failure or other criteria will reveal if this trend becomes significant. A previous study reported higher proportions of total NK-cells (identified with CD16 as a surface marker) in patients at the time of revision surgery [89]. The present study did not identify total NK-cells using CD16 as a marker, but instead, CD56 (NCAM glycoprotein) was used to identify NK- and NKT-cells (in the absence or presence of CD3, respectively). The comparison of the two studies suggests that there may be a higher proportion of NKT-cells in peripheral blood of patients with failed MPE but not with failed MM implants. NKT-cells recognize lipid antigens, therefore this may suggest an interaction of polyethylene particles in MPE patients with endogenous lipids and/or

cognate receptors via hydrophobic effects causing NKT-cell recognition and expansion [93]. However, the present study did not examine NKT-cell activation or cell concentrations that would be required to confirm this potential interaction. Furthermore, the MM group sample size is small and remains to be increased to confirm the observed trend. Overall, there seems to be a difference in the NKT-cell population as a function of bearing type, but larger sample sizes and analysis of NKT-cell activity are required for further conclusions.

Peripheral blood lymphocytes were also analyzed for subsets of T- and B-cells. The ratio of CD4⁺ to CD8⁺ T-cells was significantly higher in the MM group when compared to the control group, while the MPE group was not found to be significantly different from either the MM or the control group. As previously discussed, these results corroborated with those of previous studies reporting an increase in the CD4⁺/CD8⁺ ratio in patients with orthopaedic implants [70–72]. Indeed, Hart *et al.* [72] specifically reported a weak CD8⁺ lymphopenia in the peripheral blood of patients with a metal articulation. The authors also showed a positive correlation between the extent of lymphopenia and the level of chromium and cobalt ions in peripheral blood. In the present study, absolute counts of lymphocytes were not measured and therefore, changes in the CD4⁺/CD8⁺ ratios in MM patients cannot be attributed with certainty to a decrease in circulating CD8⁺ T-cells. Nevertheless, the ratios indicate that there is a decreasing number of circulating CD8⁺ T-cells relative to CD4⁺ T-cells in failed MM patients.

It has been proposed that elevated metal ion levels may be the cause for the observed decreases in cytotoxic lymphocyte concentrations, as the number of circulating CD8⁺ T-cells has been shown to be inversely correlated to the blood concentrations of cobalt and chromium ions [72]. *In vitro* study has supported this hypothesis at concentrations between 10 to 100 μM for both chromium and cobalt ions [94]. However, blood ion concentrations generally do not reach such levels in MM patients. For example, Hart *et al.* reported median values of 1.7 and 2.3 ppb for cobalt and chromium, respectively, in patients with unilateral MM implants which correspond to less than 0.5 μM [72]. Thus, toxicity directly in the peripheral blood environment is likely not the cause of the observed decrease in lymphocyte numbers. On the other hand, much higher concentrations of metal ions have been reported in the synovial fluid than in the peripheral blood of patients with failed MM implants, with mean concentrations up to 33 and 120 μM for cobalt and chromium, respectively [34]. Thus, the decreased concentrations of circulating CD8⁺ T-cells in MM patients may be due to ion toxicity in the periprosthetic environment; however it would not explain the specificity to CD8⁺ T-cells.

A previous report has shown that MM patients exhibit elevated levels of circulating HLA-DR⁺CD8⁺ T-cells, which indicates activation of this T-cell subset [37]. Also, it has been shown that the T-cell population downregulates CD28 expression in MM patients, suggesting cell activation and prolonged exposure to antigen [65]. Thus, if CD8⁺ T-cells impart an effector role in an immune response to metal wear, then the chronic presentation of antigen and activation of the CD8⁺ T-cells may result in down-regulation of

their response and even cell death [95]. This could therefore provide an alternative explanation to the lower percentage of CD8⁺ cells in the MM group.

4.2 Naive and Memory Lymphocytes

In the presence of a cell-mediated hypersensitivity reaction, T- and/or B-cells develop into memory/effector cells in an antigen specific response. Therefore, since implant-related hypersensitivity reactions have been thought to be T-cell mediated, one of the objectives was to measure the proportion of memory lymphocytes to determine whether a specific subset of T- or B-cells were primed and activated in MM patients. In particular, the percentages of memory (and naïve) T-and B-cells were evaluated using CD45RO and CD27 cell surface markers, to determine whether there was an increase in the relative proportion of memory T-cells (CD45RO⁺) and memory B-cells (CD27⁺) in patients with failed MM implants.

A significant difference was observed in the total memory T-cell populations in peripheral blood between the three groups, but post-hoc tests did not identify specific group differences. Nevertheless, both MM and MPE groups showed larger spread in the result distributions and a trend for higher mean percentages when compared to the control group. This may indicate an increased T-cell activity in some patients with failed implants. While both implant groups exhibit a similar trend, it is unclear whether this trend is the consequence of similar causes in both implant groups. Although MPE patients primarily accumulate PE wear, they also have some potential for similar metal sensitivities due to implant components. Alternatively, because the control group mean age was much lower

than both MM and MPE patient groups (35 versus 55 and 66, respectively), the observed trend may be due to age-related changes in T-cell phenotype. Larger sample sizes and specific grouping based on causes of failure or other criteria will reveal if this trend becomes significant.

A recent study by Hallab et al. aimed to provide evidence of T-cell-mediated activation to implant component metals *in vitro* [62]. The study included patients with a history of metal allergy, patients with poorly performing MPE implants, and patients with well-performing MM implants. The authors reported that patients from all the three groups, who had a metal sensitivity reaction showed highly differential activation profiles of lymphocytes to the component metals. These included either T-cell-mediated-, B-cell-mediated-, or mixed T- and B-cell-mediated reactions to component metals. The present study differs in that early activation markers were not tested among patient groups after metal salt challenge but instead, the proportion of lymphocytes exhibiting memory phenotype were evaluated in patients with failed implants for both MM and MPE *ex vivo* for evidence of activation of the immune system *in vivo*. The current study did not identify a significantly higher mean percentage of memory T- and B-cells in MM patients. However, there was an increased memory T-cell percentage in some MM and MPE patients as well as an increased memory B-cell percentage in some MM patients, which support the conclusion drawn by Hallab *et al.* of a person-dependent association of the cell-mediated response to metal allergen.

4.3 T-Cell Intracellular Cytokine Profile

Further analysis of the T-cell subsets in peripheral blood included the expression of type 1 (IFN- γ) and type 2 (IL-4) T-cell cytokine profiles. IL-17 was also evaluated, which is a potent stimulator of bone resorption [84]. The relative proportion of T-cells expressing IL-4 and IL-17 remained low in all groups. However, the percentage of CD8⁺ T-cells expressing IFN- γ was significantly higher in the MPE group when compared to control group. This indicates a higher proportion of type 1 T-cells in the peripheral blood of failed MPE patients. On the other hand, there was no significant difference in the mean percentages between MM and both MPE and control groups. Results corroborated those of Granchi *et al.* who previously reported cytokine expression levels in supernatants of PBMCs isolated from patients with stable MM and MPE implants at 18-36 month follow-up and stimulated with phytohemagglutinin. The authors showed higher levels of IFN- γ expression in MPE patients when compared to control subjects [70]. Interestingly, this study was based on patients with stable implants whereas the present study included only patients with failed implants. This suggests that the increase in IFN- γ may be specific to MPE and particularly PE wear, but not the failure of the implants. With respects to MM group, there was no significant difference in the expression of IFN- γ compared to both MPE and control groups. This suggests once again, that the higher percentage of IFN- γ expressing-CD8⁺ T-cells is implant-type dependent.

The histological observations of lymphocytic aggregates in MM periprosthetic tissues [36,47,50] are consistent with the pathophysiology surrounding delayed-type

hypersensitivity reactions [96]. However, the exact nature of the lymphocytic reaction is still under debate. The lymphocytic infiltrates in MM periprosthetic tissues have been shown to be predominantly CD4⁺ T-cells suggesting a DTH response over types 1-3 hypersensitivity responses, which are largely mediated by B-cells. Nevertheless, it has become apparent that it is difficult to easily classify hypersensitivity responses. For example, atopic dermatitis (AD) has long been associated to type 1 hypersensitivity response, dominated by B-cell production of IgE and IgG [97]. However T-cells are now also considered an important factor in AD, where type 2 T-cell production of IL-4 has been implicated in the elicitation of the B-cell response by induction of B-cell IgE and IgG4 production [97]. Intracellular cytokine analysis has been previously used to evaluate the balance of IL-4-producing T-cells (type 2 T-cells) to IFN- γ and IL-2-producing T-cells (type 1 T-cells) in AD patients [98]. It was shown that a decrease of the type 1 response rather than an increase in type 2 response was occurring in these patients, indicating a dysregulation of the type 1/type 2 cytokine balance towards a type 2 response. In DTH responses, type 1 T-cells (producing IFN- γ) have been reported to play a key role [76,77]. However, the exact roles of CD4⁺ and CD8⁺ T-cells are still a subject of debate. While originally CD4⁺ T-cells were thought to be the primary type 1 effector T-cells in DTH, it has since been proposed that in contact hypersensitivity (CHS), the DTH reaction may be elicited by CD8⁺ T-cells rather than CD4⁺ T-cells, as demonstrated in a CD4⁺ T-cell knockout mouse model to contact allergens [99]. Both clinical and experimental studies have supported this hypothesis, indicating a role for CD4⁺ T-cell immunoregulation and CD8⁺ T-cell effector functions in response to model haptens [99,100].

The finding that the proportion of IFN- γ ⁺ T-cells in MM patients was not higher than either MPE or control subjects was not expected if a DTH reaction is predominant in these patients. MM patients do, however, present with CD8⁺ T-cell lymphopenia in peripheral blood [72]. Therefore, although the proportion of IFN- γ producing CD8⁺ T-cells did not differ significantly between MM and both MPE and control groups, the overall level of IFN- γ production by CD8⁺ cells in the MM group may be considerably lower. Nevertheless, this would need to be confirmed by quantitative analysis of CD8⁺ T-cell counts and IFN- γ production. Indeed, not all CD8⁺ effector T-cells produce and secrete cytokines following stimulation. Therefore, other roles for this subset in MM patients not evaluated in the current study, such as cytotoxic functions or immunoregulatory roles warrant further investigation.

The present study did not indicate a shift in cytokine expression in MM patients to support a type 1 effector function in CD8⁺ T-cells. However, the absence of significant changes in the cytokine expression in peripheral blood does not exclude the potential role of synovial T-cells in the local immune response around the implant, especially considering the T-cell infiltrates observed in histological studies of early MM failures [36,47,50].

4.4 Lymphocyte Phenotype and Circulation

Peripheral blood contains only about 2% of the total body lymphocyte population, whereas they may spend hours or days within lymph nodes [101,102]. Thus, a small change in lymphocyte trafficking through lymphoid organs or an inflamed tissue may not be easily observable in the proportions of lymphocyte subpopulations in the peripheral

blood. One possible reason for the absence of differences with regards to the T- B- and NK-cells in the peripheral blood of patients in the MM, MPE and control groups could therefore be the trafficking of hapten-specific T-cells through the periprosthetic tissues and lymphatics, thereby being inaccessible for analysis in the peripheral blood. Therefore, further investigation of synovial fluid may identify specific roles for the lymphocyte subsets and identify further differences between the groups. Comparisons of the synovial fluid between MM and MPE groups indicated significant differences between the two groups for the B-cells, with larger percentages in the MM group. Previous histological analyses have reported occasional B-cell infiltrates in the synovial tissues of MM patients [50]. Nevertheless, no other differences were observed between the synovial fluid lymphocyte populations in the two patient groups.

A previous case study has reported on the oligoclonality of synovial lymphocytes in a MM patient, indicating active T-cell response to a local antigen [67]. This case study proposed a predominant type 1 response by identifying IFN- γ in the periprosthetic tissues, but not IL-4, by RT-PCR. However, the authors did not identify whether CD4⁺ or CD8⁺ T-cells (or both) were the primary effector T-cells. Unfortunately, insufficient volumes of synovial fluid prevented the intracellular cytokine analysis in the majority of cases in the present study for comparison. Nevertheless, no significant differences were observed between MM and MPE groups with regards to the proportions of T-cell naive vs. memory. However, larger sample sizes are required to confirm these results.

The current study indicated that the predominant lymphocyte population in MM patient synovial fluid was CD4⁺ T-cells, which corroborates previous histological analysis of periprosthetic tissues [36]. However, similar result was found with the MPE patients, and therefore, it does not appear to be specific to a certain bearing type, at least in the synovial fluid. Interestingly, the CD8⁺ T-cell distribution data was found to be significantly different in the synovial fluid when compared to blood for MM patients (median: 36.3% and 23.4%, respectively). The overall higher percentages of CD8⁺ T-cells in synovial fluids could suggest selective recruitment of these cells in the periprosthetic tissues in MM patients. However, while not statistically significant, a similar trend was observed in the MPE group. When Hart *et al.* reported the inverse correlation of CD8⁺ T-cell counts and Co/Cr blood ion levels, they hypothesized that the reduced CD8⁺ T-cells in the peripheral blood of MM patients may be caused by metal-related diversion of the CD8⁺ T-cell population out of circulation [72]. The results of the present study also suggest altered trafficking of CD8⁺ T-cells in MM patients, which would corroborate Hart *et al.* hypothesis. Interestingly, however, similar trends (although not significant) were observed in MPE patients. This would suggest that this altered CD8⁺ T-cell trafficking may not be specific to metal wear and could also arise in the presence of polyethylene wear.

Unsurprisingly, in both MM and MPE failed implants, higher percentages of memory T-cells were observed in the synovial fluid when compared to peripheral blood. While only memory CD4⁺ (but not CD8⁺) T-cell distribution data was significantly different between the blood and synovial fluid of the MM group, the difference was significant for both memory CD4⁺ and CD8⁺ T-cells in the MPE group. The memory B-cell distribution data was

also found to be significantly different in the synovial fluid when compared to blood for MM patients, with higher percentages observed in the synovial fluid. However, while not statistically significant, a similar trend was observed in the MPE group. Interestingly, overall, less B-cells were detected in the synovial fluid compared to peripheral blood for both implant groups.

Larger sample sizes are still required to verify these trends and results, in particular the synovial fluids. Analysis of more synovial samples will also allow verifying the trend for higher proportions of NK-cells in the synovial fluid of MM patients compared to MPE patients (the difference between the two group was not significant).

5 Conclusions and Future Considerations

The current study has shown that the trend for higher NKT-cell proportions in peripheral blood from patients with failed hip implants may be a consequence of bearing type as it may only occur in MPE implants. In any case, larger sample sizes are required to reveal if this trend becomes significant. The lower proportion of CD8⁺ T-cells in peripheral blood of MM patients compared to control also supports previous studies reporting CD8⁺ T-cell lymphopenia in the circulation of patients with failed MM implants. The current study has also found that, despite the significant difference observed between the means of three groups, the proportion of memory T-cells in the peripheral blood of MM patients was not significantly different from either MPE or control groups. Interestingly, the variance (reflecting the spread of the populations) was significantly different between the three

groups. Furthermore, the T-cell cytokine expression analysis showed only a significant difference in IFN- γ producing CD8⁺ T-cells, with MPE patients exhibiting a significantly higher percentage than control subjects. Therefore, overall, the current study did not find evidence, through the evaluation of memory T-cells and cytokine expression, of a DTH response at the systemic level (peripheral blood). Limitations of this analysis includes the potential for subsets within the memory T-cell pool that were not evaluated as well as other mechanisms of T-cell function, such as CD8⁺ cytotoxicity and cross-talk with other cells. A number of reports have identified differences within the T-cell population in patients with failed MM implants, such as: (1) increased T-cell infiltrates in periprosthetic tissues [36]; (2) reduced CD8⁺ T-cell counts in peripheral blood [9]; (3) increased proportions of CD8⁺ T-cells expressing activation associated MHC class II receptor HLA-DR in peripheral blood [37]; and (4) type 1 cytokine signals from MM periprosthetic tissue lymphocytes [67], which suggest that T-cells are involved in the reactivity to MM implants. Therefore, results observed in the T-cell populations (i.e., memory and cytokine expression) would need to be confirmed with larger sample sizes. Further investigation into the pathology of MM related T-cell reactivity should also focus on the analysis of T-cells in synovial fluid and/or periprosthetic tissues in patients with failed MM implants. Similarly, while no differences in the percentages of peripheral blood total T-cells expressing IFN- γ were observed, the percentages of total T-cells expressing IL-4 and IL-17 expression remained low. An alternative analysis may include quantitation of their expression in synovial fluid, using, for example, ELISA.

Due to increasing reports on systemic changes of the CD8⁺ T-cell subset and the lack of difference in IFN- γ expression in the current study, further characterization may include the evaluation of CD8⁺ T-cell activation and subset phenotype, either by cellular markers or cytotoxic activity, which may be altered in MM patients, and therefore better understand their possible role in the pathology around failed MM implants. Levels of apoptosis may also be evaluated which could indicate whether synovial T-cells are predisposed to cell death, and may provide further explanation to MM-related CD8⁺ T-cell lymphopenia.

The presence of B-cells has been previously described as occasionally present within the periprosthetic tissues of failed MM patients, which has been a matter of debate for the proposed DTH reaction occurring in these patients [50]. Within the current study, results showed a significant difference between the synovial fluid of the MM patients compared to the MPE patients for the total B-cells (both naive and memory), with overall larger percentages in the MM patients. There was also a significant difference between the synovial fluid and the peripheral blood of the MM group for the memory B-cells (with overall larger percentages in the synovial fluid), while the difference was not statistically significant for the MPE group. Interestingly, both MM and MPE groups had less overall B-cells (both naive and memory) in synovial fluid than in peripheral blood. To further investigate the role of B-cells and whether they are part of the aetiology of MM failures caused by an adverse tissue reaction, the B-cell population may also be compared between patients with well-performing implants and those with failed implants. This may include *ex vivo* stimulation assays, through both T-cell-dependent and independent

models of B-cell stimulation, to analyze their secretion of IL-10, immunoglobulins, RANKL, and TNF- α in order to evaluate the activity of B-cells *in vivo*. Using isolated immunoglobulins from MM patients, potential MM-related antigens may be identified by performing 2-dimensional western blots of proteins isolated from periprosthetic tissues or synovial fluid.

The size of the patient groups was a limitation for the present study, especially for synovial fluid, as well as the age disparity between the implant groups and the control group for peripheral blood. Future studies may be able to better match the mean age of the control group with that of the implant groups. However, due to the differences in the demographics of MM and MPE patients (MM resurfacings are primarily implanted in younger male patients), it will likely not be possible to match the mean ages of these two groups. Finally, further research on the outcome of MM implants should also include the comparison of failed MM implant patients with patients with well-performing implants, which is currently ongoing in the lab. Such comparison will possibly identify whether the observed differences within the lymphocyte distributions are associated to the implant failure. Ultimately, with a better understanding of the mechanisms involved in the tissue reactions around failed MM implants, it may become possible to modulate the response in affected individuals and/or determine patient predisposition to early failure, therefore allowing for better patient selection for MM implants.

References

1. Canadian Institute for Health Information. *Hip and Knee Replacements in Canada - Canadian Joint Replacement Registry (CJRR) 2008-2009*. Ottawa, ON, Canada; 2009.
2. Shimmin A, Beaulé PE, Campbell P. Metal-on-metal hip resurfacing arthroplasty. *The Journal of bone and joint surgery. American volume*. 2008;90(3):637-54.
3. Brown SR, Davies WA, Deheer DH, Swanson AB. Long-Term Survival of McKee-Farrar Total Hip Prostheses. *Clinical Orthopaedics and Related Research*. 2002;(402):157-163.
4. Pramanik S, Agarwal AK, Rai KN. Chronology of Total Hip Joint Replacement and Materials Development. *Trends in Biomaterials & Artificial Organs*. 2005;19(1):15-26.
5. Semlitsch M, Willert HG. Clinical wear behaviour of ultra-high molecular weight polyethylene cups paired with metal and ceramic ball heads in comparison to metal-on-metal pairings of hip joint replacements. *Proceedings of the Institution of Mechanical Engineers. Part H, Journal of engineering in medicine*. 1997;211(1):73-88.
6. Catelas I, Campbell P a, Bobyn JD, Medley JB, Huk OL. Wear particles from metal-on-metal total hip replacements: effects of implant design and implantation time. *Proceedings of the Institution of Mechanical Engineers, Part H: Journal of Engineering in Medicine*. 2006;220(2):195-208.
7. Jantsch S, Schwiigerl W, Zenz P, Semlitsch M, Fertschak W. and Trauma Surgery Long-term results after implantation of Mc Kee-Farrar total hip prostheses *. *Archives of Orthopaedic and Trauma Surgery*. 1991;110:230-237.
8. Australian Orthopaedic Association. *National Joint Replacement Registry*. 2010. Available at: http://www.dmac.adelaide.edu.au/aoanjrr/documents/aoanjrrreport_2010.pdf.
9. Gallo J, Kaminek P, Ticha V. Particle disease: A comprehensive theory of periprosthetic osteolysis: A review. *Biomedical papers*. 2002;146(2):21-28.
10. Catelas I, Jacobs JJ. Biological Activity of Wear Particles. *AAOS Instructional Course Lectures*. 2010;59:3-16.
11. Hallab NJ, Jacobs JJ. Biologic effects of implant debris. *Bulletin of the NYU hospital for joint diseases*. 2009;67(2):182-8.
12. Holt G, Murnaghan C, Reilly J, Meek RMD. The biology of aseptic osteolysis. *Clinical orthopaedics and related research*. 2007;460(460):240-52.
13. Yasuda H, Shima N, Nakagawa N, et al. Osteoclast differentiation factor is a ligand for osteoprotegerin/osteoclastogenesis-inhibitory factor and is identical to TRANCE/RANKL. *Proceedings of the National Academy of Sciences of the United States of America*. 1998;95(7):3597-602.

14. Takayanagi H, Ogasawara K, Hida S. T-cell-mediated regulation of osteoclastogenesis by signalling cross-talk between RANKL and IFN-g. *Nature*. 2000;408:600-605.
15. Ingham E, Fisher J. Biological reactions to wear debris in total joint replacement. *Proceedings of the Institution of Mechanical Engineers. Part H, Journal of engineering in medicine*. 2000;214(1):21-37.
16. Kim KJ, Rubash HE, Wilson SC, D'Antonio J a, McClain EJ. A histologic and biochemical comparison of the interface tissues in cementless and cemented hip prostheses. *Clinical orthopaedics and related research*. 1993;(287):142-52.
17. Goodman SB. Wear particles, periprosthetic osteolysis and the immune system. *Biomaterials*. 2007;28(34):5044-8.
18. Kaufman AM, Alabre CI, Rubash HE, Shanbhag AS. Human macrophage response to UHMWPE, TiAlV, CoCr, and alumina particles: Analysis of multiple cytokines using protein arrays. 2007.
19. Chiba J, Rubash HE, Kim KJ, Iwaki Y. The characterization of cytokines in the interface tissue obtained from failed cementless total hip arthroplasty with and without femoral osteolysis. *Clinical orthopaedics and related research*. 1994;(300):304-12.
20. Ishiguro N, Ito T, Kurokouchi K, et al. mRNA expression of matrix metalloproteinases and tissue inhibitors of metalloproteinase in interface tissue around implants in loosening total hip arthroplasty. *Journal of biomedical materials research*. 1996;32(4):611-7.
21. Stea S, Visentin M, Granchi D, et al. Cytokines and osteolysis around total hip prostheses. *Cytokine*. 2000;12(10):1575-9.
22. Thomson A, Lotze M. *The Cytokine Handbook*. 4th ed. London: Elsevier Science; 2003.
23. Wei S, Kitaura H, Zhou P, Ross FP, Teitelbaum SL. IL-1 mediates TNF-induced osteoclastogenesis. *Journal of Clinical Investigation*. 2005;115(2).
24. Zwerina J, Hayer S, Tohidast-Akrad M, et al. Single and combined inhibition of tumor necrosis factor, interleukin-1, and RANKL pathways in tumor necrosis factor-induced arthritis: effects on synovial inflammation, bone erosion, and cartilage destruction. *Arthritis and rheumatism*. 2004;50(1):277-90.
25. Clohisy JC, Teitelbaum S, Chen S, Erdmann JM, Abu-Amer Y. Tumor necrosis factor-alpha mediates polymethylmethacrylate particle-induced NF-kappaB activation in osteoclast precursor cells. *Journal of orthopaedic research: official publication of the Orthopaedic Research Society*. 2002;20(2):174-81.
26. Childs LM, Goater JJ, O'Keefe RJ, Schwarz EM. Efficacy of etanercept for wear debris-induced osteolysis. *Journal of bone and mineral research: the official journal of the American Society for Bone and Mineral Research*. 2001;16(2):338-47.

27. Yang S-Y, Wu B, Mayton L, et al. Protective effects of IL-1Ra or vIL-10 gene transfer on a murine model of wear debris-induced osteolysis. *Gene therapy*. 2004;11(5):483-91.
28. Wilkinson JM, Hamer AJ, Stockley I, Eastell R. Polyethylene wear rate and osteolysis: critical threshold versus continuous dose-response relationship. *Journal of orthopaedic research: official publication of the Orthopaedic Research Society*. 2005;23(3):520-5.
29. Rieker CB, Scho R, Ko P. Development and Validation of a Second-Generation Metal-on-Metal Bearing Laboratory Studies and Analysis of Retrievals. *Orthopedics*. 2004;19(8):5-11.
30. Doorn PF, Campbell P a, Worrall J, et al. Metal wear particle characterization from metal on metal total hip replacements: transmission electron microscopy study of periprosthetic tissues and isolated particles. *Journal of biomedical materials research*. 1998;42(1):103-11.
31. Campbell P, Ma S, Yeom B, et al. Isolation of predominantly submicron-sized UHMWPE wear particles from periprosthetic tissues. *Journal of biomedical materials research*. 1995;29(1):127-31.
32. Visentin M, Stea S, Squarzoni S, et al. A new method for isolation of polyethylene wear debris from tissue and synovial fluid. *Biomaterials*. 2004;25(24):5531-7.
33. Urban RM, Jacobs JJ, Tomlinson MJ, et al. Dissemination of wear particles to the liver, spleen, and abdominal lymph nodes of patients with hip or knee replacement. *The Journal of bone and joint surgery. American volume*. 2000;82(4):457-76.
34. Davda K, Lali FV, Sampson B, Skinner JA, Hart A. An analysis of metal ions in the joint fluid of symptomatic patients with metal-on-metal hip replacements. *Journal of Bone and Joint Surgery (Br)*. 2011;93-B(6):738-745.
35. Savarino L, Granchi D, Ciapetti G, et al. Effects of metal ions on white blood cells of patients with failed total joint arthroplasties. *Journal of biomedical materials research*. 1999;47(4):543-50.
36. Pandit H, Vlychou M, Whitwell D, et al. Necrotic granulomatous pseudotumours in bilateral resurfacing hip arthroplasties: evidence for a type IV immune response. *Virchows Archiv: an international journal of pathology*. 2008;453(5):529-34.
37. Hailer NP, Blaheta R a, Dahlstrand H, Stark A. Elevation of circulating HLA DR+ CD8+ T-cells and correlation with chromium and cobalt concentrations 6 years after metal-on-metal hip arthroplasty. *Acta orthopaedica*. 2010;82(1):6-12.
38. Daniel J, Pynsent PB, McMinn DJW. Metal-on-metal resurfacing of the hip in patients under the age of 55 years with osteoarthritis. *The Journal of Bone and Joint Surgery*. 2004;86(2):177-184.
39. Long WT, Dorr LD, Gendelman V. An American Experience With Metal-on-Metal Total Hip Arthroplasties A 7-Year Follow-Up Study. *East*. 2004;19(8):29-34.
40. Delaunay C. Metal-on-metal bearings in cementless primary total hip arthroplasty. *The Journal of Arthroplasty*. 2004;19(8):35-40.

41. Park M-S, Chung W-C, Yoon S-J, Cho H-M, Kwon S-H. Eleven-year follow-up of second-generation metal-on-metal total hip arthroplasty. *Journal of orthopaedic surgery (Hong Kong)*. 2010;18(1):15-21.
42. Underwood R, Matthies A, Cann P, Skinner JA, Hart AJ. A comparison of explanted Articular Surface Replacement and Birmingham Hip Resurfacing components. *Journal of Bone & Joint Surgery (Br)*. 2011;93(9):1169-1177.
43. Catelas I, Petit A, Vali H, et al. Quantitative analysis of macrophage apoptosis vs. necrosis induced by cobalt and chromium ions in vitro. *Biomaterials*. 2005;26(15):2441-53.
44. Catelas I, Petit A, Zukor DJ, Antoniou J, Huk OL. TNF- α secretion and macrophage mortality induced by cobalt and chromium ions in vitro-Qualitative analysis of apoptosis. *Biomaterials*. 2003;24(3):383-391.
45. Fleury C, Petit A, Mwale F, et al. Effect of cobalt and chromium ions on human MG-63 osteoblasts in vitro: morphology, cytotoxicity, and oxidative stress. *Biomaterials*. 2006;27(18):3351-60.
46. Keegan GM, Learmonth ID, Case CP. Orthopaedic metals and their potential toxicity in the arthroplasty patient: A review of current knowledge and future strategies. *The Journal of bone and joint surgery. British volume*. 2007;89(5):567-73.
47. Davies AP, Willert HG, Campbell PA, Learmonth ID, Case CP. An unusual lymphocytic perivascular infiltration in tissues around contemporary metal-on-metal joint replacements. *The Journal of bone and joint surgery. American volume*. 2005;87(1):18-27.
48. Mahendra G, Pandit H, Kliskey K, et al. Necrotic and inflammatory changes in metal-on-metal resurfacing hip arthroplasties. *Acta orthopaedica*. 2009;80(6):653-9.
49. Willert HG, Buchhorn GH, Fayyazi A, Lohmann CH. Histopathological changes around metal/metal joints indicate delayed type hypersensitivity. Preliminary results of 14 cases. *Osteologie*. 2000;9(3):165-179.
50. Willert HG, Buchhorn GH, Fayyazi A, et al. Metal-on-metal bearings and hypersensitivity in patients with artificial hip joints. A clinical and histomorphological study. *Journal of Bone and Joint Surgery*. 2005;87(1):28-36.
51. Pandit H, Whitwell D, Gibbons CLM, et al. Pseudotumours associated with metal-on- metal hip resurfacings. *The Journal of Bone and Joint Surgery*. 2008;90(7):847-851.
52. Campbell P, Ebramzadeh E, Nelson S, et al. Histological features of pseudotumor-like tissues from metal-on-metal hips. *Clinical orthopaedics and related research*. 2010;468(9):2321-7.
53. Kwon Y-M, Ostlere SJ, McLardy-Smith P, et al. "Asymptomatic" Pseudotumors After Metal-on-Metal Hip Resurfacing Arthroplasty Prevalence and Metal Ion Study. *The Journal of arthroplasty*. 2011;26(4):511-518.

54. Langton DJ, Jameson SS, Joyce TJ, et al. Early failure of metal-on-metal bearings in hip resurfacing and large-diameter total hip replacement: A consequence of excess wear. *The Journal of bone and joint surgery. British volume*. 2010;92(1):38-46.
55. Thyssen JP, Linneberg A, Menné T, Johansen JD. The epidemiology of contact allergy in the general population--prevalence and main findings. *Contact dermatitis*. 2007;57(5):287-99.
56. Basketter DA, Briatico-Vangosa G, Kaestner W, Lally C, Bontinck WJ. Nickel cobalt and chromium in consumer products: a role in allergic contact dermatitis. *Contact Dermatitis*. 1993;28:15-25.
57. Hallab N, Anderson S, Caicedo M, et al. Immune responses correlate with serum-metal in metal-on-metal hip arthroplasty. *The Journal of Arthroplasty*. 2004;19(8):88-93.
58. Park Y-soo, Moon Y-wan, Lim S-jae, et al. Early Osteolysis Following Second-Generation Metal-on-Metal Hip Replacement. *J Bone Joint Surg Am*. 2005;87:1515-1521.
59. Hallab N, Merritt K, Jacobs J. Metal sensitivity in patients with orthopaedic implants: a prospective study. *Journal of Bone & Joint Surgery*. 2001;83-A(3):428-436.
60. Granchi D, Cenni E, Trisolino G, Giunti A, Baldini N. Sensitivity to implant materials in patients undergoing total hip replacement. *Journal of biomedical materials research. Part B, Applied biomaterials*. 2006;77(2):257-64.
61. Kwon Y-M, Thomas P, Summer B, et al. Lymphocyte proliferation responses in patients with pseudotumors following metal-on-metal hip resurfacing arthroplasty. *Journal of orthopaedic research: official publication of the Orthopaedic Research Society*. 2010;28(4):444-50.
62. Hallab NJ, Caicedo M, Epstein R, McAllister K, Jacobs JJ. In vitro reactivity to implant metals demonstrates a person-dependent association with both T-cell and B-cell activation. *Journal of biomedical materials research. Part A*. 2010;92(2):667-82.
63. Choi Y, Woo KM, Ko SH, et al. Osteoclastogenesis is enhanced by activated B cells but suppressed by activated CD8(+) T cells. *European journal of immunology*. 2001;31(7):2179-88.
64. Loh J, Fraser J. Metal-derivatized Major Histocompatibility Complex: Zeroing in on Contact Hypersensitivity. *Journal of Experimental Medicine*. 2003;197(5):549-552.
65. Whittingham-Jones PM, Dunstan E, Altaf H, et al. Immune responses in patients with metal-on-metal hip articulations: a long-term follow-up. *The Journal of arthroplasty*. 2008;23(8):1212-8.
66. Effros RB. Loss of CD28 expression on T lymphocytes: a marker of replicative senescence. *Developmental and comparative immunology*. 1997;21(6):471-8.
67. Thomas P, Summer B, Sander C a, et al. Intolerance of osteosynthesis material: evidence of dichromate contact allergy with concomitant oligoclonal T-cell infiltrate and TH1-type cytokine expression in the peri-implantar tissue. *Allergy*. 2000;55(10):969-72.

68. Issekutz TB, Chin GW, Hay JB. Lymphocyte traffic through chronic inflammatory lesions: differential migration versus differential retention. *Clinical and experimental immunology*. 1981;45(3):604-14.
69. Seabrook T, Au B, Dickstein J, et al. The traffic of resting lymphocytes through delayed hypersensitivity and chronic inflammatory lesions: a dynamic equilibrium. *Seminars in immunology*. 1999;11(2):115-23.
70. Granchi D, Savarino L, Ciapetti G, et al. Immunological changes in patients with primary osteoarthritis of the hip after total joint replacement. *The Journal of Bone and Joint Surgery*. 2003;85-B:758-764.
71. Hart AJ, Hester T, Sinclair K, et al. The association between metal ions from hip resurfacing and reduced T-cell counts. *Journal of Bone and Joint Surgery (Br)*. 2006;88(4):449-54.
72. Hart AJ, Skinner JA, Winship P, et al. Circulating levels of cobalt and chromium from metal-on-metal hip replacement are associated with CD8+ T-cell lymphopenia. *Journal of Bone and Joint Surgery (Br)*. 2009;91(6):835-42.
73. Vanchit J, Hock J, Short L, Glasebrook A, Galvin R. A Role for CD8+ T Lymphocytes in Osteoclast Differentiation in Vitro. *Endocrinology*. 1996;137(6):2457-2463.
74. Skapenko A, Schulze-Koops H. Analysis of Th1/Th2 T-cell subsets. *Methods in molecular medicine*. 2007;136(4):87-96.
75. Silvennoinen-Kassinen S, Ikäheimo I, Karvonen J, Kauppinen M, Kallioinen M. Mononuclear cell subsets in the nickel-allergic reaction in vitro and in vivo. *The Journal of allergy and clinical immunology*. 1992;89(4):794-800.
76. Probst P, Kuntzlin D, Fleischer B. Th2-Type Infiltrating T Cells in Nickel-Induced Contact Dermatitis. *Cellular Immunology*. 1995;165:134-140.
77. Sell S. Delayed Hypersensitivity. In: *Immunology, Immunopathology & Immunity*. 5th ed. Stamford, Connecticut, USA: Appleton & Lange; 1996:445-462.
78. Takayanagi H. Osteoimmunology and the effects of the immune system on bone. *Nature reviews. Rheumatology*. 2009;5(12):667-76.
79. Hallab NJ, Caicedo M, Finnegan A, Jacobs JJ. Th1 type lymphocyte reactivity to metals in patients with total hip arthroplasty. *Journal of orthopaedic surgery and research*. 2008;3:6.
80. Hercus B, Revell PA. Phenotypic characteristics of T lymphocytes in the interfacial tissue of aseptically loosened prosthetic joints. *Journal of materials science. Materials in medicine*. 2001;12(10-12):1063-7.

81. Hercus B, Saeed S, Revell P a. Expression profile of T cell associated molecules in the interfacial tissue of aseptically loosened prosthetic joints. *Journal of materials science. Materials in medicine*. 2002;13(12):1153-6.
82. Gao Y, Grassi F, Ryan MR, et al. IFN- γ stimulates osteoclast formation and bone loss in vivo via antigen-driven T cell activation. *Bone*. 2007;117(1).
83. Abu-Amer Y. IL-4 abrogates osteoclastogenesis through STAT6-dependent inhibition of NF- κ B. *The Journal of clinical investigation*. 2001;107(11):1375-85.
84. Kotake S, Udagawa N, Takahashi N, et al. IL-17 in synovial fluids from patients with rheumatoid arthritis is a potent stimulator of osteoclastogenesis. *The Journal of clinical investigation*. 1999;103(9):1345-52.
85. Raza K, Scheel-Toellner D, Lord JM, et al. The assessment of T-cell apoptosis in synovial fluid. *Methods in molecular medicine*. 2007;136(7):117-38.
86. National Laboratory for HIV Immunology. Canadian guidelines for flow cytometric immunophenotyping. *NLHI - Population and Public Health - Health Canada*. 2001:1-49.
87. Machura E, Mazur B, Pieniasek W, Karczewska K. Expression of naive/memory (CD45RA/CD45RO) markers by peripheral blood CD4+ and CD8 + T cells in children with asthma. *Archivum immunologiae et therapiae experimentalis*. 2008;56(1):55-62.
88. Zubler R. Naive and memory B-cells in T-cell dependent and T-independent responses. *Springer Semin Immun*. 2001;23:405-419.
89. Case CP, Langkamer VG, Lock RJ, et al. Changes in the proportions of peripheral blood lymphocytes in patients with worn implants. *Journal of Bone and Joint Surgery (Br)*. 2000;82(5):748-54.
90. Kusaba M, Honda J, Fukuda T, Oizumi K. Analysis of type 1 and type 2 T cells in synovial fluid and peripheral blood of patients with rheumatoid arthritis. *The Journal of Rheumatology*. 1998;2(8):1466-1471.
91. Pala P, Hussell T, Openshaw PJ. Flow cytometric measurement of intracellular cytokines. *Journal of immunological methods*. 2000;243(1-2):107-24.
92. McDonald JH. *Handbook of Biological Statistics*. Baltimore: Sparky House; 2008.
93. Mallevaly T, Clarke AJ, Scott-Browne JP, et al. A molecular basis for NKT cell recognition of CD1d-self-antigen. *Immunity*. 2011;34(3):315-26.
94. Akbar M, Brewer JM, Grant MH. Effect of chromium and cobalt ions on primary human lymphocytes in vitro. *Journal of immunotoxicology*. 2011;8(2):140-9.

95. Zhou S, Ou R, Huang L, Price GE, Moskophidis D. Differential Tissue-Specific Regulation of Antiviral CD8+ T-Cell Immune Responses during Chronic Viral Infection. *Journal of Virology*. 2004;78(7):3578-3599.
96. Coombs RRA, Gell PG. The Classification of Allergic Reactions Underlying Disease. In: *Clinical Aspects of Immunology*. Blackwell Science; 1963:317-337.
97. Spielberg HL. Fc Receptors for IgE and Interleukin-4 Induced IgE and IgG4 Secretion. *Journal of Investigative Dermatology*. 1990;94:49S-52S.
98. Jung T, Lack G, Schauer U, et al. Decreased frequency of interferon-gamma and interleukin-2-producing cells in patients with atopic diseases measured at the single cell level. *Journal of Allergy and Clinical Immunology*. 1995;96:515-527.
99. Bour H, Peyron E, Gaucherand M, et al. Major histocompatibility complex class I-restricted CD8+ T cells and class II-restricted CD4+ T cells, respectively, mediate and regulate contact sensitivity to dinitrofluorobenzene. *European journal of immunology*. 1995;25(11):3006-10.
100. Abe M, Kondo T, Xu H, Fairchild RL. Interferon-g inducible protein (IP-10) expression is mediated by CD8+ T cells and is regulated by CD4+ T cells during the elicitation of contact of hypersensitivity. *Journal of Investigative Dermatology*. 1996;107:360-366.
101. Rosenberg Y, Anderson A, Pabst R. HIV-induced decline in blood CD4/CD8 ratios: viral killing or altered lymphocyte trafficking? *Immunology Today*. 1998;19(1):10-17.
102. Halin C, Mora JR, Sumen C, von Andrian UH. In vivo imaging of lymphocyte trafficking. *Annual review of cell and developmental biology*. 2005;21:581-603.
103. Nistala K, Moncrieffe H, Newton KR, et al. Interleukin-17-producing T cells are enriched in the joints of children with arthritis, but have a reciprocal relationship to regulatory T cell numbers. *Arthritis and rheumatism*. 2008;58(3):875-87.

Appendix A: Patient Group Demographics

Table 10: Demographics of patient samples analysed.

Patient ID*	Age	Gender	Years <i>in Situ</i>	Bearing**	Implant Make	Blood Analysis*** (extracellular/intracellular)		Synovial Fluid Analysis** (extracellular/intracellular)		Criteria for exclusion from analysis
H26	58	M	4	MM/Res	ConservePlus	+				
H27	50	M	1	MM/Res	ConservePlus	+				
H28	47	M	0.25	MM/Res	ConservePlus	+				Fracture
H29	67	M	25	MPE	PCA cup	+				
H30	45	M	1	MM/Res	ConservePlus	+				
H31	48	M	1	MM/Res	ConservePlus	+				
H32	60	M	3	MM/Res	ConservePlus	+				
H33	79	M	4	MM/THR	ProfemurZ/ ConservePlus	+		+		
H34	55	F	2	MM/THR	ConservePlus	+				
H35	56	M	1.5	MM/Res	ConservePlus			+		
H36	40	F	10	MPE	Duraloc	+				Rheumatoid Arthritis
H37	41	M	3	MM/Res	ConservePlus	+		+		
H38	76	F	4	CC	AML/Duraloc	+				Insufficient CC cases
H39	59	F	4	MPE	Trident/Crossfire	+	+			
H40	47	F	4	MM/Res	ConservePlus					Post-operative
H42	52	M	4	CPE	SecurFit	+	+			Insufficient CPE cases
H43	63	M	8	MPE	Duraloc	+	+			
H44	65	M	1	MPE	Trident/Accolade	+	+			Infection
H45	52	F	3	MM/Res	ConservePlus	+	+	+		
H46	61	F	5	MPE	Unknown	+	+			
H47	74	F	3.5	MPE	SecurFit/Trident			+	+	
H48	40	M	1	MM/Res	ConservePlus	+	+			Post-operative
H49	66	M	21	MPE	PCA cup	+	+			
H50	49	M	2	MPE	Accolade	+	+			
H51	67	M	20	MPE	Unknown	+	+			
H53	79	M	10	MPE	Unknown	+	+	+	+	
H55	43	F	1	MM/Res	Corin/Cormet	+	+			
H56	55	F	18	CPE	Duraloc	+	+	+	+	Insufficient CPE cases

Table 10 (continued)

Patient ID*	Age	Gender	Years <i>in Situ</i>	Bearing**	Implant Make	Blood Analysis*** (extracellular/intracellular)		Synovial Fluid Analysis** (extracellular/intracellular)		Criteria for exclusion from analysis
H57	77	M	11	MPE	Zimmer	+	+			
H58	73	F	13	MPE	AML/Duraloc	+	+			
H60	52	M	2	MM/Res	ConservePlus	+	+			Exploratory
H61	78	F	11	MPE	AML	+	+			
H63	83	M	7	MPE	SecurFit	+	+			
H64	44	M	3	MPE	Unknown	+	+	+		
H67	54	M	3	MM/Res	ConservePlus	+	+			Exploratory
H68	48	F	2	MM/Res	ConservePlus	+	+			
H70	73	M	14	MPE	Duraloc	+	+	+		
H72	53	M	4	MM/Res	ConservePlus	+	+	+		
H73	44	F	25	MM/Res	Unknown	+	+		+	Rheumatoid Arthritis
H74	60	F	13	MPE	Unknown	+	+	+		
H76	80	M	15	MPE	AML/Endurance			+		
H78	72	M	2	MM/THR	Dynasty/Profemur	+	+	+		
H80	81	F	12	MPE	Zimmer	+	+			
H81	45	F	12	MPE	Unknown	+	+			
H82	77	M	4	MM/THR	Profemur/BFH	+	+			
H83	67	F	2	MM/THR	Profemur/BFH	+	+	+		
H84	50	M	3.5	MM/Res	ConservePlus	+	+			
H85	63	F	10	MPE	AML/Duraloc	+	+			
H86	72	F	19	MPE	PCA cup	+	+			
H87	70	F	18	MPE	Biomet	+	+			
HC1	29	M	0	None	-	+	+			
HC2	23	M	0	None	-	+	+			
HC3	40	F	0	None	-	+	+			
HC4	33	F	0	None	-	+	+			
HC5	45	F	0	None	-	+	+			
HC6	31	M	0	None	-	+	+			
HC7	29	F	0	None	-	+	+			
HC8	38	F	0	None	-	+	+			

Table 10 (continued)

Patient ID*	Age	Gender	Years <i>in Situ</i>	Bearing**	Implant Make	Blood Analysis*** (extracellular/intracellular)		Synovial Fluid Analysis** (extracellular/intracellular)		Criteria for exclusion from analysis
HC9	29	F	0	None	-	+	+			
HC10	42	M	0	None	-	+	+			
HC11	20	M	0	None	-	+	+			
HC12	21	F	0	None	-	+	+			
HC13	39	M	0	None	-	+	+			
HC14	86	M	0	None	-	+	+			
HC15	28	M	0	None	-	+	+			

* Patient ID's are labelled with the 'H' prefix, while healthy control volunteers were denoted by the 'HC' prefix.

** Bearing types are differentiated as metal-on-metal resurfacing (MM/Res) or total hip replacement (MM/THR), Metal-on-polyethylene (MPE), ceramic-on-ceramic (CC) and ceramic-on-polyethylene (CPE).

*** Indicating whether sample (blood and/or synovial fluid) analyses were performed for the extracellular and/or intracellular panels of flow cytometry tests.

Appendix B: Flow Cytometry Acquisition Protocols

Acquisition protocols were setup as laid out in section 2.4. The acquisition detector settings were optimized for both peripheral blood and synovial fluid (Table 11). Each fluorochrome detector settings were optimized for identification of the positive and negative populations. The detector settings for each antibody were tested. However the optimized voltages remained the same for antibodies with the same conjugated fluorochrome.

Table 11: Detector settings for Flow cytometry analysis of peripheral blood and synovial fluid lymphocyte subpopulations.

Detector Channel	Blood (extracellular)		Synovial Fluid (extracellular)		Blood (intracellular)		Synovial Fluid (intracellular)	
	Volts	Gain	Volts	Gain	Volts	Gain	Volts	Gain
FS	552	5	552	5	552	7.5	552	7.5
SS	182	20	646	20	182	20	646	20
FL1	380	N/A	400	1	460	1	436	1
FL2	362	N/A	380	N/A	340	N/A	345	N/A
FL3	413	N/A	470	N/A	390	N/A	390	N/A
FL4	400	N/A	450	N/A	410	N/A	385	N/A
FL5	440	N/A	540	N/A	460	N/A	470	N/A

For the optimization of antibody concentrations, singly stained cell suspensions were acquired over a dilution series, starting at 2 times the concentration recommended by the manufacturer. For example, the Becton Dickinson anti-human CD3-PE-Texas-Red conjugate, the antibody was titrated over 6 concentrations. For each antibody concentration, the mean fluorescence and separation of the positive and negative population's cells were evaluated for optimal antibody concentrations (Figure 15). The

optimal concentrations of antibodies were determined qualitatively, based on the separation of the positive and negative populations at the lowest possible concentration of antibody. In the example illustrated below (Figure 15), it was determined that a concentration of 0.0625µg/test was sufficient for staining of the CD3⁺ lymphocyte population.

The optimum concentration for each antibody, under both extracellular and combination of extra- and intracellular staining, are laid out in section 2.4.2 (Table 3). For example, the concentration of anti-CD3 required for extracellular staining of 500,000 cells, to be followed by fixation and intracellular staining, was found to be 0.125 µg/test versus 0.0625 µg/test for extracellular only.

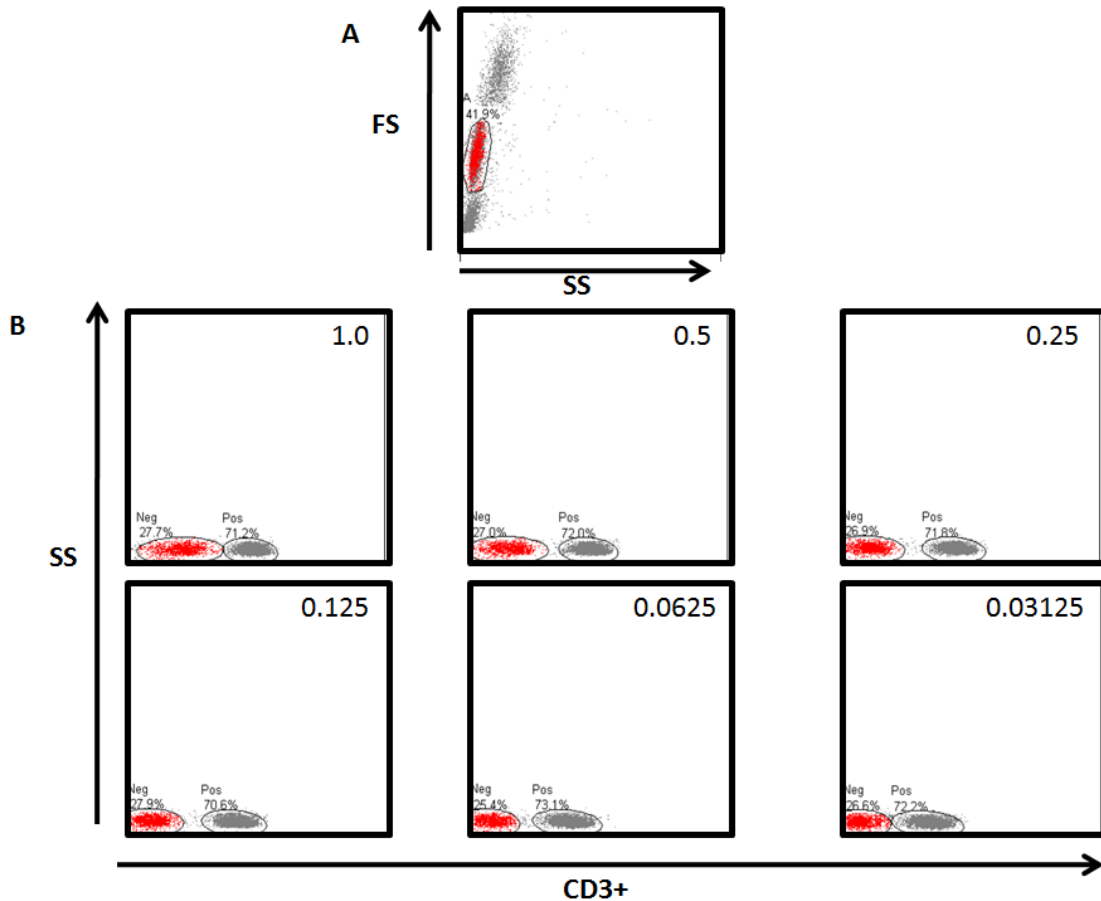


Figure 15: Acquisition data from the titration of anti-CD3-PE-Texas Red. (A) Representative FS/SS indicating the lymphocyte "A" gated population; (B) Dot plots of the SS/FL3 detectors gated on the lymphocyte population only ("A" gate). Insets indicate antibody concentration ($\mu\text{g}/\text{test}$).

Compensation, of spectral overlap, was then performed to ensure single-colour antibody detection in each of the five detectors, as laid out in section 2.4. The final compensation matrices were determined for both extracellular and combination extra/intracellular staining of peripheral blood and synovial lymphocytes (Figure 16). Figure 17-20 depict the single colour controls for peripheral blood and synovial fluid following the final setup of the compensation matrix. These single colour controls were run as controls for each experiment prior to acquisition of test samples. In each case, no overlap of antibody detection was observed between channels.

A

	FL1	FL2	FL3	FL4	FL5
FL1		1.2	3.3	2.4	1.3
FL2	20.2		14.2	3.5	5.9
FL3	5	35		2.2	1
FL4	1.6	12.5	50		1.5
FL5	1.5	1.1	6.1	25.7	

B

	FL1	FL2	FL3	FL4	FL5
FL1		16.2	13.5	7.4	1.3
FL2	4.6		23.0	24.5	4.0
FL3	10.0	67.0		16.5	4.5
FL4	10.6	45.0	71.5		6.5
FL5	1.5	9.1	80.0	25.7	

C

	FL1	FL2	FL3	FL4	FL5
FL1		1.2	3.3	2.4	2.9
FL2	20.0		14.2	3.5	2.9
FL3	10.0	60.0		6	5
FL4	1.6	23.0	50		4.5
FL5	1.5	4.5	12.5	25.7	

D

	FL1	FL2	FL3	FL4	FL5
FL1		16.2	13.5	7.4	1.3
FL2	4.6		23.0	24.5	3.7
FL3	14.0	67.0		16.5	4.5
FL4	12.5	50.0	71.5		6.5
FL5	1.5	9.1	8.0	25.7	

Figure 16: Compensation matrices for five-colour flow cytometry of peripheral blood and synovial lymphocytes. Extracellular-only staining for (A) peripheral blood, and (B) synovial fluid lymphocytes. Combination of extra- and intra-cellular staining for cytokine expression in (C) peripheral blood, and (D) synovial fluid lymphocytes.

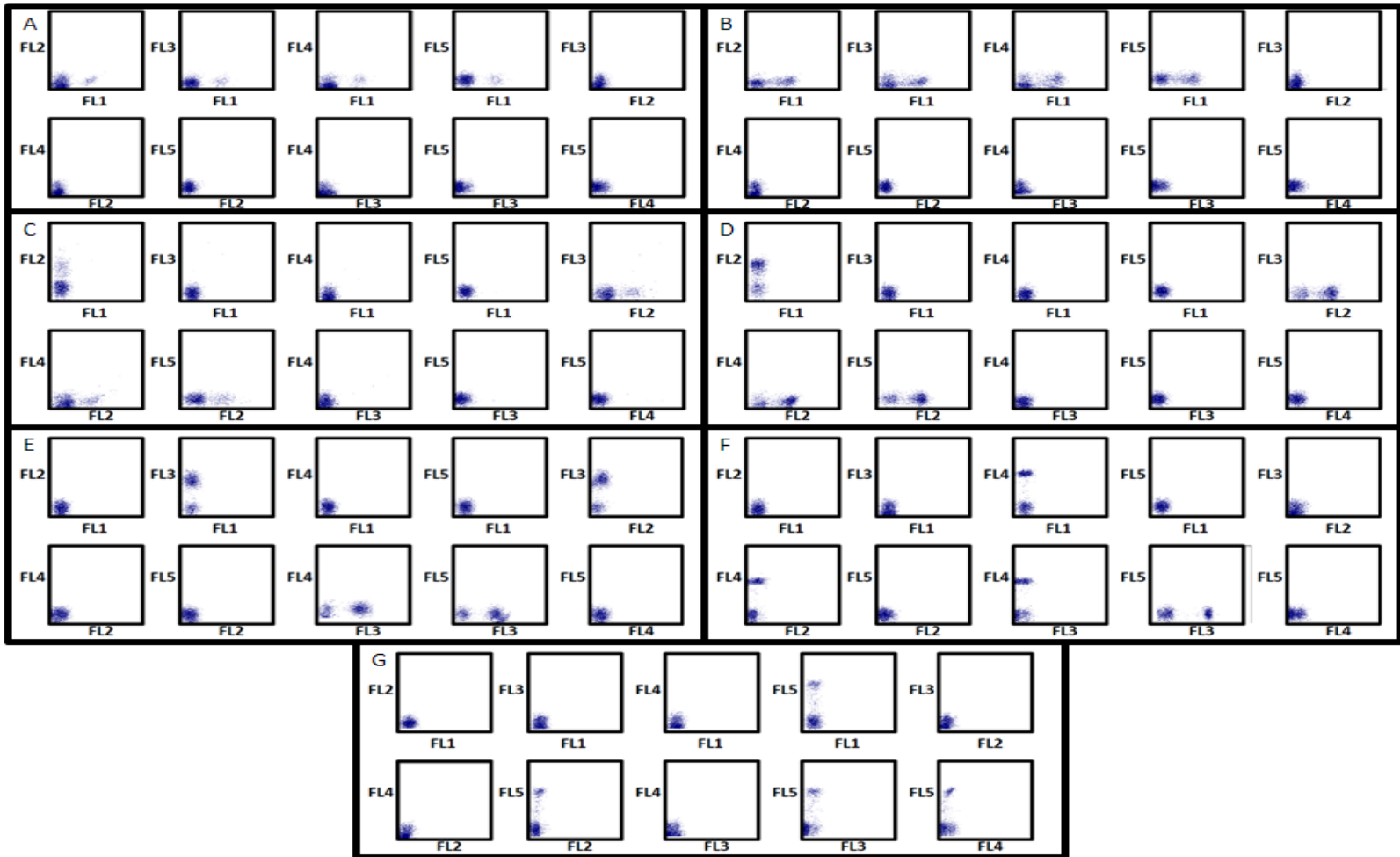


Figure 17: Single-colour antibody control dot-plots, for antibodies used in the extracellular panels for peripheral blood lymphocytes: (A) CD19; (B) CD45RO; (C) CD56; (D) CD27; (E) CD3; (F) CD4; and (G) CD8.

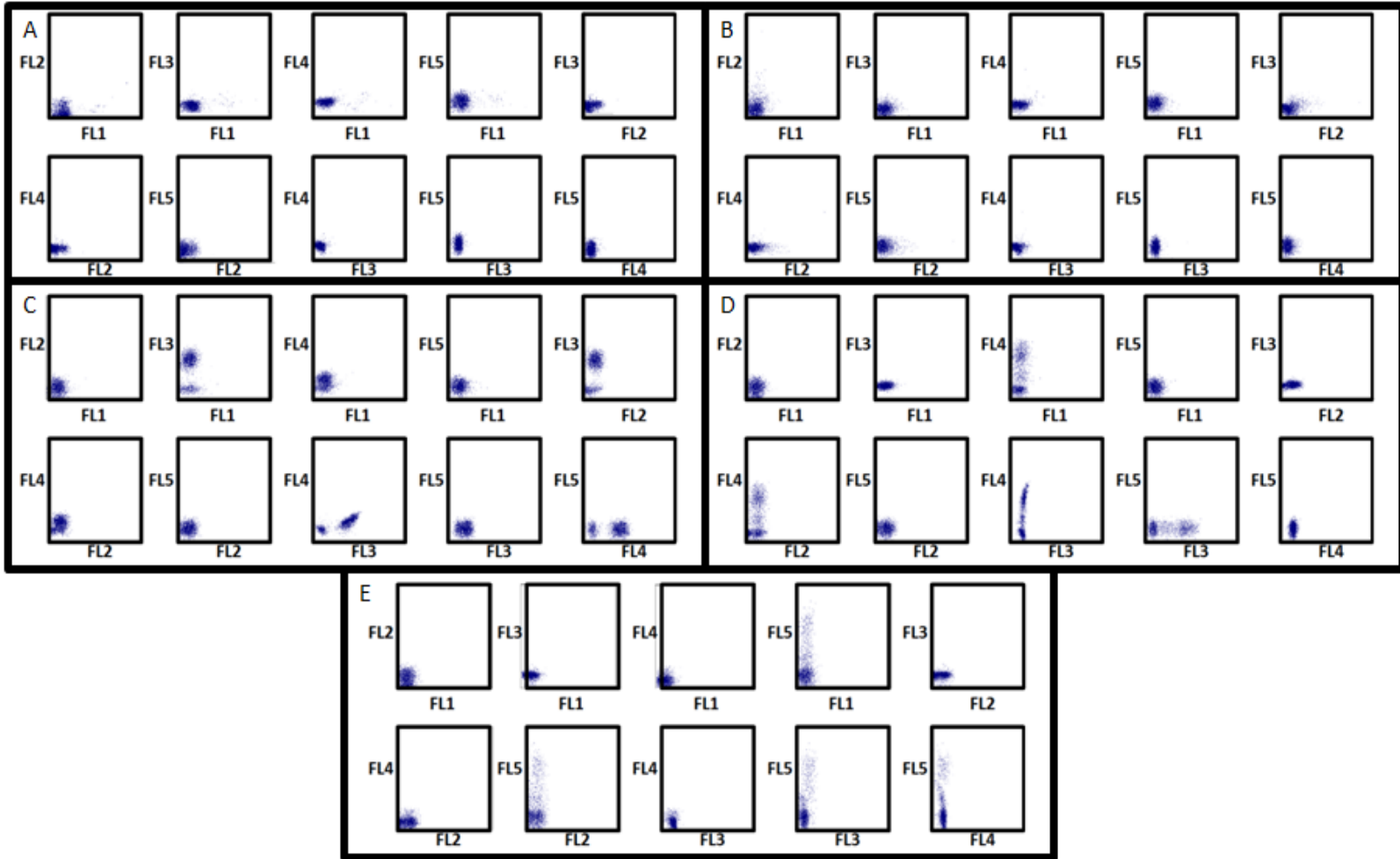


Figure 18: Single-colour antibody control dot-plots, used in the intracellular cytokine analysis panel for peripheral blood lymphocytes: (A) IL-17; (B) IL-4; (C) CD3; (D) CD4; and (E) IFN- γ .

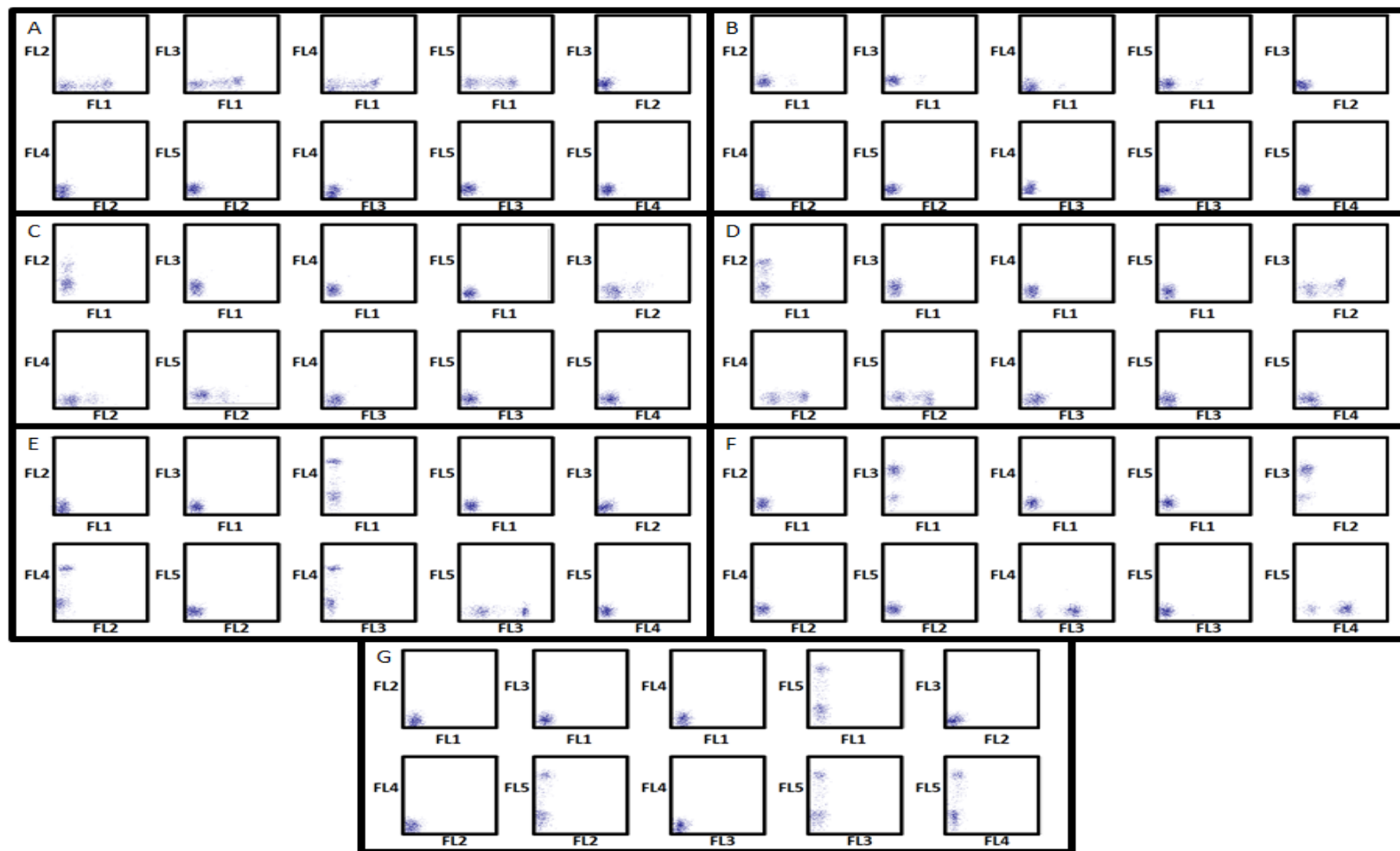


Figure 19: Single-colour antibody control dot-plots, for antibodies used in the extracellular panels for synovial fluid lymphocytes: (A) CD19; (B) CD45RO; (C) CD56; (D) CD27; (E) CD3; (F) CD4; and (G) CD8.

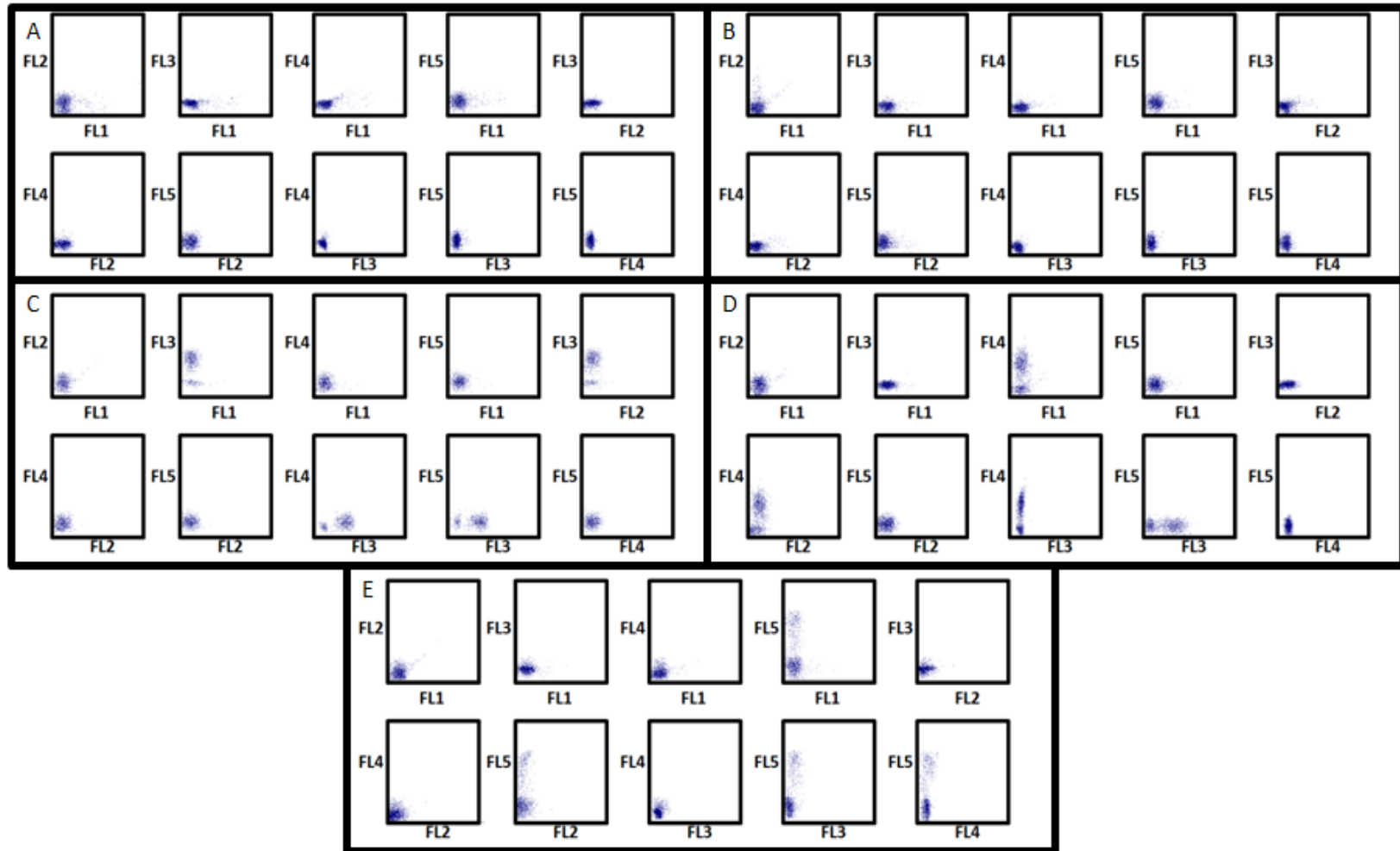


Figure 20: Single-colour antibody control dot-plots, used in the intracellular cytokine analysis panel for synovial fluid lymphocytes: (A) IL-17; (B) IL-4; (C) CD3; (D) CD4; and (E) IFN- γ .

Appendix C: Comparison of New Antibody Clones

Following June 15th, 2011, two new antibodies from Becton Dickson were used as alternatives to the original Beckman Coulter clones, for CD3 and CD19 (Table 3). Patients H80-87 and controls 14 and 15 were performed with these new antibodies. Initial experiments were performed to compare these new antibodies with the original ones using blood sample from patient H80. Firstly, following titration for the optimal concentrations of the new antibodies (as per Appendix B, single-colour controls were run. The negative and positive populations for the new antibodies were evaluated against the original antibodies (Figure 21-22). Results showed similar cell populations. There was slightly less visible separation of the positive and negative populations for CD3. However, this did not interfere with gating the populations (Figure 22). The positive and negative populations for both antibodies were within each other's standard deviations, at less than 1%. It was therefore concluded that there was no need to change the detector and compensation settings for the new antibodies.

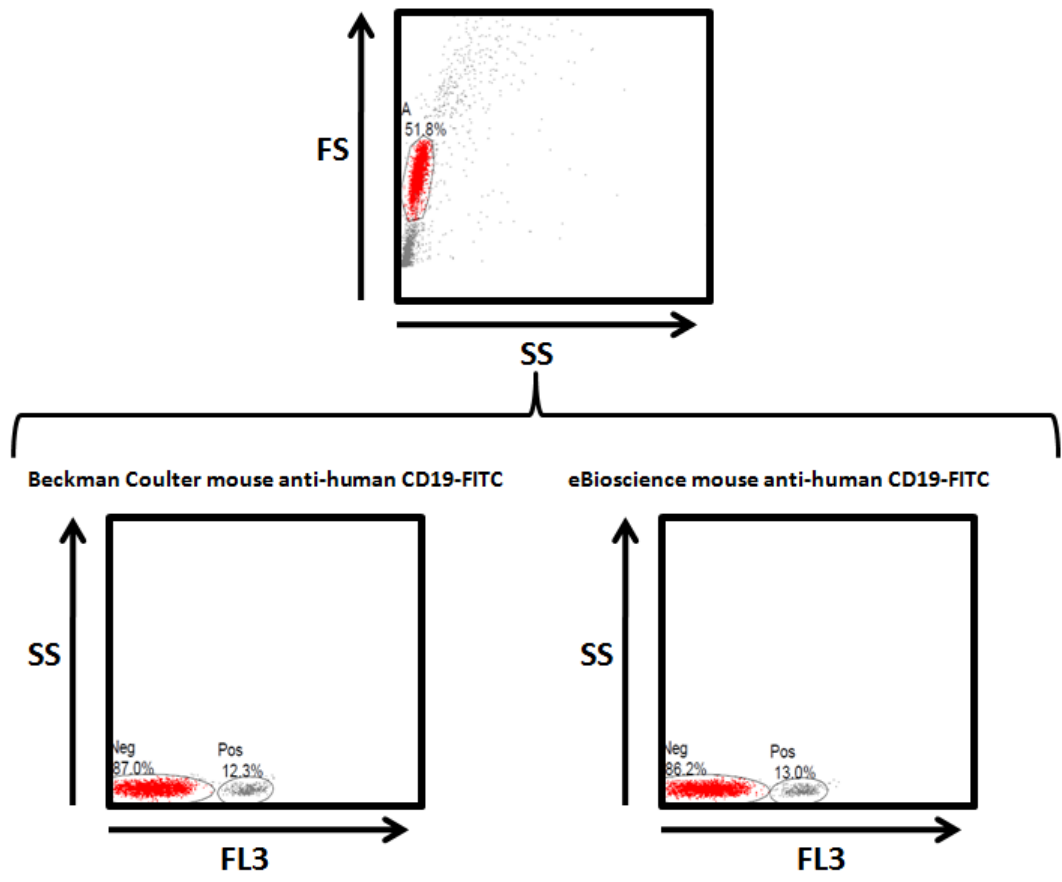


Figure 21: Evaluation of CD19 antibodies by single-colour extracellular staining.

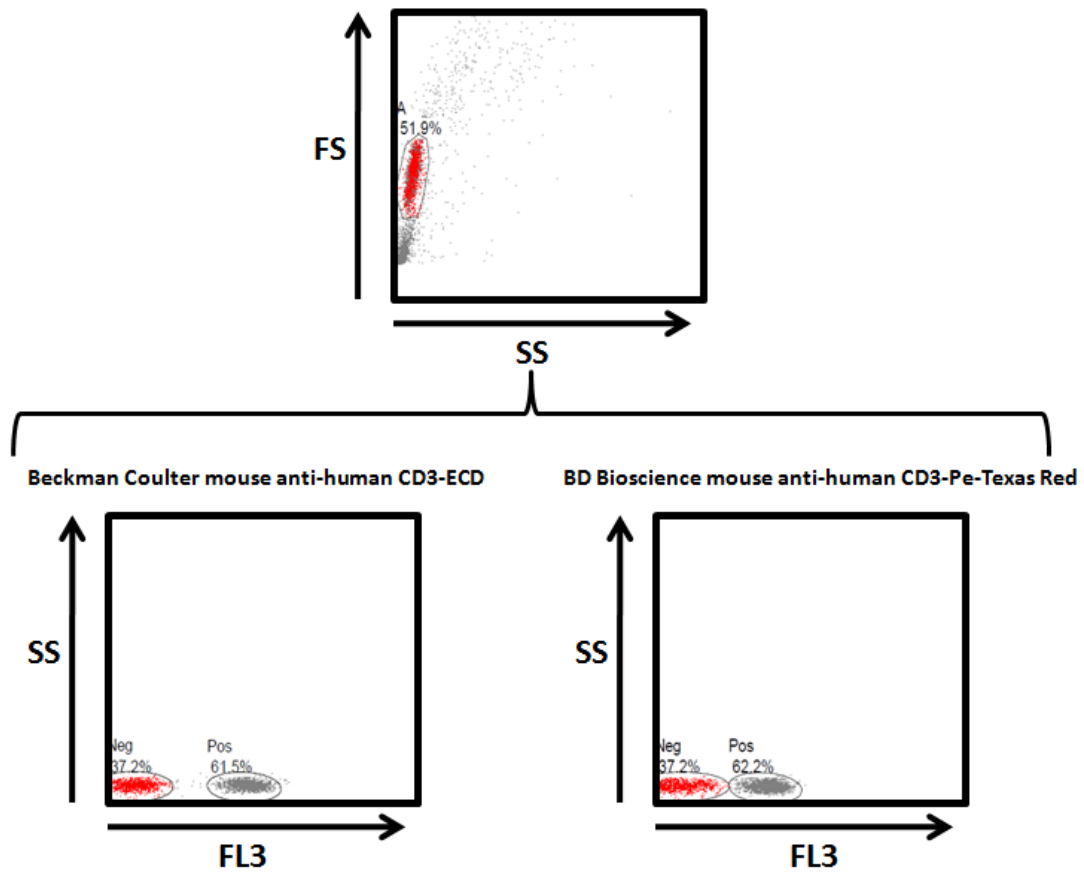


Figure 22: Evaluation of CD3 antibodies by single-colour extracellular staining.

Cell populations were then compared for the CD3 antibody, using the new vs. the original antibodies after cell fixation and permeabilization to simulate the conditions performed when analyzing intracellular cytokine staining (Figure 23). Once again, results showed similar cell populations when using the original and the new antibodies.

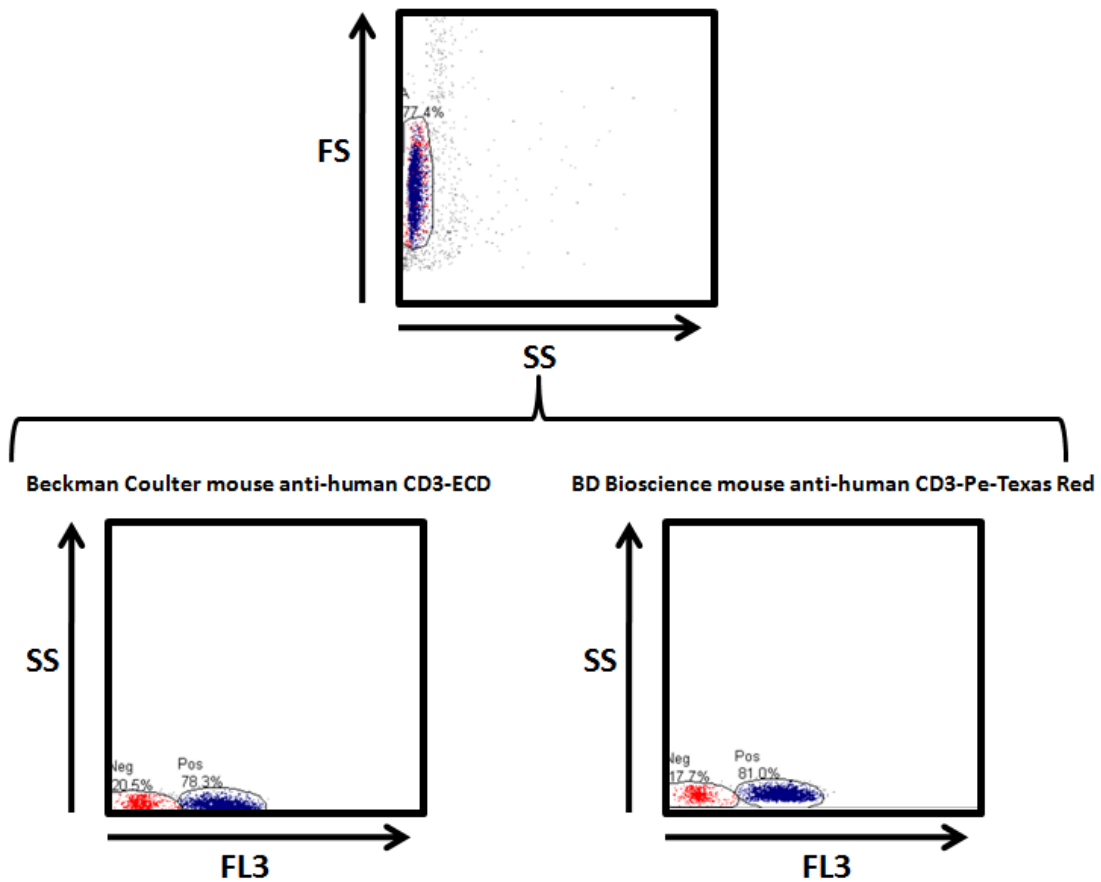


Figure 23: Evaluation of CD3 antibodies by single-colour extracellular staining of stimulated lymphocytes, followed by fixation and permeabilization.

Finally, each test panel (Table 4) was then evaluated using the new antibodies, run in parallel with the original antibodies as per the methods described in sections 2.4.2 and 2.4.3. The results from each test were compared by a Student's T-test which revealed no statistically significant differences, when varying the antibody clone (Table 12-15).

Table 12: T-cell phenotype analysis using the two alternative CD3 antibodies. Results are expressed as mean +/- STD.

Antibody*	% CD3⁺ (T-cells)	% CD3⁺CD4⁺ (T _h cells)	% CD3⁺CD8⁺ (T _c cells)	% CD45RO⁺ T_h cells (Memory)	% CD45RO⁺ T_c cells (Memory)
BC	61.44 _{+/-0.56}	73.14 _{+/-0.06}	23.58 _{+/-0.59}	65.03 _{+/-0.69}	22.83 _{+/-0.07}
BD	62.22 _{+/-0.86}	72.80 _{+/-1.21}	23.42 _{+/-0.48}	64.84 _{+/-0.04}	22.02 _{+/-0.88}

Table 13: B-cell phenotype analysis using the two alternative CD3 and CD19 antibodies. Results are expressed as mean +/- STD.

Antibody*	% CD3⁺ (T-cells)	% CD19⁺ (B-cells)	% CD19⁺CD27⁺ (Memory B-cells)
BC	61.10 _{+/-0.28}	12.75 _{+/-0.21}	29.34 _{+/-1.79}
BD/EB	60.17 _{+/-0.47}	13.10 _{+/-0.01}	30.74 _{+/-1.07}

Table 14: Lymphosum analysis using the two alternative CD3 and CD19 antibodies. Results are expressed as mean +/- STD.

Antibody*	% CD3⁺ (T-cells)	% CD19⁺ (B-cells)	% CD3⁻CD56⁺ (NK cells)	% CD3⁺CD56⁺ (NKT cells)
BC	60.86 _{+/-0.97}	12.54 _{+/-0.64}	19.31 _{+/-0.23}	1.34 _{+/-0.05}
BD/EB	61.14 _{+/-0.16}	12.68 _{+/-0.06}	18.95 _{+/-0.21}	1.45 _{+/-0.06}

Table 15: Intracellular cytokine expression analysis using the two alternative CD3 antibodies. Results are expressed as Mean +/- STD.

Antibody*	% CD3⁺CD4⁺ (T _h cells)	% CD3⁺CD4⁻ (T _c cells)	% CD3⁺CD4⁺ (T _h cells)		
			% IL-17	% IFN	% IL-4
BC	55.26 _{+/-1.05}	24.32 _{+/-0.40}	0.71 _{+/-0.03}	11.96 _{+/-0.40}	0.15 _{+/-0.05}
BD	56.66 _{+/-0.32}	23.18 _{+/-0.56}	0.71 _{+/-0.09}	12.21 _{+/-0.32}	0.24 _{+/-0.02}

* Beckman Coulter (BC) CD3 and CD19 were replaced with different clones from Becton Dickson (BD) and eBioscience (EB), respectively

Appendix D: T-Cell Cytokine Stimulation Protocol Development

Concentration of PMA for Stimulation

Intracellular cytokine expression was first optimized based on current protocols for T-cell cytokine expression profiling [91,90,103]. The optimum concentration of phorbol-12-myristate (PMA) to stimulate T-cells has been reported to be between 10-50 ng/mL [91]. To determine the optimum concentration for the present study, cells were stimulated as per section 2.4.2 with varying concentrations of PMA, from 0-50ng/mL, and the optimum concentration was determined by optimization of recoverable cells and maximum cytokine expression.

The number of recoverable cells, following 5.5 hour incubation in the presence of varying PMA concentrations, was enumerated under light microscopy with a Neubauer haemocytometer (Figure 24). Increasing concentrations of PMA resulted in lower recoverable cell numbers across the range of PMA concentrations. Increasing concentration of PMA up to 15 ng/mL significantly increased the expression of all cytokines. However, no differences were observed when increasing concentration above 15 and up to 50 ng/mL. There was a trend for higher cytokine expression at the highest PMA concentration (50 ng/mL) for all cytokines evaluated, but the difference was not statistically significant by one-way ANOVA (Figure 25). Based on these results, the optimum concentration of PMA for T-cell cytokine expression analysis was determined to be 15 ng/mL.

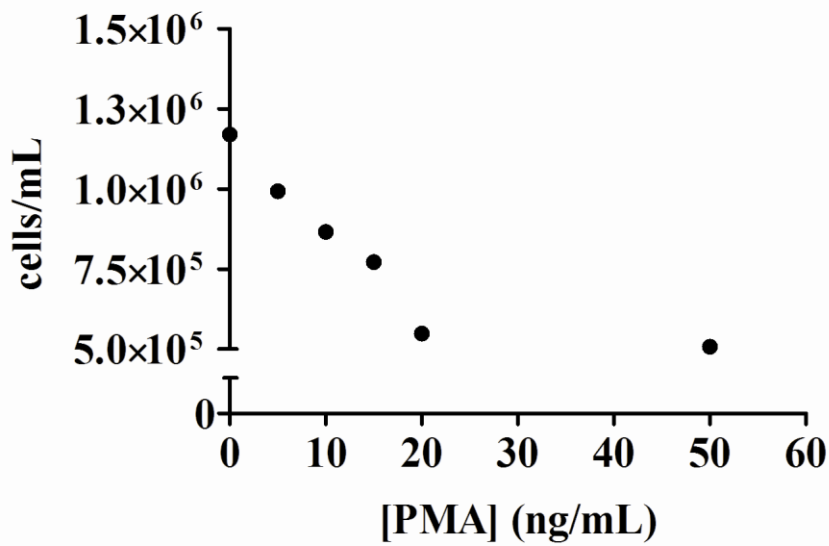


Figure 24: Recoverable cells following 5.5 hour incubation, in the presence of 1 μ M ionomycin, GolgiPlug and varying concentrations of PMA.

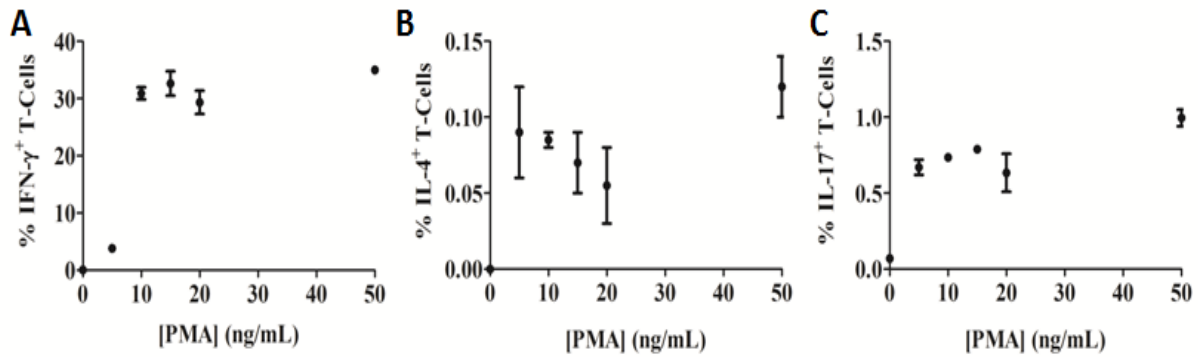


Figure 25: T-cell cytokine expression with varying concentrations of PMA. Graphs show percentages of cells expressing (A) IFN- γ ; (B) IL-4; and (C) IL-17.

Optimization of incubation time for cytokine stimulation

Incubation time was initially evaluated between 0 and 24 hours. Cells were stimulated as per section 2.4.4, for varying incubation periods (0, 3, 5.5, 9, and 24 hours). Maximum cytokine expression was found after 5.5 hours for IFN- γ , while there was no observable maximum for IL-4 (Figure 26A and D). IL-17 expression was maximum at the 24 hour time point (Figure 26E and F). However, the ability to identify CD4⁺ T-cells from CD4⁻ T-cells degraded at the 9 and 24 hour time points. Down-regulation of CD4 has been reported during extended stimulation with PMA, causing CD4⁺ T-cells to become indistinguishable from the CD4⁻ T-cell population [91]. Thus distinguishing the CD4⁺ and CD4⁻ T-cell subsets became unreliable at these two time points. In perspective, at the 24-hour time point, the number of events in the CD4⁺ gate had dropped drastically and represented less than 25% of the T-cell population, despite being 60% of the T-cell population in original sample. On the other hand, at all other time points, the percentage of CD4⁺ T-cells was maintained around 60%. Based on these results and considering that the incubation time for these cytokines has been previously reported to be between 4-6 hours, the time point chosen for the current study was 5.5 hours.

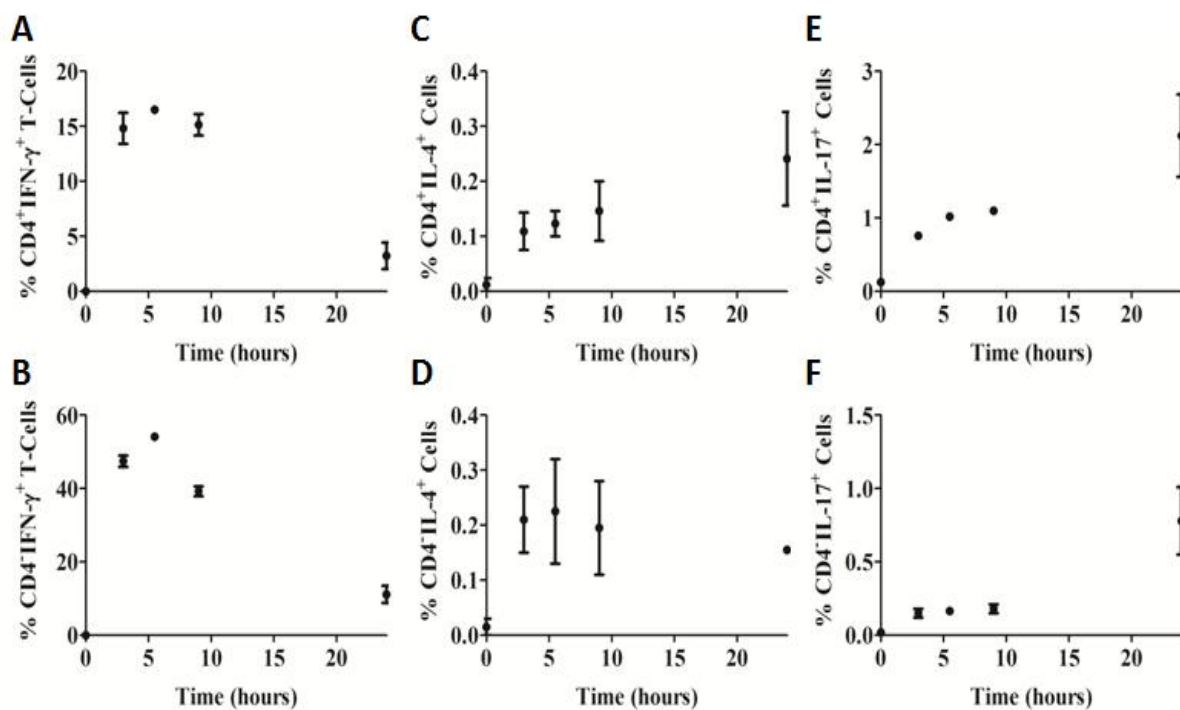


Figure 26: Cytokine expression of CD4⁺ and CD4⁻ (CD8) T-cells over a time course of 24 hours. Graphs show percentages of cells expressing (A-B) IFN- γ ; (C-D) IL-4; and (E-F) IL-17.

Appendix E: Raw Data collected from Flow Cytometry Analysis

The raw data from flow cytometry acquisition was processed to percentages from the total number of events in the appropriate gates for that cell type. Example calculations for the extracellular results are illustrated below (Table 16), followed by the mean results (Table 17).

Table 16: Example calculations for Extracellular lymphocyte phenotyping.

% CD4 and % CD8	CD4/CD8 ratio
Where, y = CD3 ⁺ CD4 ⁺ or CD3 ⁺ CD8 ⁺ T-cells	
$\% y = \frac{x \text{ events}}{CD3^+ \text{ events}}$	$CD4/CD8 \text{ ratio} = \frac{CD4^+ \text{ events}}{CD8^+ \text{ events}}$
% Memory T-cells	% Memory B-cells
Where, y = CD4 ⁺ or CD8 ⁺ T-cells	
$\% y \text{ memory T-cells} = \frac{y \text{ CD3}^+ \text{ CD45RO}^+ \text{ events}}{y \text{ CD3}^+ \text{ events}}$	$\% \text{ memory B-cells} = \frac{CD19^+ \text{ CD27}^+ \text{ events}}{CD19^+ \text{ events}}$
% T-cells, B, NK, and NKT-cells	
Where y = CD3 ⁺ CD56 ⁻ (T-) or CD19 ⁺ (B-), or CD3 ⁻ CD56 ⁺ (NK) or CD3 ⁺ CD56 ⁺ (NKT) cells.	
$\% y\text{-cells} = \frac{y \text{ events}}{(CD3^+ CD56^- \text{ events} + CD19^+ \text{ events} + CD3^- CD56^+ \text{ events} + CD3^+ CD56^+ \text{ events})}$	

Table 17: Extracellular phenotyping results.

Sample	Type	ID	% CD4	% CD8	CD4/CD8	% Memory CD4	% Memory CD8	% Memory T	% Memory B	% T-cells	% B-cells	% NK-cells	% NKT-cells
Blood	MM	26	88.93%	10.97%	8.11	77.00%	61.20%	75.61%	63.26%				
Blood	MM	27							49.10%				
Blood	MM	30	83.58%	13.12%	6.37	67.50%	34.68%	60.97%	42.15%				
Blood	MM	31	78.23%	16.97%	4.61	81.30%	34.00%	69.37%	24.17%				
Blood	MM	32	65.66%	34.33%	1.91	96.70%	62.20%	83.64%	14.26%				
Blood	MM	33	77.16%	19.49%	3.96	83.70%	44.28%	75.90%	29.83%				
Blood	MM	34	81.47%	18.50%	4.40	68.57%	46.08%	64.39%	4.92%				
Blood	MM	37	66.17%	30.05%	2.20	34.17%	33.09%	32.55%	26.92%				
Blood	MM	45	47.91%	48.02%	1.00	47.26%	30.91%	37.49%					
Blood	MM	55	76.87%	21.11%	3.64	37.15%	33.50%	35.63%	19.52%				
Blood	MM	68	73.43%	24.31%	3.02	46.61%	26.87%	40.76%	26.64%	79.61%	8.26%	12.12%	2.54%
Blood	MM	72	67.98%	27.01%	2.52	49.75%	42.99%	45.43%	43.56%	80.22%	10.10%	9.68%	1.13%
Blood	MM	78	85.62%	11.94%	7.17	46.39%	70.27%	48.11%	24.80%	69.59%	14.22%	24.50%	2.22%
Blood	MM	82	66.60%	32.49%	2.05	34.86%	22.48%	30.52%	17.84%	76.45%	8.93%	14.62%	3.83%
Blood	MM	83	74.91%	23.38%	3.20	32.20%	14.14%	27.42%	11.45%	69.62%	19.98%	10.40%	1.14%
Blood	MM	84	71.64%	24.51%	2.92	69.75%	53.86%	63.17%	19.72%	74.20%	19.60%	6.20%	1.13%
Blood	MPE	29	54.35%	42.39%	1.28	60.00%	16.30%	39.52%	36.00%				
Blood	MPE	39	41.67%	53.53%	0.78	52.20%	40.28%	43.31%	11.28%				
Blood	MPE	43	76.09%	19.56%	3.89	65.70%	48.30%	59.44%	8.73%				
Blood	MPE	46	82.61%	16.69%	4.95	41.75%	53.75%	43.46%	6.07%				
Blood	MPE	49	79.89%	19.25%	4.15	61.29%	58.73%	60.27%	27.87%				
Blood	MPE	50	68.89%	29.51%	2.33	53.37%	36.06%	47.40%	13.21%				
Blood	MPE	51	64.29%	30.06%	2.14	98.57%	70.70%	84.62%	4.53%				
Blood	MPE	53	45.87%	54.89%	0.84	51.40%	17.20%	33.02%	21.91%				

Table 17 (continued)

Sample	Type	ID	% CD4	% CD8	CD4/CD8	% Memory CD4	% Memory CD8	% Memory T	% Memory B	% T-cells	% NK-cells	% B-cells	% NKT-cells
Blood	MPE	57	72.09%	25.77%	2.8	65.92%	52.05%	60.93%	31.36%				
Blood	MPE	58	74.15%	17.70%	4.19	35.50%	18.24%	29.55%	23.82%	81.78%	15.28%	2.94%	9.97%
Blood	MPE	61	75.83%	22.61%	3.35	54.31%	60.68%	54.90%	15.30%	55.18%	15.16%	29.67%	9.87%
Blood	MPE	63	77.96%	19.49%	4	65.36%	30.89%	56.97%	37.10%	52.57%	20.21%	27.22%	1.33%
Blood	MPE	64	74.27%	23.26%	3.19	66.77%	60.22%	63.59%	13.66%	67.58%	12.20%	20.22%	2.05%
Blood	MPE	70	77.42%	21.23%	3.65	60.12%	61.99%	59.70%	34.81%	66.68%	8.11%	25.20%	5.37%
Blood	MPE	74	83.77%	13.18%	6.36	28.32%	38.00%	28.73%	29.84%	76.54%	9.64%	13.82%	0.86%
Blood	MPE	80	73.74%	24.95%	2.96	63.42%	22.19%	52.30%	28.95%	65.22%	14.23%	20.55%	1.81%
Blood	MPE	81	60.60%	36.75%	1.65	53.06%	25.27%	41.09%	41.03%	78.89%	9.41%	11.70%	3.67%
Blood	MPE	85	42.71%	46.06%	0.93	87.32%	18.59%	45.86%	28.22%	80.34%	11.64%	8.02%	16.86%
Blood	MPE	86	71.55%	26.23%	2.73	36.32%	29.96%	33.84%	11.80%	71.74%	14.98%	13.29%	3.48%
Blood	MPE	87	70.27%	22.01%	3.19	67.18%	68.40%	62.26%	9.96%	72.53%	17.26%	10.21%	7.84%
Synovial	MPE	47	76.82%	19.16%	4.01	82.04%	57.37%	74.02%	7.03%	87.20%	5.64%	0.91%	5.42%
Synovial	MPE	53	63.04%	33.84%	1.86	94.84%	47.37%	75.82%	59.20%	84.33%	10.32%	0.99%	4.36%
Synovial	MPE	64	73.09%	23.09%	3.17	92.51%	108.83%	92.75%	20.10%	92.19%	5.12%	1.23%	1.46%
Synovial	MPE	70	39.44%	52.93%	0.75	90.71%	91.63%	84.28%	40.05%	94.10%	3.63%	1.02%	1.24%
Synovial	MPE	74	43.42%	56.58%	0.77	89.90%	91.93%	91.05%	22.22%	90.26%	6.51%	0.23%	2.99%
Synovial	MPE	76	51.75%	41.31%	1.25	61.91%	56.25%	55.28%	34.57%	79.11%	13.19%	2.59%	5.12%
Synovial	MM	33	63.05%	36.95%	1.71	91.06%	73.45%	84.55%	25.00%				
Synovial	MM	35	77.16%	22.84%	3.38	98.91%	87.12%	96.22%	36.84%				
Synovial	MM	37	74.05%	25.95%	2.85	36.30%	26.89%	33.86%	29.00%				
Synovial	MM	45	60.75%	39.25%	1.55	87.40%	63.63%	78.07%	49.21%	75.87%	14.38%	8.31%	1.43%
Synovial	MM	72	63.70%	36.30%	1.75	82.13%	47.09%	69.41%	36.99%	92.21%	3.84%	1.79%	2.16%
Synovial	MM	78	54.11%	45.89%	1.18	94.88%	93.02%	94.03%	32.84%	66.38%	21.26%	6.62%	5.74%

Table 17 (continued)

Sample	Type	ID	% CD4	% CD8	CD4/CD8	% Memory CD4	% Memory CD8	% Memory T	% Memory B	% T-cells	% NK-cells	% B-cells	% NKT-cells
Synovial	MM	83	71.20%	28.80%	2.47	57.95%	20.47%	47.16%	35.54%	72.49%	16.01%	8.24%	3.26%
Blood	Control	1	54.18%	40.12%	1.35	56.44%	38.79%	46.14%	30.46%				
Blood	Control	2	61.87%	34.98%	1.77	34.15%	12.75%	25.59%	8.52%	78.41%	11.81%	9.78%	2.25%
Blood	Control	3	61.89%	30.35%	2.04	60.66%	40.70%	49.89%	31.56%	70.07%	21.74%	8.19%	0.50%
Blood	Control	5	64.14%	32.43%	1.98	59.04%	45.34%	52.57%	40.50%	74.55%	9.20%	16.25%	
Blood	Control	6	80.24%	20.81%	3.86	36.22%	25.70%	31.47%	29.48%	69.85%	12.85%	17.30%	1.08%
Blood	Control	7	45.23%	47.66%	0.95	64.73%	28.39%	42.81%	17.61%	72.89%	13.17%	13.94%	6.95%
Blood	Control	8	63.22%	32.76%	1.93	53.80%	44.78%	48.68%	44.27%	58.15%	18.43%	23.42%	4.55%
Blood	Control	9	71.05%	26.37%	2.69	30.55%	25.04%	28.31%	38.95%	73.31%	10.36%	16.33%	2.16%
Blood	Control	10	61.66%	34.11%	1.81	47.79%	25.95%	38.32%	44.76%	74.64%	9.23%	16.13%	2.09%
Blood	Control	11	68.17%	23.12%	2.95	50.90%	59.93%	48.56%	13.78%	81.00%	11.94%	7.06%	4.55%
Blood	Control	12	73.00%	22.35%	3.27	29.17%	15.35%	24.72%	12.85%	74.13%	17.25%	8.62%	1.91%
Blood	Control	13	62.81%	30.65%	2.05	55.14%	33.68%	44.96%	18.77%	63.92%	27.69%	8.39%	5.14%
Blood	Control	14	51.05%	40.43%	1.26	69.86%	29.96%	47.78%	25.33%	72.89%	14.00%	13.11%	5.20%
Blood	Control	15	72.23%	26.44%	2.73	46.93%	61.30%	50.10%	24.96%	76.89%	11.27%	11.85%	6.37%
Blood	Control	16	64.52%	31.02%	2.08	49.16%	37.32%	43.30%	30.20%	67.68%	7.73%	24.59%	2.77%

Intracellular cytokine expression data was calculated using the total number of cytokine expressing T-cells divided by the total number of T-cells of that phenotype, i.e. CD4+ (T_h) and CD4-, assumed to be primarily T_c. Example calculations are given below (Table 18), followed by the mean results (Table 19).

Table 18: Example calculations for Extracellular lymphocyte phenotyping.

% T-cell Cytokine expression (IL-4, IL-17 and IFN-γ)

Where:

y = CD3⁺CD4⁺ or CD3⁺CD4⁻

z = IL-4⁺ or IL-17⁺ or IFN-γ⁺

$$\% z^+ y^+ \text{ T-cells} = \frac{z^+ y^+ \text{ events}}{y^+ \text{ events}}$$

Table 19: T-cell cytokine expression results

Sample	Type	ID	% CD4 IFN-γ	% CD8 IFN-γ	% CD4 IL-4	% CD4 IL-17	% CD8 IL-4	% CD8 IL-17
Blood	MM	26						
Blood	MM	27						
Blood	MM	30						
Blood	MM	31						
Blood	MM	32						
Blood	MM	33						
Blood	MM	34						
Blood	MM	37						
Blood	MM	45	14.62%	47.72%	0.20%	1.51%	0.21%	0.21%
Blood	MM	55	11.70%	35.71%	0.15%	1.81%	0.06%	0.50%
Blood	MM	68	15.14%	53.47%	0.14%	1.43%	0.03%	0.30%
Blood	MM	72	17.58%	27.71%	0.16%	1.52%	0.48%	0.15%
Blood	MM	78	10.14%	62.01%	0.02%	1.27%	1.01%	1.07%

Table 19 (continued)

Blood	MM	82	5.41%	54.91%	0.13%	0.35%	0.59%	0.23%
Blood	MM	83	6.76%	14.31%	0.15%	0.69%	0.09%	0.28%
Blood	MM	84	25.05%	56.94%	0.51%	2.01%	0.85%	0.24%
Blood	MPE	29						
Blood	MPE	39	17.67%	72.08%	0.23%	2.92%	0.07%	0.40%
Blood	MPE	43	20.35%	61.15%	0.04%	1.68%	0.07%	0.30%
Blood	MPE	46	11.19%	67.77%	0.30%	1.13%	0.23%	0.45%
Blood	MPE	49	12.99%	61.08%	0.19%	0.72%	0.05%	0.16%
Blood	MPE	50	13.84%	36.68%	0.04%	3.47%	0.02%	0.68%
Blood	MPE	51	18.29%	55.52%	0.08%	3.64%	0.49%	1.37%
Blood	MPE	53	7.59%	61.87%	0.04%	0.58%	0.08%	0.18%
Blood	MPE	57	14.01%	37.08%	0.20%	1.74%	0.71%	0.05%
Blood	MPE	58	11.99%	85.69%	0.02%	0.48%	0.00%	0.42%
Blood	MPE	61	6.80%	42.88%	0.24%	0.64%	0.17%	0.35%
Blood	MPE	63	9.57%	50.95%	0.14%	2.18%	0.59%	0.70%
Blood	MPE	64	14.12%	54.40%	0.16%	0.90%	0.18%	0.29%
Blood	MPE	70	14.38%	58.23%	0.10%	0.31%	0.18%	0.15%
Blood	MPE	74	6.60%	33.92%	0.13%	0.51%	0.00%	0.06%
Blood	MPE	80	14.64%	76.45%	0.04%	2.05%	0.27%	0.47%
Blood	MPE	81	11.22%	31.94%	0.09%	0.70%	0.32%	0.13%
Blood	MPE	85	20.48%	64.10%	0.46%	2.94%	0.35%	0.08%
Blood	MPE	86	14.17%	81.76%	0.04%	0.54%	0.15%	0.15%
Blood	MPE	87	8.98%	49.97%	0.15%	0.84%	0.36%	0.16%
Synovial	MPE	47	19.19%	33.12%	0.17%	1.64%	0.76%	0.66%
Synovial	MPE	53	37.48%	57.10%	8.81%	8.98%	0.74%	6.56%
Synovial	MPE	64						
Synovial	MPE	70						
Synovial	MPE	74						
Synovial	MPE	76						
Synovial	MM	33						
Synovial	MM	35						
Synovial	MM	37						
Synovial	MM	45						
Synovial	MM	72	23.38%	47.32%	1.14%	1.21%	1.54%	3.38%
Synovial	MM	78						
Synovial	MM	83						
Blood	Control	1	17.82%	49.28%	0.31%	0.80%	0.68%	0.33%
Blood	Control	2	10.76%	20.37%	0.24%	1.40%	0.22%	0.35%
Blood	Control	3	27.27%	63.45%	0.21%	3.65%	0.49%	0.71%
Blood	Control	5	30.17%	32.63%	0.17%	1.68%	0.11%	1.31%
Blood	Control	6	15.15%	30.02%	0.15%	1.12%	0.11%	0.37%

Table 19(continued)

Sample	Type	ID	% CD4 IFN-γ	% CD8 IFN-γ	% CD4 IL-4	% CD4 IL-17	% CD8 IL-4	% CD8 IL-17
Blood	Control	7	25.78%	59.41%	0.18%	3.10%	0.37%	0.43%
Blood	Control	8	8.96%	30.16%	0.14%	1.05%	0.24%	0.29%
Blood	Control	9	16.52%	29.27%	0.15%	0.95%	0.19%	0.19%
Blood	Control	10	8.55%	37.02%	0.11%	1.12%	0.14%	0.13%
Blood	Control	11	15.56%	61.78%	0.14%	2.81%	0.69%	0.93%
Blood	Control	12	6.68%	20.17%	0.14%	1.18%	0.32%	0.60%
Blood	Control	13	14.19%	32.18%	0.24%	0.87%	0.05%	0.09%
Blood	Control	14	16.55%	28.84%	0.14%	0.88%	0.02%	0.07%
Blood	Control	15	5.98%	42.06%	0.14%	0.48%	0.17%	0.50%

Appendix F: Peripheral Blood Lymphocyte Population Distributions

As per section 2.5 the T- and B-cell lymphocyte populations were analyzed using one-way ANOVA under the assumption of near-normal distributions. The distributions for the patient groups, MM, MPE, and control subjects were evaluated qualitatively using normal probability plots for the peripheral blood data. Deviations from the expected normal values were minimal, with the exceptions of the NK, NKT and cytokine expression of IL-4 and IL-17 (Figure 28, Figure 32, and Figure 33). Cytokine expression, NK- and NKT-cell populations were therefore analyzed without the assumption of normality as described in section 2.5.

Due to small sample sizes, for the synovial fluids, no evaluation of normality was performed and non-parametric analysis was performed as laid out in section 2.5.

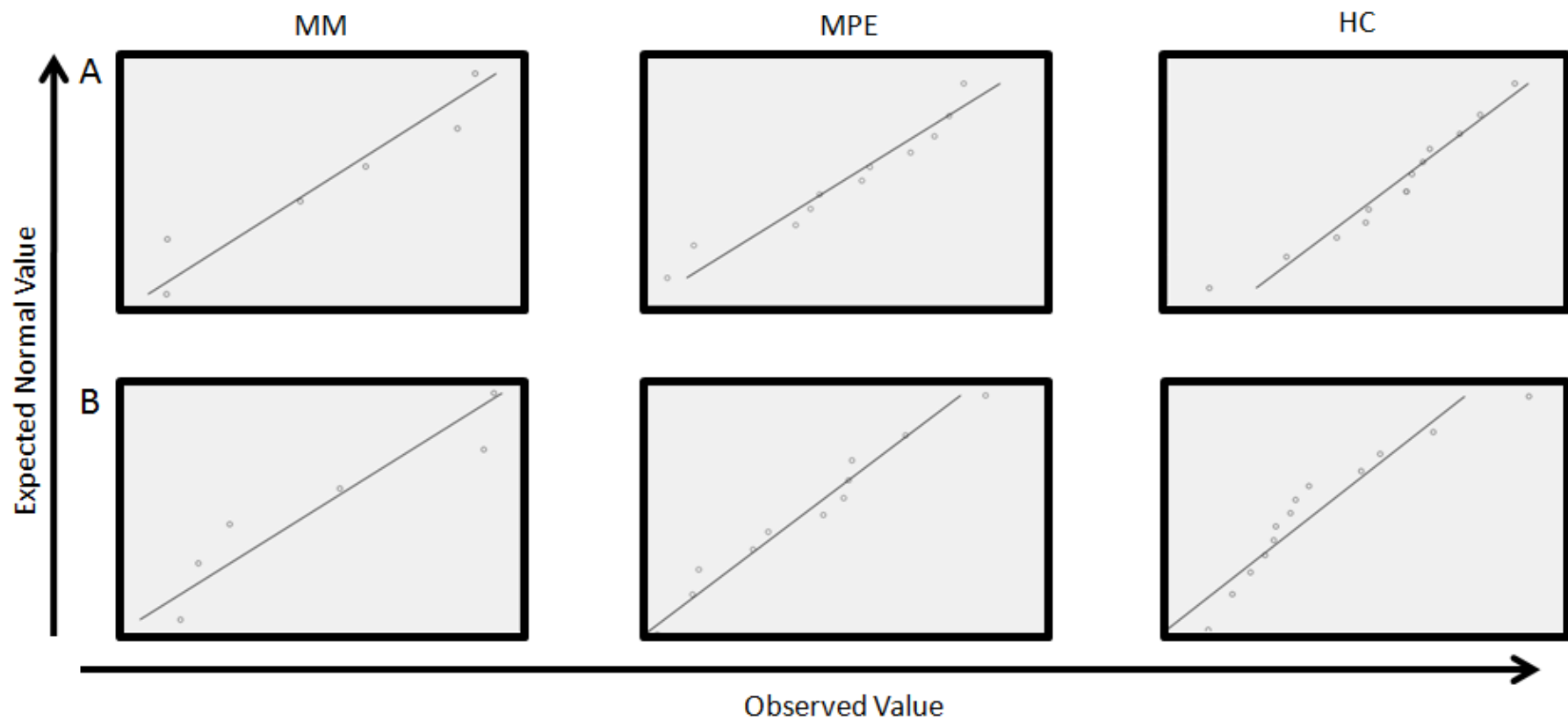


Figure 27: Normal distribution plots for the T- and B-cell peripheral blood lymphocyte populations (A and B, respectively), separated by patient groups (MM, MPE and control (HC)).

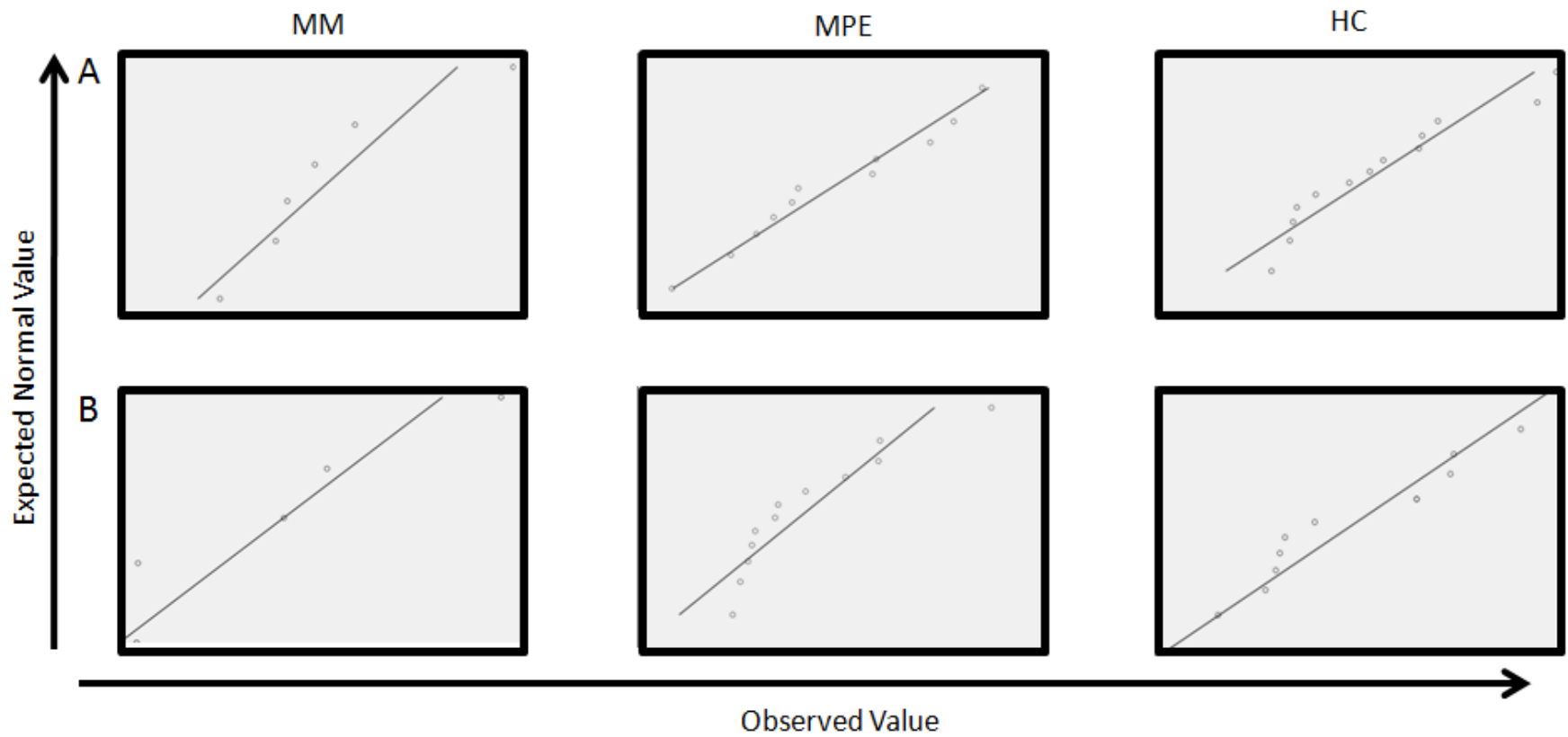


Figure 28: Normal distribution plots for the NK- and NKT-cell peripheral blood lymphocyte populations (A and B, respectively), separated by patient groups (MM, MPE and control (HC)).

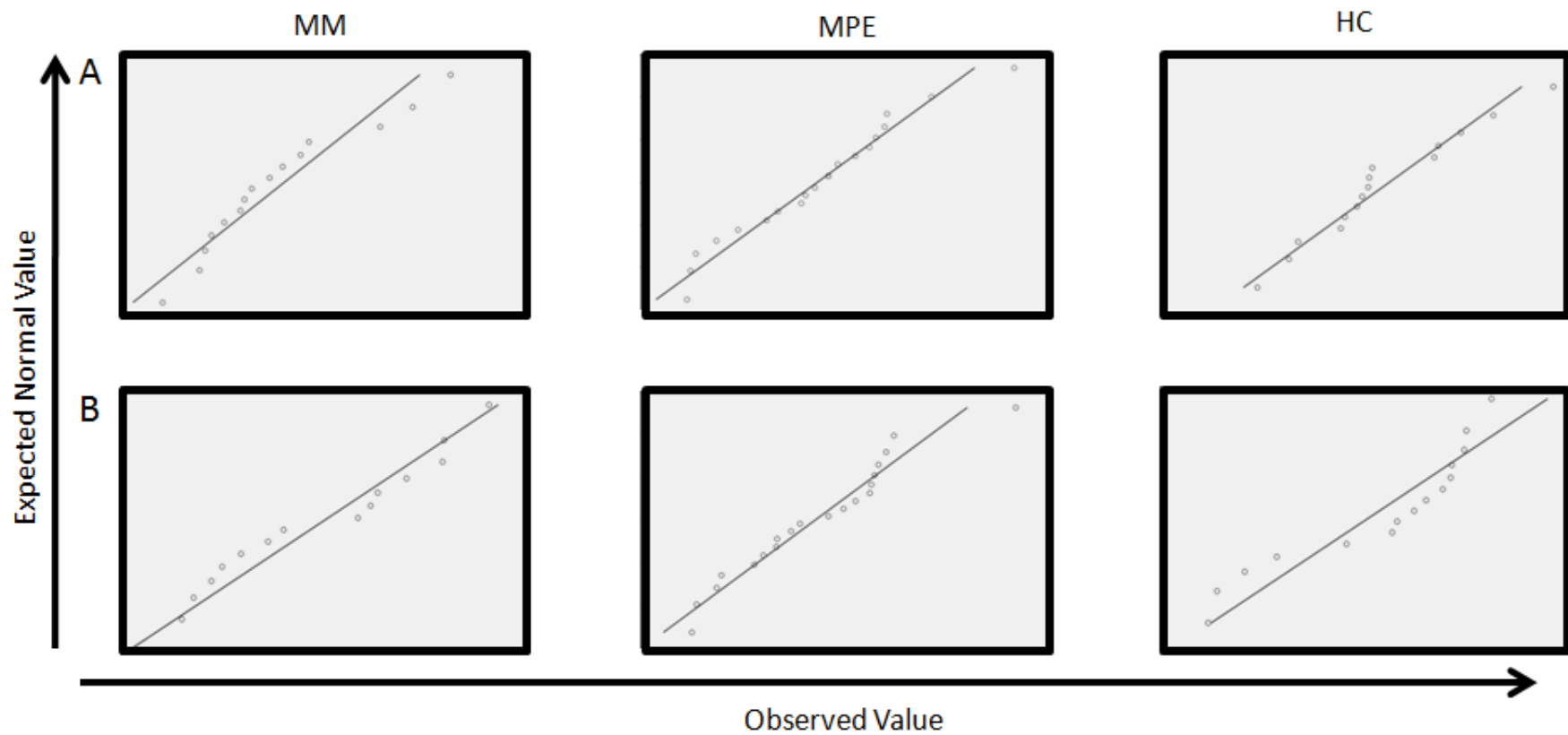


Figure 29: Normal distribution plots for the CD4/CD8 ratios and the percentages of memory ($CD45RO^+$) T-cell peripheral blood lymphocyte populations (A and B, respectively), separated by patient groups (MM, MPE and control (HC)).

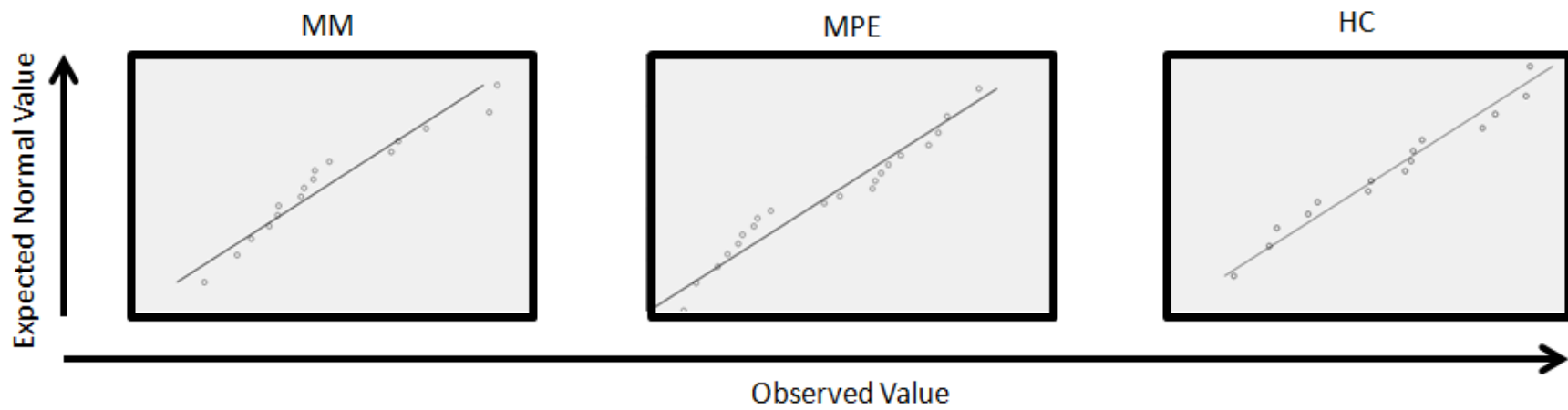


Figure 30: Normal distribution plots for the percentages of memory B-cells, separated by patient groups (MM, MPE, and control (HC)).

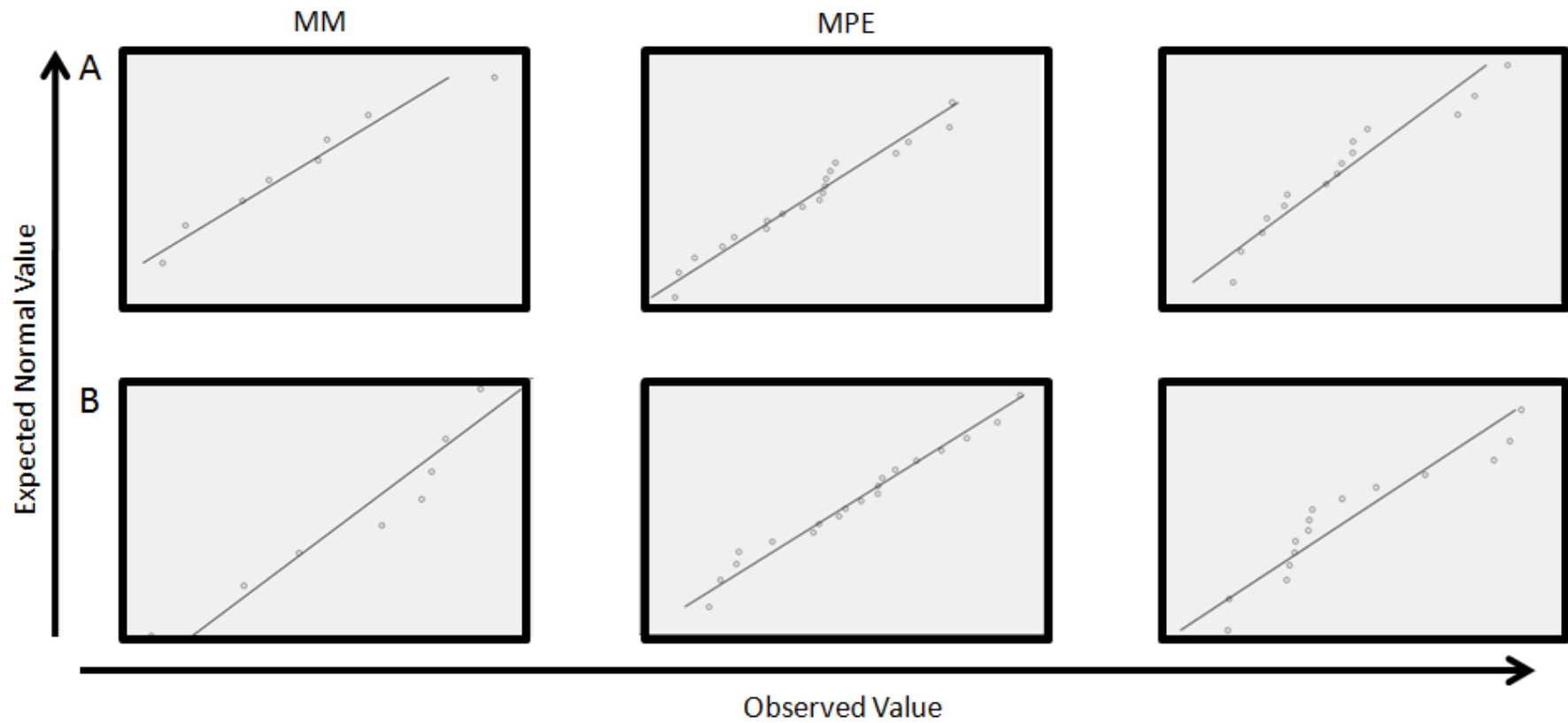


Figure 31: Normal distribution plots for the percentages of IFN- γ cytokine expression in peripheral blood CD4⁺ and CD4⁻ (CD8⁺) T-cells (A and B, respectively), separated by patient groups (MM, MPE, and control (HC)).

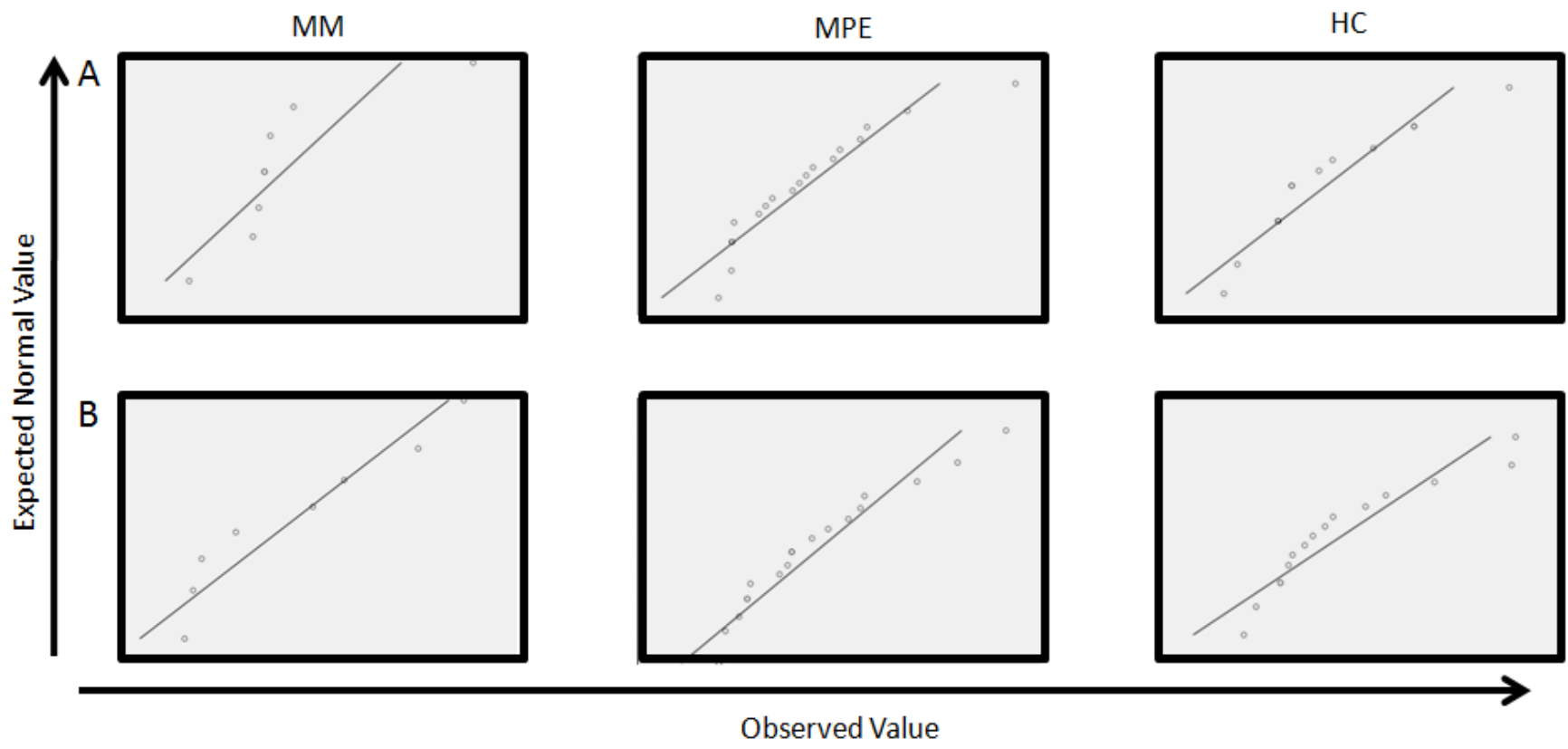


Figure 32: Normal distribution plots for the percentages of IL-4 cytokine expression in peripheral blood CD4⁺ and CD4⁻ (CD8⁺) T-cells (A and B, respectively), separated by patient groups (MM, MPE, and control (HC)).

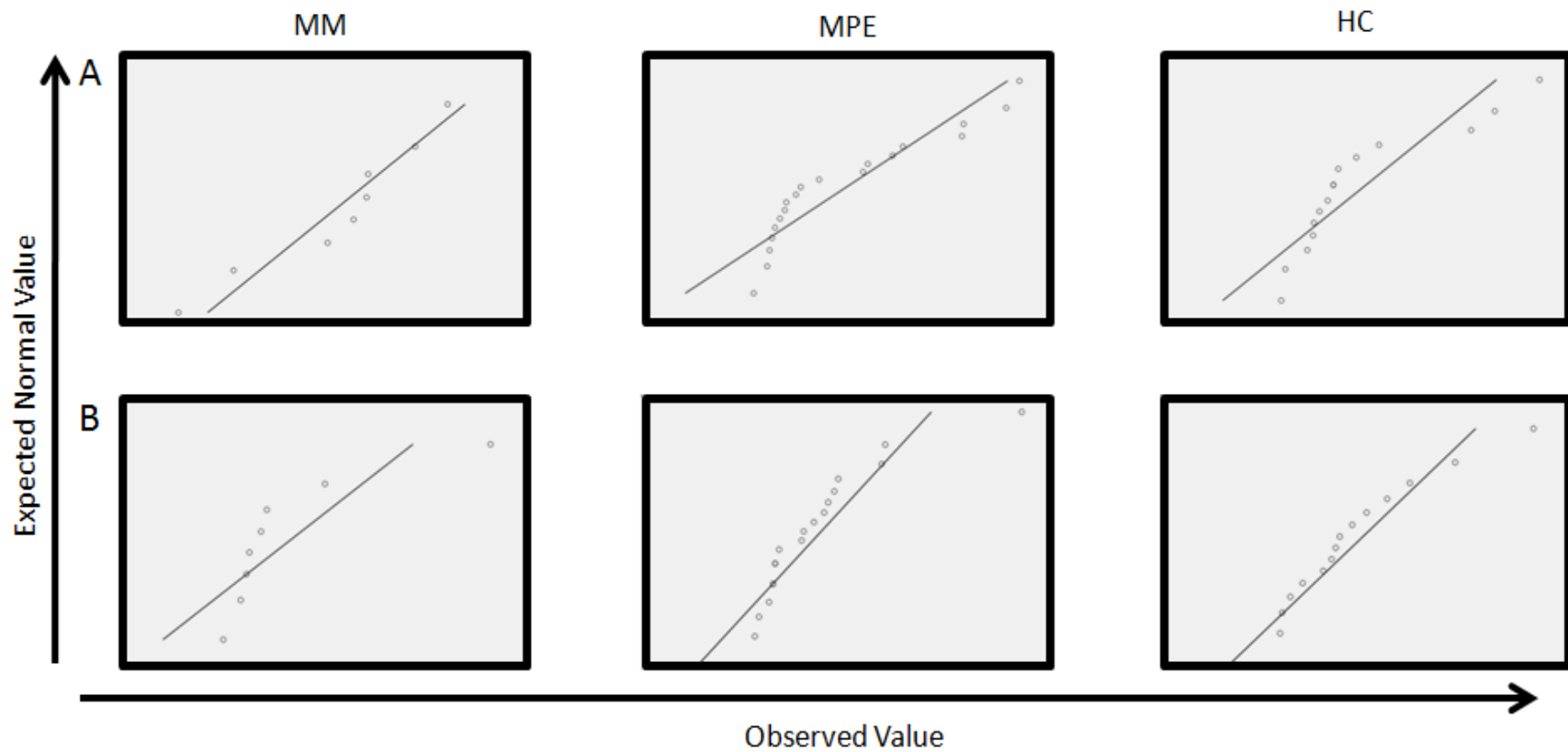


Figure 33: Normal distribution plots for the percentages of IL-17 cytokine expression in peripheral blood CD4⁺ and CD4⁻ (CD8⁺) T-cells (A and B, respectively), separated by patient groups (MM, MPE, and control (HC)).